

Student Organization for Aerospace Research Atlantis II

Sounding Rocket

Team 43 Project Technical Report for the 2018 IREC

J. Martens¹, X. Cui², H. Stoldt³, L. Alacoque⁴, T. Messinger⁵, A. Hamilton⁶, Wm. K. van der Meulen⁷, A. Deshpande⁸
University of Calgary, Calgary, AB, T2L 1B3, Canada

The following report details the hybrid powered sounding rocket design put forth by the Student Organization for Aerospace Research (SOAR) at the University of Calgary. The sounding rocket officially known as Atlantis II, is SOAR's entry into the 2018 Intercollegiate Rocket Engineering Competition at Spaceport America, New Mexico. SOAR's vision is for Atlantis II to achieve a target altitude of 30,000-feet above ground level. To accomplish this task, Atlantis II is powered by a student researched and designed hybrid rocket motor using paraffin wax as fuel, and nitrous oxide as an oxidizer. The rocket measures 17 feet in length, and 7 inches in diameter, and will be carrying an 8.8 lb scientific payload. This payload aims to measure the efficacy of different materials used to shield humans, and other biological systems, from the increased levels of radiation in space. A new composite material was developed by the University of Calgary to be usable for space wear while providing the required radiation shielding - specifically, the range of radiation that composes "cosmic radiation". Our payload also records the temperature distribution along the length of the rocket nose cone, and collects flight spin and speed information. This data, in combination with acceleration, GPS and barometer data from our main avionics system, will be highly valuable in improving our overall rocket and engine design.

¹ Undergraduate, Mechanical Engineering, 2500 University Dr NW, Calgary, AB T2N 1N4

² Undergraduate, Mechanical Engineering, 2500 University Dr NW, Calgary, AB T2N 1N4

³ Undergraduate, Mechanical Engineering, 2500 University Dr NW, Calgary, AB T2N 1N4

⁴ Undergraduate, Mechanical Engineering, 2500 University Dr NW, Calgary, AB T2N 1N4

⁵ Undergraduate, Mechanical Engineering, 2500 University Dr NW, Calgary, AB T2N 1N4

⁶ Undergraduate, Mechanical Engineering, 2500 University Dr NW, Calgary, AB T2N 1N4

⁷ Undergraduate, Electrical Engineering and Computer Science, 2500 University Dr NW, Calgary, AB T2N 1N4

⁸ Undergraduate, Mechanical Engineering, 2500 University Dr NW, Calgary, AB T2N 1N4

Nomenclature

F_y	=	Y component of the resultant pressure force acting on the vehicle
m_{dry}	=	mass of rocket when descending
a	=	acceleration
v_o	=	opening velocity
v_{term}	=	terminal velocity
$SA/inch$	=	Shear area per inch
π	=	pi
D_{max}	=	maximum minor diameter of the internal thread
D_{min}	=	minimum pitch diameter of the external threads
N	=	threads per inch
\dot{m}_{spi}	=	mass flow rate single phase flow
\dot{m}_{hem}	=	mass flow rate at homogeneous equilibrium
$A_{injection}$	=	Area of the injection plate orifices
ρ	=	density
ΔP	=	Pressure differential
S_n	=	Entropy at location n
\dot{m}_{Dyer}	=	Dyer mass flow equation for non-homogeneous non-equilibrium
κ	=	kappa, non-equilibrium parameter
Δh	=	change in enthalpy
t_{cr}	=	thickness of combustion casing
P	=	Pressure
R	=	Radius for combustion chamber equations
S	=	cylindrical stress
e	=	efficiency
C_nH_{2n+1}	=	chemical formula for paraffin wax with n=20-30
A_t	=	nozzle throat area
A_1	=	nozzle inlet area
A_e	=	nozzle exit area
A_p	=	parachute nominal area
M_1	=	Mach number at nozzle inlet
M_t	=	Mach number at nozzle throat
M_e	=	Mach number at nozzle exit
k	=	specific heat ratio
σ	=	dimensionless factor accounting for variation of row and mu values across boundary layer
h_g	=	heat transfer coefficient
T_w	=	wall temperature
T_o	=	stagnation temperature
γ	=	ratio of specific heats in heat transfer equations
ϖ	=	temperature exponent of viscosity equation
Pr	=	Prandtl number
r_c	=	throat radius of curvature
μ	=	viscosity
g	=	gravitational acceleration
D^*	=	throat diameter for heat transfer equations
A^*	=	throat area for heat transfer equations
C^*	=	characteristic velocity for heat transfer equations
C_p	=	specific heat at constant pressure
C_d	=	Coefficient of drag

I. Introduction

The Atlantis II sounding rocket is the Student Organization for Aerospace Research's (SOAR's) entry in the 2018 Intercollegiate Rocket Engineering Competition (IREC) at Spaceport America, New Mexico. The Atlantis II will be the third sounding rocket that SOAR has entered into the IREC event over the years, featuring SOAR's second SRAD motor, making it the second SOAR rocket attempting a target altitude of 30,000-feet. In 2016, SOAR entered its first IREC event with a basic Commercial off the Shelf (COTS) rocket that reached an altitude of 9,200-feet, and placed middle of the group at 22 out of 40 teams. For the 2017 competition, SOAR entered a new rocket, a Student Researched and Developed (SRAD) hybrid rocket. This rocket placed 3rd in its category.

SOAR is run and operated by students from multiple disciplines and faculties including mechanical engineering, electrical engineering, physics, and computer science. The team has two academic advisors, Dr. Craig Johansen from Mechanical Engineering, and Dr. Chris Cully from the Faculty of Science. SOAR is an extracurricular club where students do not receive any additional credits for their work but instead have the opportunity to reinforce engineering principles learned in class and apply them to real-world aerospace applications with time and resource constraints. SOAR helps students gain experience in manufacturing, design, teamwork, and project management - an opportunity that is not readily offered in the classroom. SOAR has positioned itself to thrive in the future with strong support from academic advisors, an aerospace sponsor, core team members, and new recruits.

The objective of the club is to provide members with the ability to learn about physics and engineering with a hands-on approach. The projects provide education in space sciences through the creation and completion of various projects from start to finish. The club also creates awareness on campus about space research at the University of Calgary, as well as related projects from the Canadian Space Agency with the intent to further student knowledge and motivate/interest future researchers.

The Atlantis II rocket name was chosen to signify that this is the team's second iteration of this size and class of rocket. The project has numerous stakeholders that offered valuable resources and knowledge needed to complete the Atlantis II hybrid sounding rocket. The project received generous contributions from the University of Calgary Schulich School of Engineering and from the Faculty of Science, who provided funding, workspace, and resources necessary to attend the competition in New Mexico. SOAR also received a significant amount of help and materials from the fantastic team at Luxfer Gas Cylinders in Calgary. Lastly, the University of Calgary Rothney Astrophysical Observatory generously donated the space in their static test facility for SOAR's use.

II. System Architecture Overview

The Atlantis II is a 17-foot length, 7-inch diameter sounding rocket with a target altitude of 30,000-feet., primarily made of student researched and designed components. The exterior of the rocket is made out of two carbon fiber filament wound body tubes and a composite overwrapped pressure vessel (carbon fiber wrapped on an aluminum 6061-T6 liner) as the oxidizer tank. The top section of the rocket comprises a fiberglass composite nose cone with an aluminum tip, drogue parachute and a scientific payload. The top carbon fiber tube contains the main parachute, avionics and recovery systems. A 7-foot pressure vessel makes up the middle section of the rocket where the nitrous oxide oxidizer is contained. This section attaches to the combustion chamber assembly via a radial - axial joint. The aluminum combustion chamber assembly is encased by a carbon fiber body tube, which houses the injector feed system, combustion chamber, fuel grain, motor control system, and nozzle. Three symmetric and replaceable clipped delta fins made out of basswood wrapped with multiple layers of carbon fiber are bolted through the rocket body tube.



Figure 1: Cross-sectional view of the Atlantis II sounding rocket.

A. Aero-structures Subsystems

1.1 Nose Cone

The shape of the nose cone was determined using OpenRocket, a rocket simulation software that was used to model the Atlantis II. Identical simulations were executed with varying nose geometry and the results were analyzed in the areas of drag, velocity and acceleration. Shown below is a table outlining the primary results and ultimate decision of designing a nose cone with $\frac{1}{2}$ Power geometry. Furthermore the fineness ratio had to be analysed to conclude the optimal length to diameter ratio. This analysis was also completed with OpenRocket software in the same manner. The final result was a nose cone modelled with $\frac{1}{2}$ Power series geometry and 6:1 fineness ratio resulting in minimum drag and maximum altitude and velocity (details in Appendix VI).

Table 1: Nose Cone Geometry and Respective Assessment at Varying Mach Speeds

Type of Nose Cone	Optimum Range (Mach) [45]	Drag at Mach 1.2	Surface Area
$\frac{3}{4}$ Power	(0.8-0.9), (1.6-2.2) and 2+	3	1
$\frac{1}{2}$ Power	(0.8 -1.8)	1	2
LD Haack Series	(0.8 – 1.35), (1.75- 2.2)	2	3

On a number scale where the larger the number the lower the ranking, i.e. the worse it is in a category in comparison

In conjunction with the connecting body tubes of the Atlantis II the base of the nose cone has a diameter of 7" and corresponding to the 6:1 fineness ratio the final length is 42". This ensured that the internal volume of the nose cone is large enough to house the payload system and consequently reduced the length of body tubes and the rocket's overall weight and surface area.

To determine the potential pressures, heat transfer and overall fluid mechanics of the Atlantis II nose cone the geometry described previously was modelled and simulated in Solidworks and ANSYS software. Upon completing the simulations it was found the largest potential forces were 130 kPa (gauge) at fluid velocities of 450 m/s parallel to length of nose cone and 17 m/s perpendicular. From this data ANSYS composite simulation was conducted to determine that 4 ply of 6 oz E-glass fiberglass and Aeropoxy PR2032 laminating resin was needed to withstand flight loads. Fiberglass was decided upon to ensure the nose cone is radio frequency transparent, lightweight and with high strength capabilities. Maximum temperature was located at the stagnation point at the tip of the rocket and calculated to be 130 °C. An aluminum tip was manufactured to withstand the stagnation temperatures during flight and it was verified that temperatures during flight would be low enough to ensure that the PR2032 epoxy would not reach glass transition state or deform along the length of the nose cone. Details are available in Appendix VI.

1.1.1 Drogue Connection:

The line connecting the nose cone to the drogue chute is threaded through the upper bulkhead at the base of the nose cone. It enters on one side, passes underneath the payload and then exits on the other. Both the entry and exit holes have a rounded profile to avoid having the parachute cord on a sharp 90 degree angle.

1.1.2 Body Tube Connection:

The nose cone connects the upper body tube via a number of small nylon bolts. They bolt into a 3.5" long section of $\frac{1}{8}$ " wall Aluminum pipe protruding from the upper body tube. One inch of the tube is epoxied permanently into the upper body tube and two and a half inches protrude into the bottom of the nose cone. The nylon bolts are designed to fail in shear when the recovery system is triggered. The number of nylon bolts used modulates the amount of pressure built up in the upper body tube and nose cone before the nose cone is released and will be set through experimental testing.

1.2 Rocket Body Tubes

The SOAR team endeavored to make its own body tubes once again this year. They had to be strong but also light, which made composites very appealing. SOAR had our body tubes filament wound with carbon fiber because

of the superior strength of filament wound tubes. The angle of the windings and the number of layers (4) were based off of the results obtained from ANSYS FEA software and a simulation prepared to test various loading conditions. Due to restrictions imposed by our mandrel and the sponsor's winding setup, the lowest angle we could achieve was 33° (all angle from the longitudinal). Because most of the loads experienced by the body tubes are expected to be axial or bending loads, this became the winding angle for our first layer. The 4th layer (farthest from the center of the cylinder) was set to be 85° to ensure good compression of the interior layers and to give some amount of compressive strength. Since our body tubes will primarily be under axial loading, we considered the following possibilities for the orientation of our winding angles, and tested them using FEA simulations.

Our loading cases are as follows (further info available in Appendix VI):

Flight Loads: Axial Force: -3515N(Compressive) Bending Moment: 231.2 Nm Shear Force: 209.7N

Parachute Deployment Loads: Axial Force: 2920N Bending Moment: 806 Nm Shear Force: 290.4N

The winding orientation which resulted in the highest Factor of Safety - [33,33,33,85]. The results of the different orientation of the winding angles are shown below. Failure of the body tubes was checked against the Maximum Principal Failure Criterion.

Table 2: Factor of Safety for Different Fiber Winding Angles

	Parachute Deployment				Flight Loads			
	Layer 1	Layer 2	Layer 3	Layer 4	Layer 1	Layer 2	Layer 3	Layer 4
33,85,-33,85	15.7	5.3	8.3	3.9	36.2	13.2	19.2	9.0
33,33,33,85	15.5	11.3	7.2	3.1	33.9	26.5	15.6	7.6

The reason why the first winding angle orientation was not chosen despite having a higher minimum Factor of Safety is because of the low Factor of Safety in layer 2 of 5.3 during parachute deployment. Since there will primarily be axial loading, having a layer at 85 would have not provided any support except through it's epoxy strength. With the second orientation there is no layer which is experiencing sudden drop on Factor of Safety. It is also important to note that in these simulations all loads were applied evenly around the entire circumference of the body tube, which would not necessarily be the case in the real rocket, especially for axial loads applied by the motor mount system (see 2.4).

1.3 Radax (radial-axial) Joints

As stated, radax joints are used to couple the rocket sections. Each joint consists of two aluminum (6061-T6) cylinder modules, which are coupled together using 16 #8 steel bolts angled at 30° from the longitudinal axis of the rocket. This design allows any loads which the rocket experiences to be distributed chiefly axially along the bolts; as such, our coupling system effectively withstands high tensile/bending loads during groundwork, parachute deployment, and flight descent [41].

The rocket has two radax joints, one each above and below the main pressure vessel. The length of the radax joints is actually not primarily useful for strength (See Appendix VI) but for the ease of alignment with the rocket body tube that it creates. Because the bottom radax joint is adjacent to the motor mount, which provides a realignment location, the bottom radax joint was designed to be shorter than the top one, which has no such alignment mechanism nearby.

1.4.1 Upper Bulkhead:

The purpose of the upper bulkhead is to hold the payload in the nose cone during flight, but also allow easy removal when on the ground. To accomplish this, we separated it into two parts. One has an L-shaped cross section and is permanently epoxied to the interior of the nose cone and the other is a flat circular plate that connects to the bottom of the threaded rods that make up the main structure of the payload. Nut plates are riveted onto the top of the L-shaped piece, allowing the payload and it's mounting plate to bolt in from the bottom. The peak loading this part

was designed for is the peak drogue loading, calculated at 4500 N, since there is a chance this load could be fully applied to the nose cone if slack remains in the section of line between the nose cone and the main rocket while the section of line between the drogue and the nose cone is already pulled taut.

1.4.2 Lower Bulkhead:

The purpose of the lower bulkhead is to provide a secure attachment location for our parachutes. The structure is designed to hold on to a large centered forged steel eye bolt, positioned at the center of the rocket. It is permanently epoxied into the upper body tube and milled out of piece of solid 6061-T6 aluminum. The epoxy bond gap around the bulkhead and all other components epoxied into the body tubes was left at a slightly large 0.02" since it was known in advance that our body tube mandrel / form is not perfectly round.

1.5 Motor Attachment

The purpose of the motor attachment is to transfer largely axial load from the combustion chamber to the rest of the rocket airframe. Since the section of body tube right above the combustion chamber is made out of fiberglass and we do not have a nice way of filament winding strong fiberglass body tubes, we decided to avoid having the fiberglass take the motor load by connecting the motor mount directly to the carbon fiber tube just above the fiberglass section.

The motor's force is carried across the fiberglass body tube by four equally spaced lengths of aluminum square tube, positioned to butt right up against the inner wall of our rocket's body and thereby providing the maximum amount of bending strength.

Since our combustion chamber is smaller than the ID of the rocket, an adapter plate was bolted on to the top of the chamber to provide a mounting surface right at the inside wall of the body tube. The square tubes are then bolted both into the adapter plate at the top of the engine and into aluminum blocks permanently epoxied into the rocket just above the transition back to our filament wound carbon fiber body tubes. To make the whole assembly accessible, the bottom body tube, fins and tail fairing can be removed by undoing eight bolts and sliding it off.

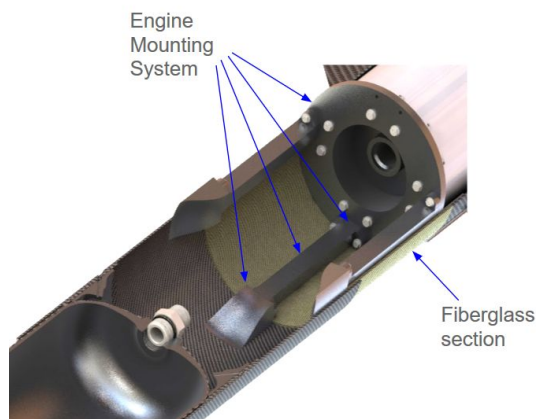


Figure 2: Engine Mounting System

1.6 Tail Fairing

The tail fairing will be present simply to ease the transition from the ~7.25" OD rocket body to the smaller diameter combustion chamber exhaust nozzle to allow for less turbulence generated at that point. It will be made from 3-4 layers of 8 HS carbon fiber. It is not expected to take any major loading and so its structure was not verified using composite FEA software, but rather is determined by past composite structure experience. The tail fairing is easily replaceable and attached to the rest of the rocket by three small bond plates and #8 bolts in shear loading.

1.7 Fins

The purpose of the fin design is to create a fin that will provide stability for the rocket through all stages of flight, while at the same time adding the minimum possible amount of drag. To achieve this, a method for accurately and quickly modelling the rocket stability through different fin iterations was required. OpenRocket software was chosen for this purpose as the primary method for determining stability, and one of two methods for estimating the drag contribution from the fins. Aerolab was used as a secondary source for drag numbers, to compare with OpenRocket, as OpenRocket is not optimized for supersonic calculations [42]. An article in the Apogee newsletter (Why Should You Airfoil Your Rocket's Fins?) mentions that a fin is at its optimum when it is designed with three things – an efficient plan-form, proper symmetrical airfoil, and a precise radial taper. Two main forms of fin planform were examined and contrasted to determine which provided superior aerodynamic properties with equivalent stability. The two planforms were clipped delta and symmetrical trapezoid. Both designs utilized a diamond shaped airfoil, and a radial taper, as mentioned in the Apogee article. OpenRocket simulations showed that with an equal planform area, both geometries provided roughly the same stability throughout ascent, but the clipped

delta design provided a lower drag coefficient in our velocity range. Figures plotting the drag coefficients of each geometry against time are available in Appendix VI.

The pressure drag during the supersonic portion of flight is higher for the Trapezoidal fin. This was verified by running the same geometries through Aerolab. Since drag is related to velocity squared, a model of drag force versus time showed a lower total drag on the clipped delta geometry, which equated to an increased apogee. Due to this, the clipped delta geometry was chosen.

The exact geometry of the fins were then determined in order to satisfy the stability requirements: namely that the rocket be stable at all times throughout the ascent, and always maintain a stability margin between 2.0 and 6.0 (for nominal stability). At the time of the first launch lug departing the launch rail, the rocket is designed to be travelling at a speed of 118ft/s, which is above the minimum speed for launch rail departure stability.

In order to prevent excess drag and stability, a fin mounting system was designed such that multiple different sizes of fins may be attached to the rocket, in order to adapt both to varying wind conditions at launch. An added benefit of this system is that it allows us to adapt quickly and efficiently to changes in the actual rocket weight / CG / CP locations compared to our initial design.

A downside of this mounting system is that due to the requirements for this mounting system, the base of the fin had to be kept identical for each iteration, which constrained some aspects of the geometry, such as sweep angle, at the price of modularity.

The failure case of fin flutter was also examined for our geometry. Critical velocity for fin flutter was calculated using an equation from Apogee Newsletter [43] which is a variation of the equation proposed by Dennis Martin in his NASA paper on flutter calculations [44]. Using this equation, the critical velocity for the fin geometry was calculated to be 787m/s, which is much higher than our maximum velocity of 530m/s.

The structure of the fins consists of a core of laser-cut basswood ribs stacked together to form the desired 3D geometry. To add the required strength, a lay-up of carbon fiber is done. As a means of attaching the fins onto the body tube so that they are easily replaceable, mounting plates are epoxied to the outside of the body tubes. Bolts are then threaded through the mounting plates and into aluminum inserts embedded inside the base of the fins. This system of mounts and fins was designed such that the failure mode will be the bolts in tension, so that any failure can be quickly and easily repaired by simply installing a new set of fins. That failure mode was confirmed to be the one that occurs by a destructive test of a prototype fin.

The three fins will be positioned evenly around the body of the tube by using a CNC routed plywood alignment plate. Then they will be aligned with the body tube's longitudinal axis with a straight slotted piece of sheet metal bent to an angle. With this jig holding the fins and their mounts in position, the mounting plates will be permanently attached allowing replacement of fins with no additional alignment required.



Figure 3: Fin Prototype just prior to failure

B. Recovery Subsystems

2.0 Design

A dual deployment system was chosen for the recovery subsystem of this rocket. This involves the use of a drogue and main parachute and systems to release each parachute. The drogue parachute deployment utilizes two Raptor CO₂ systems. This allows for a dual deployment by ejecting the nose cone from the body tube, which simplifies the rocket design by using only one parachute compartment. The main parachute release utilizes a student designed system based off the commercially available Tender Descender [39]. The entire recovery system is shown below in both the drogue parachute deployment stage and the main parachute deployment stage. In addition to the student designed flight computer, a redundant commercially available flight computer powered by a separate battery sends the signals for drogue and main parachute deployment. The commercially available flight computer was chosen to be an Eggtimer Quantum to meet regulation and altitude requirements. When the rocket reaches apogee, the student designed flight computer will send a signal to the two Raptor CO₂ systems, pressurizing the parachute compartment to break shear pins that connect the nose to the rocket body. With the nose cone separated, the drogue parachute can deploy. If the first signal fails to trigger the CO₂ systems, the Eggtimer will send a delayed signal as backup. Once the rocket descends to an altitude of 1500 ft, a signal and a delayed signal from the Eggtimer are sent

to release the main parachute.

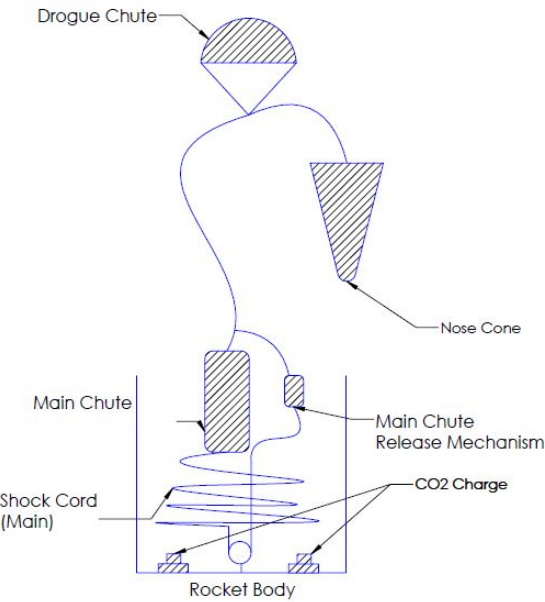


Figure 4: Rocket Descent under Drogue Chute

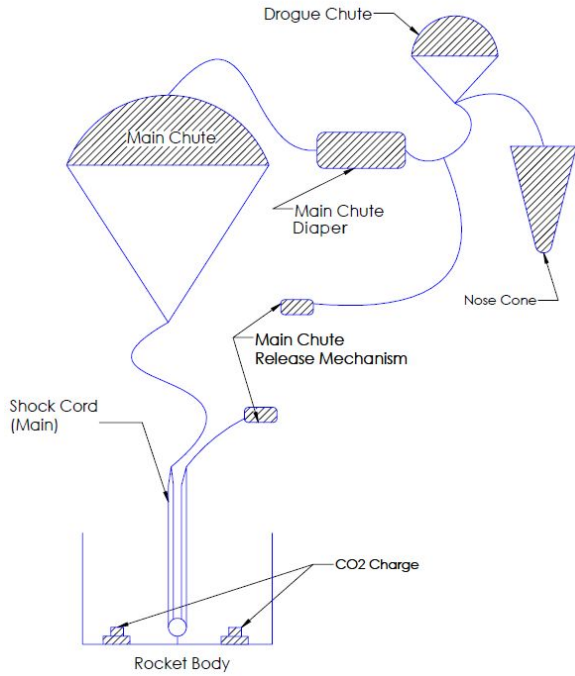


Figure 5: Rocket Descent under Main Chute

2.1 Force Calculation

Two parachute opening force methods were used in predicting the forces experienced by both the drogue parachute and the main parachute [35]. Both methods use the drag force equation to predict the parachute opening force. The first method assumes the weight of the rocket body is large enough that the opening of the parachute does not actually reduce the velocity of the rocket by a significant amount in that instant. This is called the infinite mass case and over predicts all opening force scenarios [37].

$$F = \frac{1}{2} v_o^2 \rho C_d A_p$$

The second method involves including a force reduction factor. For a small parachute with a heavy payload, the second method approaches that of the first method. However, as the canopy loading, defined as the weight of the payload over the effective drag area of the parachute, decreases, the parachute opening force predicted by the second method also decreases relative to the first method. The first method was used in designing both the main and the drogue parachutes as the overestimation of parachute opening forces predicted by this method provides a safety factor. The force calculation used for the current drogue parachute assumes a 6 sec delay after apogee. The vertical velocity reached in combination with the horizontal velocity of the rocket calculated from Open Rocket is used in determining the total drogue opening force with a predicted value of 1012lbs. The air density versus altitude for a high air density environment was taken to account for a safety factor [40]. After the drogue parachute was designed, the main parachute opening load was calculated to be 1866lbs, based on the steady state descend velocity of the drogue at 1500ft above ground level.

2.2 Drogue Parachute

A cross design was chosen for the drogue parachute based on three factors: stability, drag coefficient and ease of manufacture thereby increasing reliability. The drogue parachute reduces the rocket to a reasonable freefall velocity for the main parachute to open [35]. The minimum main parachute force is achieved by reducing the drogue

parachute steady state descent velocity while accounting for wind drift to ensure the rocket does not drift outside the designated landing zone. Maximum wind speed versus altitude was taken from an airport near Spaceport America and simulations were run to estimate the rocket drift distance. The estimated rocket weight and an estimated coefficient of drag of 0.63 were used in determining the nominal diameter of the drogue parameter and a 8.5ft nominal diameter drogue chute was selected. The estimated terminal velocity at 1500ft is predicted to be 66ft/s. The canopy fabric was chosen to reduce both oscillatory and rotational instability. It was determined that 1.1oz fabric at 80-120cfm porosity would be both strong and stable enough during descent. The canopy porosity and geometric porosity was selected to reduce rotational and oscillatory instability. See Appendix VII for engineering drawing.

The design was then further refined through the data collected by the US military tests [32-35]. With the results from the force calculation, the canopy strength was determined. The number of suspension lines as well as the line length was chosen as a trade off optimization between weight and effective drag [32]. 15ft of $\frac{1}{4}$ " kevlar shock cord will be used for the drogue parachute as this provides sufficient strength during the parachute opening phase. An unfurling test of the drogue parachute was performed at running speed and the drogue opened successfully.

2.3 Main Parachute

The main chute was chosen based on its ability to bring the rocket to the ground at a safe speed. Four different designs were considered, and a conical design was chosen based on weight, stability, ease of construction, coefficient of drag, and opening force. The ease of construction originally played large influence. From an estimated drag coefficient of 0.95, the main parachute was chosen to have a nominal diameter of 25ft. This gives the rocket vertical landing velocity of 18ft/s. A low number of 16 suspension lines was chosen to reduce the chances of entanglement and to prolong the parachute opening time. The longer opening time spreads the parachute opening forces over a longer time interval. Based on the force calculations, the suspension line and canopy rating were determined. A low 0-3cfm porosity rating was selected to maintain the previously estimated drag coefficient of 0.95. The number of gores were chosen to match the number of suspension lines. Based on findings in literature, bias panels were used in the construction of the gores to better handle canopy loads [35]. The number of panels on each gore was chosen based manufacturing limitations. See Appendix VII for engineering drawing.

After consulting with the team's academic advisor, it was decided to outsource manufacturing of both the drogue and the main parachutes to increase reliability. The optimal conical angle of 27.5 degrees was chosen to maximize drag. The vent hole ratio was chosen based on the minimum size required to reduce oscillation to an acceptable amount. This value is found by comparing data from low Reynolds number parachutes with commercially available parachutes that experiences high Reynolds numbers like that by the main parachute at around 2.3e6. The main parachute will be connected to the rocket by 15ft of $\frac{1}{2}$ " kevlar shock cord as this provides sufficient strength during the parachute opening phase. Finally, an optimization analysis was run to minimize the main parachute weight. This was done by increasing and decreasing the suspension line length as this which varies the drag coefficient of the parachute [36].

2.4 Drogue Parachute Release Mechanism

At an altitude above 20,000ft, conventional rocketry black powder charges become unreliable [38]. A CO2 system was chosen as a suitable alternative. See Appendix VII for engineering drawing. Most of the calculations made with regards to CO2 sizing are empirical. A convention used in rocketry is to multiply the amount of black powder needed in a ground test by a factor of five [38]. Due to uncertainties associated with vent holes and other leakage points, an estimate based on previous year's rocket was used, yielding an estimated 75 grams of CO2 required. Two Raptor CO2 will be used to eject the gas as quickly as possible because the flow out of the CO2 canisters are choked. Two e-matches will be used to trigger each Raptor systems at apogee, with the first trigger coming from the student designed flight computer and a delayed signal coming from Eggtimer Quantum. The Raptor CO2 system was tested with the Eggtimer Quantum and performed as expected.

2.5 Main Parachute Release Mechanism

The main parachute release mechanism restrains the main parachute from being released until the rocket descends to an altitude of at most 1500 ft above ground level. It is based on the working concept of the commercially available tender descender, but student designed in this case to meet the specific needs of the current drogue opening force at 1012 lbs. See Appendix VII for engineering drawing. The release mechanism consists of two parts, the main body and the pin piece [39]. The main body has three holes along the main axis, with the two holes on either side of the piece being through holes. The pin piece contains three pins that fit into the main body.

The pins on either side connects to the drogue parachute and the main parachute respectively. The side that connects to the main parachute has a shorter cord than the actual main parachute shock cord and therefore prevents the main parachute from being pulled out from the parachute compartment until the release mechanism is activated. The release mechanism works through the separation of the main body and the pin piece, allowing the shorter cord to separate. The separation happens through the trigger of black powder inside the center hole. Then the main parachute can be pulled out by the drogue. The release mechanism has been tested to the drogue parachute opening shock force and performed as expected.

C. Payload Subsystems

3.1 Scientific Experiment

The scientific payload of our rocket is to observe the effectiveness of a custom material to shield against cosmic radiation. A concern for astronauts, pilots and people in other jobs where exposure to radiation is eminent is the increased dose rate they receive. When considering how to best shield humans and other creatures from the dangerous effects of space, one must first consider what type of radiation you wish to shield against. For instance, when considering how to shield against massive particles such as alpha particles the concern is providing a thin layer of material to block the particles, as the alpha particles are damaging but easily blocked. On the other hand, high energy electromagnetic radiation is best shielded against using materials of high atomic mass. For astronauts, the protective properties would need to extend to shielding against other harsh conditions in space as well, for example the extreme temperatures and pressures. Outside of the earth's atmosphere, the radiation that you are expected to encounter is much more dangerous than the radiation that you are expected to encounter on the surface of the earth. This is because much of the radiation that you are expected to encounter when above the atmosphere is absorbed or blocked by the atmosphere. For this reason, it is very important to properly shield any biological system from dangerous sources of radiation. Some sources of radiation that are of concern include cosmic rays, radiation from the Van Allen Radiation Belts, and high intensity solar radiation rays. The payload consists of three functional units divided into three cubesat bays.

3.2 Electronics

The sensing package, i.e. the thermistors, photoresistors and such, is connected to an arduino teensy. This holds the SD card that logs all the payload sensor data. The payload radiation sensors are powered by simple but efficient Arduino Nano's running at 16MHz. To reduce the erroneous readings due to noisy output of the geiger tubes (one ionizing particle event usually produces a brief blip of noise), a denoising library is used on the Arduino. The denoising function reconciles events within a certain temporal threshold of each other into a single event, allowing us to accurately measure radiation.

3.3 Structure and Components

The upper two bays are 12 cm in height and each contain a radiation measuring unit. One of the geiger counter container is placed in the shielding material. The unshielding radiation sensor is used to record a baseline radiation profile as a function of altitude during the flight, the other is to ascertain the effectiveness of radiation shielding. The lower bay is 5 cm in height and houses the main payload computer and data logger, as well as some auxiliary sensors. The total dimensions of the payload are 10cm x 10cm x 34.1cm. Outside of the payload are ten sensors mounted into the nose cone to measure rocket rotation speed and profile the nose cone temperature gradient. A pitot tube is used to measure rocket airspeed. The three containers are separated by metal plates which have threaded rods running through them to provide structural support to the entire encasement. The payload is housed in the nose cone so as to, not only mitigate effect of the payload on the rocket but also of the rocket on the radiation sensing abilities of the payload.



Figure 6. Render of the payload contained within the Atlantis II rocket

D. Avionics Subsystems

4.1 Flight Board and Sensors (Barometer, Altimeter, IMU, GPS)

The Flight Board acts as the central system for controlling the rocket and is has been custom designed and in-house fabricated for this purpose. At the heart of the board is a STM32F4 micro-controller unit (MCU). The reasons the chip was selected are due to its low power usage compared to full OS alternatives like a Raspberry Pi, its high reliability (it has regular commercial use), and past experience as some members have successfully used it in a similar projects.

The board is connected to launch systems via an external umbilical cord which supplies two ground lines, 12V DC power, two communication channels, and a select line (active high to determine if the rocket is connected to launch systems). From this connection, the power is immediately routed to a connection to the battery board which charges the onboard LiPo battery. The battery then provides 7.4V power back to the board to power the board, GPS, radio, and pressure sensors. This centralized architecture of each component only connecting to the flight board, combined with the Molex plugs which only fit one way, simplifies the wiring on the rocket.

Directly mounted to the flight board are the barometer and the inertial motion unit (IMU) (which consists of a magnetometer, accelerometer, and gyroscope). The data from these two sensors are fed to the Kalman filter to detect apogee (see section below).

Connected to the rocket, but not on the flight board, are the GPS, two pressure sensors, and a 900 MHz long range (1 watt) radio. The pressure sensors are connected to the oxidizer tank and the combustion chamber to aid in monitoring pressures and determine what venting action is necessary. The GPS is used to determine the rocket's location, primarily to track its location upon descent and landing, and is transmitted via the onboard (transmission only) radio to a (receiving only) radio on ground station. All data generated by the collection of sensors is logged and saved to an onboard SD card for later analysis.

A diagram of all of the rocket's electrical components is available in Appendix VII.

4.2 Software Systems

The software controlling the recovery system is created with safety as the foremost priority, and uses the wide array of sensors supported by the avionics. This includes, in particular, the barometer and accelerometer as the primary tools to determine apogee and perform safety checks. There are several different levels of readiness in place to ensure that the parachutes will not deploy prematurely. All software is version controlled via Git and stored on GitHub with limited write access. All changes are subjected to a review and quality assurance (QA) process and

must pass continuous integration, an automated quality checks. The software is all linted using Astyle to promote code clarity and standards.

The software is run on the main Flight Board and is built on the FreeRTOS framework, which provides a large wealth of well-tested libraries and allows safe execution of multiple threads to ensure important processes do not interfere with unimportant processes. For example, if the logging process is malfunctioning, the process to monitor for apogee will be unaffected. In the software, all variables are either allocated on the stack or in static memory. Some data is allocated in the heap before the main loop starts and is all deallocated after the main loop. This ensures there is no memory leaks which could cause a crash after a long time. Infinite loops (other than the main loop) are prohibited, every loop must have a clear termination condition.

The software in the rocket has 6 stages: PRELAUNCH, BURN, COAST, DROGUE_DESCENT, MAIN_DESCENT, and ABORT. At any point in time, if the system receives an ABORT command via UART or the rocket is found to be in an unsafe state, the software enters the ABORT stage. All other control threads are killed, the injection is closed, parachute deployment is disabled, and the vent valve is attempted to be opened to release oxidizer and prevent any further action from the rocket. The system must be power cycled in order to leave the ABORT stage. Unsafe states include the rocket not being vertical in the BURN stages and the oxidizer tank pressure reaching super critical levels.

In the PRELAUNCH phase, the injection valve is closed, parachute deployment is disabled, the venting process is enabled, and the rocket listens for a launch command via UART from the launch system. The injection valve is closed to prevent premature combustion on the launch rail. The parachute deployment is disabled to prevent premature parachute ejection from the launch rail. The venting process monitors the pressure in the oxidizer tank and opens the vent valve if the pressure/temperature in the tank are above safe levels, this is important because at this point in time the off-board launch system will be filling the tank with oxidizer during prelaunch. The rocket will also be listening for a launch command to enter the next phase, the BURN phase.

In the BURN stage, the injection valve is opened and combustion begins, this is the only stage where the injection valve is open. Parachute deployment is still disabled to prevent deployment during combustion. At this point in time the software also watches if the rocket is no longer vertical, if the rocket is no longer vertical, the ABORT stage is entered. This is to prevent a missile-like scenario, where the rocket is combusting while it is aimed horizontally. After a pre-calculated amount of time, 13 seconds, the rocket enters the COAST stage.

In the COAST stage, the injection valve is closed and the rocket prepares for apogee. The injection valve will remain closed for the remainder of the flight. Parachute deployment is now enabled and the system uses a sophisticated and well-tested Kalman filter with acceleration and pressure data to detect apogee. When apogee is detected, the drogue parachute is deployed and the system enters the DROGUE_DESCENT stage.

In the DROGUE_DESCENT stage, the system uses the Kalman filter, like in the COAST stage, to detect when an altitude of 1500ft is reached. When that altitude is reached, the main parachute is deployed and the system enters the MAIN_DESCENT phase.

In the MAIN_DESCENT phase, the system is mostly idle as this is the terminal stage. The system's main task will be to reliably send GPS coordinates back to mission control to facilitate recovery.

During all stages, the system is reading acceleration, gyroscope, magnetism, barometer, GPS, oxidizer tank pressure, and combustion tank pressure data. It is also monitoring for emergency shut off (entering the ABORT stage), logging data to an SD card, and transmitting data via UART to the radio.

4.3 Battery Boards & Battery

The battery used to control the rocket's avionics system is a 7.4V two-cell lithium polymer and board has been designed for a battery of this specification. The primary component of the battery board is an off the shelf battery charging chip (an MCP73213 OVP Dual-Cell Li-Ion Battery Charger) which protects the battery during charging and discharging. Some of its features include overvoltage protection, automatic charge termination, and thermal regulation. The board also has switch terminals for the power and battery input, and a molex connector so it can be connected to the main flight board. A schematic of the board can be found in APPENDIX VII

4.4 Kalman Filter

The on-board Kalman filter is tuned to the specific conditions of the launch. We expect to go supersonic, and so we have correspondingly decreased the dependence of the algorithm on the barometer to avoid transient behaviour introduced when travelling at transonic speeds. The accelerometer then becomes the primary source to minimize our error when comparing to our real-world state. An added benefit of the Kalman filter is that it also allows us to filter

out white noise to an extent, all while maintaining near real-time responses.

As mentioned above, the Kalman filter is used to detect apogee during the COAST stage. By looking for zero velocity within a tolerance, we have tuned the algorithm to send the signal to release the parachute slightly before apogee, even with the modest delay compared to real-world altitude by 0.1 seconds. This allows the parachute to unfurl at exactly the right moment to reduce stress on the airframe and parachute itself.

The Kalman filter also allows us to trivially deploy the main parachute on time, during the DROGUE_DESCENT stage, by looking for any altitude lower than our deployment altitude. This does not face nearly as many challenges as detecting apogee, since there is a large window where the parachute can be deployed safely without inducing too much drift.

E. Propulsion Subsystems



Figure 7. Oxidizer Tank and Propulsion System

5.1 Oxidizer Tank

A large tank is required to contain the nitrous oxide propellant. It is stored in a two-phase gas-liquid mixture. No turbo pump is required in the feed system as nitrous oxide is self-pressurizing due to its high vapor pressure. The maximum expected operating pressure is 1000 psi and this is controlled by a pressure safety valve mounted on top of the vessel which is set to 1000 psi. The design temperature of the Nitrous oxide is 25°C, chosen to match known test conditions and to be distanced from the critical temperature of 36.4°C. In order to regulate the temperature in a hot environment, nitrous oxide will be vented from the flight tank before it reaches the critical temperature, experiencing cooling by expansion. The N₂O mother bottle will be stored at a temperature below its critical temperature in an insulated shack with a cooling system.

5.1.1 Analysis and Design

The flight tank is a SRAD composite overwrapped pressure vessel (COPV). The vessel is an external tank and a structural member of the airframe. The vessel consists of an aluminum liner, isotensoid end caps with polar ports on either end. The vessel is comprised of 2 helical and 4 hoop layers. simulations were completed in ANSYS with ACP. The fiber buildup and angle was formulated based off of literature values and imported into an ANSYS simulation. A MATLAB script was used to generate the data for a look-up table (fiber orientation, volume, and fiber-epoxy ratio). The vessel was designed for a burst pressure of 3000 psi or 3x the maximum expected operating pressure (MEOP) of 1000 psi. Additional analysis details are presented in Appendix VI. The composite and filament properties were acquired from our local branch of Luxfer gas cylinders who agreed to help us construct it.

The $\frac{1}{8}$ " 6061-T6 COPV liner was welded with 4943 filler rod and heat treated back to a T6 temper before being filament wound. Since the epoxy resin used in our COPV cures at 250°F and the fact that carbon has a much lower coefficient of thermal expansion than aluminum, the liner shrinks away from the overwrap at room temperature (delamination), but contacts at a pressure under MEOP. The common industry solution to delamination is to autofrettage (yield) the liner back into the overwrap such that the liner is in residual compressive stress at zero pressure. Our ANSYS simulations show autofrettage does not occur at our proof load. A maximum principal stress failure does not occur at 3x MEOP with our liner and overwrap design.

Simulation results are available in Appendix VI

The drawings for the oxidizer tank are available in Appendix VII : COPV, COPV01, COPV02

5.2 Injector and Feed System

The feed and injection system contains all the necessary components to transport the oxidizer from the oxidizer tank into the combustion chamber. Along this system, the oxidizer is restricted to an appropriate flow rate and is atomized during injection into the combustion chamber to help facilitate combustion.

One of the difficulties encountered during the project was the selection of an appropriate valve system to control the oxidizer flow rate to the combustion chamber. One of the attractive features of hybrid rockets is the relative simplicity of implementing throttle control during operation of the motor, however in this project this avenue was

not explored. The difficulty in our system arose from the necessity of supplying high mass flow of 1.6 kg/s while maintaining a lightweight and flightworthy design that could fit into a 7" body tube. There are two main valve considerations that could fulfil these requirements.



Our first option we considered was the design of the previous vehicle, Atlantis I, injection system. The design split the flow into three lines which would connect to three solenoid valves. Each solenoid would have the capability of roughly 0.5 kg/s during a burn, based off of previous tests of the Atlantis I engine. Splitting and recombining the flow into three lines adds additional losses and more leak points and complexity.

A single compact lightweight valve-actuator assembly was sourced from Assured Automation. This valve consists of: a ball valve, an actuator, a solenoid valve and a working gas. In our case the working gas is a CO₂ canister regulated to 100 psi.

The drawings for the final injector assembly are presented in APPENDIX VI as INJE01

Figure 8. Assembled injector assembly with valves attached - full and cross-sectioned view

The challenges associated with predicting the nitrous oxide mass flow rate arise primarily from the fact that the liquid nitrous oxide is in a saturated state when it leaves the oxidizer tank. This means that the liquid exists in an equilibrium with its vapor phase and will begin to boil if the pressure in the liquid drops. As a result the entire process must be treated as a two phase flow problem, and the estimation of mass flow rates through valve and orifices must be treated as a two state flow.

The Injection system was assumed to have negligible losses until the injector plate which consists of 30 to 50 1.5 mm diameter holes. The 1.5 mm holes were chosen as they have been known to sufficiently atomize the flow [18]. The flow was modeled through the following set of equations. State 1 is before the injector plate and state 2 is after. The flow was assumed to be isenthalpic through the plate. The physical meaning of G is mass flow per unit area.

$$G = \frac{\kappa G_{SPI} + G_{HEM}}{1 + \kappa}$$

$$G_{SPI} = C_d \sqrt{2\rho_1(P_1 - P_2)}$$

$$G_{HEM} = C_d \rho_2 \sqrt{2(h_1 - h_2)}$$

$$\kappa = \sqrt{\frac{P_1 - P_2}{P_{1,sat} - P_2}}$$

Since the discharge coefficient is an empirical value ranging from 0.3 to 0.9 [18] the injector plate will be tuned to the design mass flow of 1.6 kg/s after successive tests. The plate has the capacity for 55 holes that our countersunk. The number of holes through drilled is not known during the writing of this document. An efficient method of placing the holes equidistant is hexagonal packing. The injector plate was mounted to an injection assemble that was radially bolted to the chamber and sealed with circumferential o-rings.

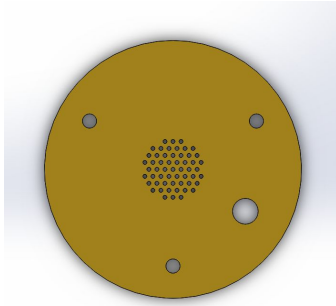


Figure 9. Injection plate showing the number and placement of 1.5mm hole

5.3 Combustion Chamber

The combustion chamber contains two major subassemblies, the combustion casing and the fuel cartridge. The arrangement of the assembly can be seen in the adjacent. As an assembly, this section of the rocket motor is the location in which the reaction between the fuel and the oxidizer takes place. The purpose of this section is to contain and direct the flows created by this process. The combustion reaction produces high temperatures and pressures that are typically controlled by flow properties upstream and downstream of the combustion chamber.

The chamber consists of a 6" OD x 0.125" wall x 23.5" 6061-T6 structural aluminum tube with 12 radial clearance holes for cap screws to retain the injector plate and nozzle housings. Inside the chamber is the fuel cartridge consisting of a 5" nominal PVC pipe wrapped in a sheet of LDPE that is epoxied to the PVC pipe. Inside the pipe there are two layers of 1/16" EPDM insulation. The fuel length is 14" with a 2" pre and a 3.5" post combustion chamber. The chamber's MEOP (maximum expected operating pressure) is 350 psi.

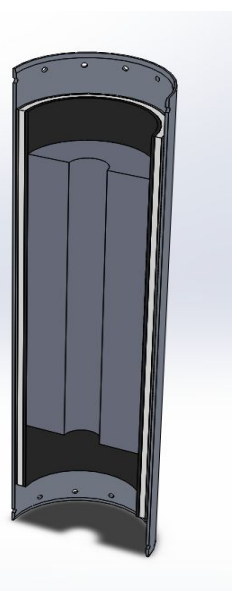


Figure 10. Cross Section of Combustion Chamber Showing Insulation and Fuel Grain
The radial and axial plane stress state of the cylinder is resolved into the following expression from thin walled pressure vessel theory . [31]:

$$\sigma = \frac{Pr}{t}$$

Using the yield stress as the maximum allowable stress, and the vessel thickness and radius, a safety factor of 4.0 is achieved with regard to the pressure.

The strength of the radial bolts and vessel bearing capacity was considered. An internal pressure of 2 x MEOP was used to design the bolt holes, number, and spacing. The resolved force of the 2x MEOP on the projected area requires each end connection to withstand 18494 lbs of force. This force was resolved into twelve, #12-24, equally spaced bolts, a more manageable requirement of 1541 lbf bearing capacity was required for each bolt. The bolts have a shear capacity of 2126 lbf [30]. The aluminum wall bearing stress was calculated using the formula:

$$\sigma = \frac{F}{dt}$$

The ultimate bearing strength of aluminum for 2.0 x diameters away was used as the maximum allowable stress. For a #12 bolt clearance the safety factor is 2.47. A hydro-test was performed at a proof load of 525 psi or 1.5x the MEOP on the combustion chamber for a time of 10 minutes. No ruptures or leaks were observed.



Figure 10. Combustion chamber assembly Hydro-test



Figure 11. Fuel cartridge with wax and insulation

The flame temperature inside the chamber is controlled by the properties of the paraffin wax fuel as well as the oxidizer to fuel ratio (O/F). The amount of fuel within this ratio follows a predictably increasing path with regression of the fuel grain and isn't controllable during burn. This makes the O/F ratio at any point during the burn strongly dependent on the mass flow rate of oxidizer flowing into the chamber from the injector assembly. The rate of oxidizer flow entering is controllable through valves and can be increased or decreased as seen fit. In general, a higher O/F ratio creates a more complete combustion reaction, producing more energy and higher temperatures.

The internal pressure of the chamber is also dependent on other parts of the assembly, most importantly the injector and nozzle assemblies. The mass of fuel added to the flow by the time it exits the chamber is small when compared to the pre-existing oxidizer mass. As given by our simulations, about 87% of the exiting mass leaving our chamber can be attributed to the oxidizer mass flowing in, indicating the mass flow rate through the injectors one of the biggest factor in the internal pressure within the chamber. However, the conditions at the exit need to be considered as well. The nozzle shape and size determine the mass flow rate leaving the system and the pressure at the entrance of the nozzle and exit of the combustion chamber. The nozzle throat diameter is the primary dimension determining the mass flow leaving the system and is most responsible for the internal pressure.

The combustion casing is the structure of the assembly, taking the stresses induced by the internal pressure. The casing is 6061-T6 aluminum tube with radial bolts on either end to attach the nozzle and injector assemblies. The design of the casing had to conform to a set of thermal and structural constraints defined by the chosen oxidizer to fuel ratio and the flow within it. With the inputs of the weight of our rocket, desired altitude and chamber pressure, our simulation gave a burn time of 13 seconds to reach our altitude goal. From established literature, it was found that the adiabatic flame temperature for our chosen O/F ratio was approximately 3000K. The burn length has a large impact on thermal protection requirements as the melting point of 6061-T6 aluminum is 855K. Therefore, if the chamber were exposed to the flame for more than a few seconds it would begin to melt. To prevent failure of the material from the internal pressure, the temperature of the walls must be kept as near the ambient outer temperature as possible. Thermal protection of the chamber walls is therefore necessary.

We decided to use EPDM sheet rubber as an ablative insulator due to its high temperature resistance and its low thermal conductivity. This decision was made based on the commonality of its use in other amateur rockets. The real ablation rate within the environment can only be found through a burn test.

5.4 Fuel Grain

A modular fuel cartridge design was desired in order to allow relative quick fuel grain installations between burns. The primary challenge was sourcing a suitable cartridge that would closely match the desired combustion chamber internal diameter. This proved to be difficult due to the relatively unusual internal diameter of 5.75".

Following manufacturing of the cartridge, the paraffin wax was melted and spin cast into it to form the fuel grain. The casing provided the molding surface for the outer diameter of the grain and an aluminum tube with centering plugs provided the internal geometry of the fuel port. The fuel is a mid-molecular weight paraffin wax selected based on its bonding strength when pour cast. The only additional component added to the wax before casting is 10% tar, which is intended to help stabilize the liquid layer which forms on top the wax during combustion. The EPDM insulation is bonded to the PVC pipe and after a 24-hour hardening period, the full assembled fuel grain is ready to be installed in the combustion chamber.

5.5 Ignition System

The ignition system consists of rocket candy pyrotechnic charge that is lit by a nichrome wire. This ignites a sparkler and a magnesium strip, when 12 volts DC are supplied. An ignition test was performed on April 21 2018.

5.6 Nozzle

The nozzle consists of three components; an aluminum nozzle shell, silicone insulation, and a graphite nozzle insert. This is depicted in the nozzle figure shown in Appendix VII. This three-part design is in order to have an interface between the combustion chamber and the nozzle, thermal insulation between the nozzle and the aluminum shell, as well as have an easily replaceable nozzle in case of design changes or worn out components. The nozzle shell attaches to the combustion chamber via a radial bolt mounting system (utilizing 12 bolts), and a 2 o-ring silicone seal between the combustion chamber and nozzle shell.

The geometry of the graphite insert is a conical converging diverging nozzle (fifteen degree diverging section), chosen for it's proven performance and ease of manufacturing. The conical convergent-divergent nozzle provides optimal geometry to allow for flow expansion, increasing the total impulse achieved. Although a bell-shaped nozzle would provide better performance, the benefits were not enough to outweigh the additional complexity in manufacturing, especially considering the geometry of the curve and the difficulty in finding a shop willing to CNC graphite. As a means of designing the nozzle geometry, we needed to know the combustion of the gases flowing through the nozzle. This is done by completing a stoichiometric balance equation which includes the reactants nitrous oxide and paraffin wax, and products nitrogen, water vapour and carbon dioxide. This is shown in the equation below:



For the stoichiometric equation we assumed n to be 28, using a value from University of Duluth, Ryan Erickson. Using this information, the ideal gas law, and NASA's CEA program, the mass fractions, heat capacities, and gas constants were calculated. The gas properties, as well as the initial conditions seen at Spaceport America from the previous year (ex. atmospheric pressure to ensure overexpanded flow for the majority of flight) provided the necessary information for calculating the throat area, exit area, and the conical contour. Using isentropic flow equations:

$$A_t = \frac{A_t M_t}{M_e} \sqrt{\left(\frac{1+\frac{k-1}{2}M_t^2}{1+\frac{k-1}{2}M_1^2}\right)^{\frac{k+1}{k-1}}} \quad A_e = \frac{A_t M_t}{M_e} \sqrt{\left(\frac{1+\frac{k-1}{2}M_e^2}{1+\frac{k-1}{2}M_t^2}\right)^{\frac{k+1}{k-1}}}$$

The summary of these calculations gives the following values: throat diameter, $D_t = 1.57$ inches, exit diameter, $D_e = 3.37$ inches, divergent length measured from throat to exit, $LD = 3.29$ inches, and area ratio $= A_e/A_t = 4.61$

After the preliminary design was established and the python coding (used for simulating flow) was completed, the nozzle was manufactured and experiments were conducted with the rest of the motor to determine the accuracy of the models created. The experiments included measurements of thrust, mass flow rate, and pressures inside the combustion chamber. From here the experimental data was used to determine the nozzle efficiency. The equations used from Sutton and Ref [18] are for adiabatic and isentropic flow and do not incorporate all the losses that occur through actual hybrid rockets. A refinement of the nozzle design can take place to get the appropriate geometry.

The nozzle insert was chosen to be made from fine-grain isomolded graphite rod procured from the GraphiteStore because of its high temperature resistance (maximum service temperature of 2850-2960 K, melting temperature of 3800-3950K), its availability, and relatively cheap price compared to alternatives. As stated, the combustion of nitrous oxide and paraffin wax creates temperatures in the nozzle of approximately 2000-3000 K.

Graphite is a common material used for nozzles because of the high temperatures experience in the nozzle, and with a short burn time of 10s, the graphite inserts should have survived several test fires. If wear becomes an issue, the graphite insert is easily replaceable as discussed above. It is noted that the graphite nozzle will erode at the throat due to the high temperatures and flow speeds, however from literature this effect has been small when dealing with low run times (less than 13 seconds)[9].

The nozzle shell will be made of aluminum 6061-T6. Aluminum does have a low temperature resistance (6061-T6: melting temperature of 855-925K) but the nozzle shell will be completely insulated using a 1/8" layer of silicone around the graphite nozzle insert. Aluminum was chosen over steel as the nozzle shell because of its low density, while still having the appropriate strength properties needed to withstand the forces encountered from the rocket airframe and combustion chamber attachments.

F. Preparation and Launch Subsystem

6.1 Rocket and Launch Pad Setup

In order to more easily facilitate the setup and lift of the rocket in to launch position, the launch tower is equipped with a lever and electric winch. The rocket may be inserted on to the launch rail while the tower is in a horizontal position, and connect the fill line and umbilical wire. All preflight tests can be made prior to lifting the tower to a vertical position.

The Ground Control and Circuits will be stored in a weatherproofed housing nearby the launch tower. In addition, a generator, air compressor, and shack for the nitrous fill bottle will be set up in appropriate spots nearby the tower. Ideally these will be placed behind tower, but all lines are long enough to allow flexibility in placement.

As required by regulation, the ignition circuit has a mechanical switch which must be turned in order to activate the system. For further security, a mechanical key switch has been used, with the key given to the launch coordinator so that the system can be activated only after setup is complete. (Note: nitrous fill and arming and firing are conducted remotely as per regulation).

6.2 Ground Control and Monitoring

For safety reasons, no personal are allowed within the vicinity of the rocket during filling and launch. In order to facilitate the filling, monitoring and ignition phases of the mission an automated ground stations has been designed and constructed.

The Ground Stations consists of a laptop computer and Arduino acting as controllers for the various systems. The laptop is connected by a wireless point to point ethernet connection (P2P), allowing direct intervention from the team in the command center if necessary. The Ground Station acts as a web server, allowing simple access with any laptop or computer connected on the other end of the P2P link.

The Ground Station commands the Arduino via the USB serial. The Arduino then forwards the packets onto Avionics via UART, or toggles the GPIO pins connected to the various relays as required. Additionally, the Arduino receives and forwards UART packets to the Ground Station via USB, providing 2 way communication between the laptop and rocket. During liftoff, the audiojack type connectors will naturally pull free from the ascending rocket, disconnecting the rocket and ground stations.

A schematic of the ground system's electronics is available in Appendix VII.

Around the launch base we intend to place 3 cameras in order to monitor the various connections to the rocket:

1. Nitrous Fill
2. Electrical Umbilical
3. Ignition

These cameras will be connected to the laptop Ground Station, and their streams will be made available to the web server.

6.3 Nitrous Fill System

In order to avoid the dangers of transporting a filled rocket, the nitrous fill system is automated. The system consists of a fill and vent valve, connected to the Ground Station, which is designed to control the filling process while being monitored remotely from the command center.

The N₂O contained in the oxidizer tank exists as a saturated two-phase liquid-vapour mixture at the temperature and pressure required for launch. As a result when the rocket is positioned vertically on the launch rail, the higher

density liquid phase pools at the bottom and the lower density vapour phase rises to the top. It is then possible to release the vapour phase from the top of the tank using a solenoid valve. Releasing the vapour from the tank will induce a temperature drop within the saturated mixture. As the vapour phase is released, the liquid phase will flash boil, producing more vapour to regain equilibrium between liquid and vapour phases. The energy required to boil the liquid phase (quantified as the latent heat of vapourization for a specific temperature and pressure) is removed from the liquid and thus causes the temperature to drop within the tank.

Venting into the ignition chamber could be dangerous as it could cause combustion and is therefore avoided. Above the connection point between the oxidizer tank and the upper shell portion of the rocket body, there is a vent valve to release N₂O to atmosphere.

In addition to the cooling effect of the N₂O venting, the mother bottle feeding the rocket will be placed in an air conditioned structure. This will both protect the mother bottle and equipment from debris, as well as ensure the Nitrous being filled into the rocket is colder than the surrounding air. The injection of cooled Nitrous will additionally assist in cooling the main tank aboard the rocket.

The nitrous fill line is ejected using a pneumatic ejector. Using pressure from the nearby compressor, the system is activated by a relay controlled by the ground station, producing a pressure which will eject the fill line.

6.4 Ignition System

The ignition process consists of shorting the power supply unit through an igniter (rocket candy) in order to produce sufficient heat to ignite the wax fuel. Control of this short is provided by two relays in series, which are controlled by the Ground Station via the Arduino's GPIO pins.

The rocket ignition sequence occurs in several steps. By placing the ignition relays in series we have created a two part ignition sequence. The first step, Arming, will be conducted after permission to fire is granted from the competition supervisors. Checks will be performed prior to sending the arming signal, which will activate the first of the two relays. In addition, after this step the N₂O fill line will be ejected. At any time between the arm and fire command, the process of firing can be aborted.

The Arming / Ignition Sequence is shown in Appendix VIII.

III. Mission Concept of Operations Overview

The Mission Concept of Operations Overview (CONOPS) consists of the following phases: ignition, liftoff, ascent, apogee, and ending descent.

A. Filling

The filling phase is defined as the event taking place between the rocket being mounted onto the launch rail and the fill lines being disconnected from the rocket. The filling phase describes the oxidizer pressure vessel being filled with nitrous oxide. Once the pressure vessel is at the appropriate levels to reach 30,000-feet this phase is complete.

B. Temperature Regulation / Venting

After the vessel is filled, the rocket will automatically vent and refill nitrous as required to keep the nitrous in the tank near its design operating temperature of 25°C. Throughout this process the mother bottles are kept cold in a small air conditioned structure.

C. Ignition

The ignition phase of the rocket launch is defined as the event between the initial ignition signal sent from the control box, and the nitrous oxide being introduced and ignited in the combustion chamber. The ignition phase will only commence by a digital switch from our launch base station. The current flowing through the nichrome wire will heat the wire and ignite the flammable paste impeded in the paraffin wax fuel grain. During this time the nitrous valves will open at a specified rate introducing nitrous oxide into the combustion chamber. The nitrous oxide will react with the heat source and paraffin wax causing the combustion reaction. The moment the rocket has a plume and is experiencing thrust, the phase transitions into liftoff.

D. Liftoff

Proceeding the ignition phase is the liftoff phase, where the rocket begins to produce thrust. Liftoff is a short phase occurring for only a few seconds, until the last launch lug leaves the launch rail. During this phase the nitrous

oxide and wax combustion is building up pressure in the chamber (300 psi) until it produces enough thrust to leave the launch rail. This phase ends once the second launch lug leaves the launch rail.

E. Ascent

The ascent phase describes the phase where the rocket climbs from the launch rail to apogee. During this phase the motor will be burning the nitrous oxide and paraffin wax. The onboard motor control system keeps the injection valve open for a precalculated amount of time, afterwards it will close the valves.

F. Apogee

The apogee event describes when the rocket reaches its peak altitude and subsequently releases the drogue and main parachute. This event is controlled by the onboard avionics located in the payload. The avionics will blow the black powder charge at apogee releasing the drogue parachutes once it receives descent data from the onboard IMU's.

G. Ending Descent

The ending descent is the phase where the main parachute releases from the commercial chute release, and descends the rocket to a safe landing. The main parachute release is programmed to open at an altitude of 1,500-feet above ground level. The parachute will slow the rocket to 18 ft/s to a safe landing. This phase ends once the rocket is grounded.

IV. Conclusion and Lessons Learned

Lessons from last year's design and build cycle (2016-2017) and experience at competition

Atlantis I was SOAR's first large scale rocket, and the first rocket for which the team attempted its own research and development of a very large majority of the systems on the rocket. Although we did design and build our rocket in a very short window of time prior to competition, we were not able to launch last year at IREC 2017. The time-crunched nature of last year's design and build cycle taught us that we need to have a more concrete plan from the start, with detailed task lists, a head start on students designing their parts and systems, and more attentive management of engineering students in charge of design. We addressed the issue of attentive management by a reconfiguration of our team structure. We addressed the issue of planning and getting a head start by having newly appointed team leads do comprehensive research reports over the summer, which allowed us to plan early and start design early.

Lessons from this year's design and build cycle (2017-2018)

Since last year we've performed many static engine tests and are confident in that system. But, since launching and testing rockets in Canada is no simple task due to a strict approval process, we have had only one opportunity to launch this past year, in which we attempted to launch Atlantis I with only one minor issue in the launch sequence preventing ignition. Because of these constrictions our team understands that our designs have not been fully field-validated. Unfortunately, due to the lack of real flight data and design validation we have been unable to learn from the rocket's systems under actual flight conditions. We have, however, been able to learn some important details from engine testing, such as an optimized launch procedure and engine firing characteristics. Additionally, we have learned the optimal way to set up the launch rail and related systems, and an improved process of organization and documentation within our engineering team. For example, we learned that in order to improve our workflow throughout the year, we need to get teams to start their designs earlier, as starting construction on some key rocket systems far in advance this year was advantageous from a time and scheduling perspective, and also from a financial perspective. Learning from this, the team is already starting to recruit new students this spring in hopes of encouraging these students to learn important engineering concepts and teamwork throughout the summer months, in order to create timely designs in the fall. This is in contrast to the standard University of Calgary method of recruiting new members in October during "clubs week", as is fairly standard at our school. We also have plans to start generating funding further in advance next time, to better assist in building our rocket's parts and systems.

This year, the SOAR team made enormous progress and learned countless new ways of doing things. We will continue to take note of every single detail we can improve on and give thought to how we can do better. We hope to have a culture of continuous improvement and come back every year more competent, organized, safe, and competitive.

APPENDIX I: System Weights, Measures, and Performance Data

Attached is the third and final progress report submitted for the Atlantis II project for the 2018 IREC at Spaceport America, New Mexico.



Spaceport America Cup

Intercollegiate Rocket Engineering Competition

Entry Form & Progress Update



Color Key

SRAD = Student Researched and Designed

v18.1

Must be completed accurately at all time. These fields mostly pertain to team identifying information and the highest-level technical information.

Should always be completed "to the team's best knowledge", but is expected to vary with increasing accuracy / fidelity throughout the project.

May not be known until later in the project but should be completed ASAP, and must be completed accurately in the final progress report.

Date Submitted:

Country:

Team ID: * You will receive your Team ID after you submit your 1st project entry form.

State or Province:

State or Province is for US and Canada

Team Information

Rocket/Project Name:

Student Organization Name:

College or University Name:

Preferred Informal Name:

Organization Type:

Project Start Date:

Projects are not limited on how many years they take

Category:

Member	Name	Email	Phone
Student Lead	Jeff Martens	jeff.L.martens@gmail.com	403-978-8454
Alt. Student Lead			
Faculty Advisor	Dr. Craig Johansen	johansen@ucalgary.ca	403-220-7421
Alt. Faculty Adviser	Dan Forre	dforre@ucalgary.ca	403-220-8594

For Mailing Awards:

Payable To:	Jeff Martens
Address Line 1:	6 Varbrook Place NW, Calgary, AB, T3A-0A2, Canada

Address Line 1:	6 Varbrook Place NW, Calgary, AB, T3A-0A2, Canada
Address Line 2:	
Address Line 3:	
Address Line 4:	
Address Line 5:	

Demographic Data

This is all members working with your project including those not attending the event.
This will help ESRA and Spaceport America promote the event and get more sponsorships and grants to help the teams and improve the event.

Number of team members

High School	0
Undergrad	48
Masters	4
PhD	0

Male	44
Female	8
Veterans	0
NAR or Tripoli	0

Just a reminder the you are not required to have a NAR, Tripoli member on your team. If your country has an equivalent organization to NAR or Tripoli, you can count them in the NAR or Tripoli box. CAR from Canada is an example.

STEM Outreach Events

If you perform any STEM related outreach events, please place a brief description here.

STEM stands for Science, Technology, Engineering, and Mathematics.

Rocket Information

Overall rocket parameters:

	Measurement	Additional Comments (Optional)
Airframe Length (inches):	196	
Airframe Diameter (inches):	7.13	
Fin-span (inches):	11.88	
Vehicle weight (pounds):	74.51	
Propellant weight (pounds):	56.4	
Payload weight (pounds):	9	
Liftoff weight (pounds):	140	
Number of stages:	1	
Strap-on Booster Cluster:	No	
Propulsion Type:	Hybrid	
Propulsion Manufacturer:	Student-built	
Kinetic Energy Dart:	No	

Propulsion Systems: (Stage: Manufacturer, Motor, Letter Class, Total Impulse)

1st Stage: SRAD Hybrid, 3.6kg (7.9lbs) of paraffin wax fuel and 22kg(48.5lbs) of nitrous oxide, O Class, 40,000 Ns.

Page 2

Total Impulse of all Motors: 40,000 (Ns)

Predicted Flight Data and Analysis

The following stats should be calculated using rocket trajectory software or by hand.

Pro Tip: Reference the Barrowman Equations, know what they are, and know how to use them.

	Measurement	Additional Comments (Optional)
Launch Rail:	Team-Provided	
Rail Length (feet):	44.396	
Liftoff Thrust-Weight Ratio:	5.79	
Launch Rail Departure Velocity (feet/second):	118	(See "Other pertinent information")
Minimum Static Margin During Boost:	3.9	
Maximum Acceleration (G):	6	
Maximum Velocity (feet/second):	1745	
Target Apogee (feet AGL):	30K	
Predicted Apogee (feet AGL):	30180	

Payload Information

Predicted Apogee (feet AGL): 50180

Payload Information

Payload Description:

Our payload will contain a radiation sensor. The designs are not yet fully worked out. Our payload will not be ejecting from the rocket. It will reside on a mount which is attached to the inside of our nosecone. The nosecone itself, though, will eject with the parachute ejection event. Our payload will have the aforementioned radiation detection experiment and therefore may be considered "functional", but obviously will not serve in function critical to the rocket's operation. It will weigh the target 4kg and will be dimensioned according to CubeSat standards with dimensions of (10cmX10cmX30cm).

Page 3

Recovery Information

Page 3

Entire rocket will be recovered as a single component. The Recovery scheme of the system will be a drogue and main parachute combination. The nose cone will be connected to the drogue parachute which will be connected to the main parachute. The main parachute will then be connected to the rest of the rocket body including the combustion chamber. The drogue parachute will deploy at apogee and the main parachute will deploy at 1500ft. Ideally apogee should occur at 30000ft above the takeoff altitude. The drogue parachute deployment will be triggered by a coupled barometer and accelerometer system when apogee is reached to resolve accelerometer error accumulation and pressure spikes saturating the barometer at supersonic velocity. The algorithm used to detect apogee accurately will be a Kalman filter. The combined system provides redundant and accurate deployment. When apogee is detected, a signal will be sent to two parachute expulsion triggers. Both triggers will be set off simultaneously and will lead to two commercially available CO₂ ejection systems. Both CO₂ system will need to be set off in order to eject the nose cone. A redundant COTS flight computer, in this case an eggtimer quantum, will send a delayed signal to the dual CO₂ systems in case the student designed signal does not trigger the CO₂ system. This COTS flight computer will act as a backup to the student designed version. For detection of 1500ft altitude for main parachute deployment, a barometer is sufficient. At this point, the main parachute will be released from its parachute bag and will inflate to bring the entire rocket down safely.

Page 4

Any other pertinent information:

(1) OXIDIZER TANK: Most noteworthy of changes to our rocket from last year's SRAD hybrid rocket engine is the development of a COPV (composite over-wrapped pressure vessel) which will be 6061 Aluminum tube (0.125" wall thickness) filament wound with carbon fiber, which will contain our nitrous oxide oxidizer. --- (2) COMBUSTION CHAMBER and INJECTION: We will be essentially resuing last year's aluminum combustion chamber design, which will be a ~6" diameter 6061-T6 aluminum tube (0.125" wall thickness) which will be ~23.5" long. The changes we plan to make to the combustion chamber this year are a removal of the flange-attachment method of affixing the nozzle and the injection system to the combustion chamber, and to go with a radial bolting configuration. Our plan is to have a similar injection system but one where we can manufacture various plates with different spray configurations to be able to swap them. Our injection feeding system will have a pneumatic valve (CO₂ cartridge-powered) which controls flow of nitrous oxide to the engine. Our launch initiation sequence will control this valve and the generation of a spark to flame our ignitor. --- (3) OXIDIZER ACTIVE COOLING SYSTEM: We plan to also employ an active cooling system, which will be present and potentially integrated with our launch rail assembly, and which will provide climate control for the oxidizer tank to remain at a desired temperature, and which will disengage safely before launch. --- (4) LAUNCH PAD AND SYSTEM: Our launch pad base is a steel square-bar frame with a winch-articulated base where we mount our tower (a radio tower with a height mentioned earlier in this document). Our tower has t-slot rail bolted to it which the rocket's launch lugs slide through. We plan to have wireless control over our launch systems via a secure method which is being developed. This wireless point-to-point system will be configured to take commands from a control station computer but with a physical button to start the actual launch sequence. --- (5) TESTING: Note - Mk.2 is this year's engine, Mk.1 is last year's engine. The engine from last year was developed by a 4th year engineering capstone group on our team. This engine has become their graduate research project and so they conduct testing at our fully-equipped engine test stand. They

with a winch-articulated base where we mount our tower (a radio tower with a height mentioned earlier in this document). Our tower has t-slot rail bolted to it which the rocket's launch lugs slide through. We plan to have wireless control over our launch systems via a secure method which is being developed. This wireless point-to-point system will be configured to take commands from a control station computer but with a physical button to start the actual launch sequence. --- (5) TESTING: Note - Mk.2 is this year's engine, Mk.1 is last year's engine. The engine from last year was developed by a 4th year engineering capstone group on our team. This engine has become their graduate research project and so they conduct testing at our fully-equipped engine test stand. They are working on smoothing out our engine's wax regression rate at the moment and perform test burns every couple of weeks. Since our new engine will be, in every way that matters most, the same as our engine from last year, we consider these tests to be validating tests of our engine's design and configuration. We will, however, be conducting further tests on the new flight combustion chamber once it is manufactured, as mentioned in the testing section. Note - our engine test stand has our engine in a "flight configuration" in that everything is connected as it would be in flight, but our test stand securely holds our engine and oxidizer tank in place with our combustion chamber horizontal and our oxidizer tank angled upwards. --- (6) Launch stability off the rail: Experimental testing to determine actual thrust curve is expected to improve our fairly conservative takeoff speed estimates to be above 100ft/s. Failing that, CFD analysis using openFoam of the rocket to determine the coefficient of restoring moment produced by the fins at the moment of launch rod clearance should prove stability off the rail -

- I hope I've managed to include any information which was missing from our last progress update!

End of File

APPENDIX II: Project Test Reports

Unfortunately during the time of this writing, the parachute deployment test has not yet been completed. Also, although many engine static tests have been done with last year's engine, this year's combustion chamber is slightly different and so we will need to perform static test firings with this new engine to validate it. As of yet, we have not completed any test firings using the new engine. These tests will be completed before competition, and are scheduled to occur beginning June 1, 2018.

Hydro-static Test Report - Pressure Vessel

For the hydro-static test report of the pressure vessel please see APPENDIX V.

Hydro-static Test Report - Combustion Chamber

For the hydro-static test report of the pressure vessel please see APPENDIX V.

APPENDIX III: Hazard Analysis

The Atlantis II project only contains one hazardous material; nitrous oxide. When handling nitrous oxide, personal protective equipment must be worn including safety glasses, and leather gloves. Transportation of the material shall be limited to only when required, and be done with the minimum number of person(s) to predict bodily harm. When transporting, the nitrous oxide shall be completely enclosed. For additional information please refer to the assembly, preflight checklists to be provided at competition.

APPENDIX IV: Risk Assessment

The following risk assessment matrix was completed showcasing all failure modes and mitigation approaches corresponding to the phases identified in the CONOPS section of the technical report.

Team	Rocket/Project Name	Date		
Team 43 - University of Calgary - SOAR	Atlantis II	23-May-18		
Hazard	Possible Causes	Risk of Mishap and Rationale	Mitigation Approach	Risk of Injury after Mitigation
Rocket body breaks during or after ignition with flying debris causing injury	Coupler tubes fail to hold pressure vessel and carbon fiber tubes together. Shearing of body from screws holding the payload Parachutes deploy before or after apogee at high speed. Carbon Fiber airframe failure from flight loads.	Medium; Student constructed payload and rocket body, with minimal testing of the strength of material and adhesives.	Solidworks and ANSYS simulations performed successfully demonstrate coupler strength for well over predicted aerodynamic loads. Numerous screws throughout payload on multiple planes to distribute stresses, and hold payload in place. Two separate electrical systems to activate parachute close to apogee. Redundant system is a COTS system. Testing will be done. Analysis suggests that the CF body tubes are capable of loads far in excess of our predicted flight loads.	Low
Recovery system deploys on ground causing blast with debris, with chance of injury	Short in wires Malfunction of code Antenna Noise Interference	Medium; student assembly of SRAD system could produce defects, software bug could cause rocket to think it's in the flight phase, and a further bug could cause our code to think it's at apogee	Multimeter test of circuit to ensure correct wiring Charges not to be primed until final assembly of rocket Algorithms will not be prepared to fire charges until a minimum acceleration is reached	Low
Rocket deviates from nominal flight path during ascent, comes in contact with personnel at high speed	Rocket is overstable or understable. Detachment of fin from body tube Nosecone becomes detached during flight Fin flutter causing failure of fins Fins are misaligned Smaller diameter motor isn't centered in larger body tube. Large defect in exterior materials	Medium; Student designed fins and rocket body.	Used design software to predict stability of the rocket. Control system detects variation from flight path and shuts down the motor. Physical testing being performed with known loads to validate design strength. Friction fit, shear pins and wind drag force hold the nosecone in place. Fins are made with two types of materials to prevent fin flutter from natural frequencies. Fins attached using a 3d printed fin jig, inspected, and measured for accuracy. Used centering rings to align motor in the center of the rocket. Materials used are visually inspected before and after assembly.	Low
Recovery system fails to	CO2 charges do not	High; Student built	Dry test performed to confirm	Low

deploy at apogee, rocket or payload comes in contact with personnel	provide enough force to release parachutes.	electronics and limited ground testing available.	forces from charge can eject parachutes.	
	Electronic system fails to register pressure differential		Electronics tested using vacuum chamber.	
	Electronics have a faulty connection unable to send signal to ignite charge		Electronics tested before launch, and two separate electrical systems in place.	
Recovery system partially deploys, rocket or payload comes in contact with personnel	Parachute becomes tangled and does not open fully.	Medium; Student packed parachutes, and charges.	Packing techniques from rocket association members to avoid tangled parachute employed.	Low
	Parachute does not deploy due to packing friction.		Table top test to ensure parachute is able to release from rocket.	
	Shock cord breaks from charge		Kevlar cord is used because of burn resistance, and tensile strength properties.	
Nitrous oxide undergoes a decomposition reaction during filling	Small pressure differential between combustion chamber and pressure vessel	Medium; hot climate, SRAD pressure vessel	Oxidizer vessel operating pressure is 3 times higher than combustion chamber pressure, therefore nitrous will not propagate back to nitrous tank	Low
			Pressure vessel failure will occur at end caps, therefore force is directed upwards rather than outwards.	
			Pressure vessel successfully hydrotested to 1.5x operating pressure (1500 psi), and designed to 2 times.	
			Pressure Vessel will have relieving device in the form of a relief valve or burst disk set to 910 psi.	
			Filling is completed remotely so no member will be near the rocket during or after filling.	
Rocket Ignition occurs before or during filling	Ignition on control box accidentally pressed	Low; Switches contained on outside of control box.	Multiple switches required to power on system, and momentary key switch needed to start ignition.	Low
	Nichrome wire heats up		Last member to leave rocket will have ignition key.	
		Medium; Student design ignitors and circuitry	Ignition system successfully tested. Low activation energy, with only a flame produced. No combustion or explosion would occur.	
Rocket falls at high decent rate	Main chute does not open	Medium; student packed parachutes.	Main chute released by commercial chute release tested in pressure chamber.	Low
	Main chute gets tangled and does not descend rocket at slow enough rate		Main chute packing optimized for low risk entanglement	
	Main chute burns from charge		Main chute surrounded by kevlar bag and kevlar blanket.	

APPENDIX V: Checklists

Assembly, preflight, and launch checklists will be fully detailed and completed in time for the competition, and will be provided at that time. Below are the hydro-static test procedure, oxidizer feed system cleaning procedure, and the static test firing procedure.

Hydro-static Test Procedure

Must be Completed and Documented Prior to Test Related Activities

Motivation: Hydro-static testing is a relatively safe way to check if a pressure vessel can meet its operating pressure requirements without leaking. All pressure vessels must be tested at 1.5 times their maximum expected operating pressure before they can be used for flight or propulsion testing.

Safety Regulations

Personal Protective Equipment

1. Eye protection must be worn by all personnel

Safety Considerations

1. First aid kit must be available and identified at test location
2. Stay out of the Line-of-Fire

Oxidizer Tank Procedure

- 1.01 _x_ Screw o-ring boss caps into the bottom OxTk end cap for drain valve
- 1.02 _x_ Screw o-ring boss caps into the top OxTk end cap, leave one open for filling with water
- 1.03 _x_ Apply oxygen compatible o-ring grease to o-rings
- 1.04 _x_ Screw in the hydro-static pump hose to the bottom end cap
- 1.05 _x_ Begin filling the oxidizer tank with water through the top end cap
- 1.06 _x_ Bleed air out of the hydro-static pump
- 1.07 _x_ Fill the oxidizer tank until it is full and then screw in the last o-ring boss cap on the top end cap
- 1.08 _x_ Check that everyone has safety glasses on
- 1.09 _x_ Record gauge pressure: _0_ psi
- 1.10 _x_ Slowly begin to increase the pressure in the oxidizer tank and check for leaking water
- 1.11 If leaking occurs go to leak procedure
- 1.12 _x_ Increase pressure to 1500 psi and hold for 10 minutes
- 1.13 _x_ Slowly decrease the pressure in the oxidizer tank
- 1.14 _x_ Wait until pressure decreases to original gauge pressure in step 1.09
- 1.15 _x_ Drain the water out of the oxidizer tank
- 1.16 _x_ Disassemble oxidizer tank
- 1.17 _x_ Oxidizer tank requires cleaning, see “Oxidizer Feed System Cleaning Procedure”

Combustion Chamber Procedure

- 2.01 Bolt hydro-test plate to lower combustion chamber section
- 2.02 Torque each bolt to 4 ft-lbs in a star pattern. Check with a torque wrench
- 2.03 Screw in o-ring boss caps
 - 2.03 a Leave one open for the hydro-static pump line
 - 2.03 b Leave one open for filling with water
- 2.04 Begin filling combustion chamber with water
- 2.05 Bleed the air out of the hydro-static pump
- 2.06 Fill combustion chamber tank until full and then screw in last o-ring boss cap
- 2.07 Check that everyone has safety glasses on
- 2.08 Record gauge pressure: 0 psi
- 2.09 Slowly begin to increase the pressure in the combustion chamber and check for leaking water
- 2.10 If leaking occurs go to leak procedure
- 2.11 Increase pressure to 500 psi and hold for 10 minutes
- 2.12 Slowly decrease the pressure in the combustion chamber
- 2.13 Wait until pressure decreases to original gauge pressure in step _____
- 2.14 Drain the water out of the combustion chamber
- 2.15 Disassemble combustion chamber

Leak Procedure

Leaking vessel: Combustion Chamber

 Stop increasing the pressure

Pressure when leak occurred:

 Document where leak occurred

Leak location: Leaking out of the flange welds

 Take pictures of leak location

 Slowly decrease pressure of system

 Wait until pressure decreases to original gauge pressure

 Drain the water out of the system

 Diss-assemble the system

 Report the leak to the Mechanical Team Lead

Reported to: _____

Reported by: _____

Personnel in Attendance

Signature of Hydro-test Lead : _____ **Date:** _____

Oxidizer Feed System Cleaning Procedure

Must be Completed and Documented Prior to Test Related Activities

Motivation:

Nitrous Oxide under high pressures has the potential to decompose into nitrogen and oxygen which rapidly raises the pressure inside the Oxidizer Feed system. This can cause catastrophic failure of the flight vehicle. The presence of hydrocarbons lowers the activation energy required for this dissociation reaction. Therefore it is important to ensure all parts of the Oxidizer Feed system have been properly cleaned.

Safety Regulations

Personal Protective Equipment

1. Eye protection must be worn all personnel
2. New, clean nitrile gloves must be worn for all cleaning processes

Safety Considerations

1. Eye wash station or equivalent must be available for use

Cleaning Checklist

Part/s Cleaned: _____

Date: _____

Cleaned by: _____ Signature: _____

Blue Gold Preparation

Amount of Blue Gold to be made: A _____

Divide A by 20: B _____

_____ Add B concentrated Blue Gold into a container and then dilute with Distilled Water until container reaches original amount A

General Procedure

- ____ Distilled water is available
- ____ Diluted Blue Gold is available
- ____ Workspace is clean of contaminants, debris, dust
- ____ Put on new, clean nitrile gloves

Oxidizer Tank Cleaning Procedure

- ____ Use lint-free towels/wipes and hand clean the end caps and threads

- Fill oxidizer tank a quarter full with blue gold cleaner
- Close off the oxidizer tank
- Let it sit, occasionally turning to a new position
- Agitate the oxidizer tank
- Drain it
- Fill part ways full with distilled water
- Agitate the oxidizer tank
- Drain it
- Fill oxidizer tank a quarter full with blue gold cleaner
- Close off the oxidizer tank
- Let it sit, occasionally turning to a new position
- Agitate the oxidizer tank
- Drain it
- Fill part ways full with distilled water
- Agitate the oxidizer tank
- Drain it
- Fill part ways full with distilled water
- Agitate the oxidizer tank
- Drain it
- Use a vacuum to suck out the remaining water
- Clean the caps with blue gold and rinse with distilled water
- Put caps on all the ports
- Hang "Cleaned for Service" tags on parts

Fitting Cleaning Procedure

- Use lint-free wipes and hand wipe all surfaces that will be exposed to nitrous oxide with Blue Gold cleaner
- Rinse surfaces with distilled water
- Air dry
- Install parts or cap them to prevent contamination
- Hang "Cleaned for Service" tags on parts

Hose Cleaning Procedure

- Use lint-free towels/wipes and hand clean the threads
- Rinse hose with blue gold
- Rinse with distilled water
- Rinse hose with blue gold

- Rinse with distilled water
- Rinse with distilled water
- Clean the caps with blue gold and rinse with distilled water
- Install into a cleaned system or Put caps on all the openings and hang a “Cleaned for Service” tag

SOAR Static Test Firing Procedure

Safety Regulations

Personal Protective Equipment

1. Eye protection must be worn all personnel working around the test apparatus/engine at all times.
2. Hearing protection is mandatory for all personnel within 500 feet of the test stand during engine test firing.
3. All personnel must wear long pants and closed toed shoes.
4. Any personnel working around the pressurized nitrous oxide system must wear a face shield and gloves

Safety Considerations

1. Prior to pre-testing setup there must be a first aid kit, a fire extinguisher (Class B or multi-class including B), and a phone for calling emergency response (land line is preferred). All participants must be aware of the location of these items and knowledgeable in how to use them.
2. A least two people present must be trained in first-aid.
 - a. One will be designated as the primary first-aider and a secondary as backup
3. No one should view the motor during firing via direct line of sight.
4. A physical barrier (wall or barricade) must be between any personnel and the engine during firing.
5. Level of authority for test firing in order of highest to lowest is Faculty Advisor, Safety Director and Propulsion Lead. The firing may not commence without the physical presence of either the Faculty Advisor or Safety Director. Additional oversight may be required and will take precedent over the order above.
6. Written procedures specifically tailored to the test must be created and approved by the Safety Director prior to testing. These procedures must include any amendments to the general rules and procedures and information specific to the test such as test goals, expected results, and additional potential hazards or risks.

Roles During Test Firing Operations

- I. **Faculty Advisor:**
 - a. Must be present for test firing
 - b. Oversees the due diligence and safety of operations
- II. **Safety Director:**
 - a. Will maintain the safety of the operation at all times
 - b. Responsible for ensuring all personnel are in appropriate locations during all stages of the test
 - c. Holds launch keys prior to launch
 - d. Cannot initiate launch
- III. **Propulsion Lead:**
 - a. In command of the test fire unless overruled by the safety director or faculty advisor
 - b. Ensures that all steps of the procedure are completed
 - c. Reviews the test procedure with all participants
 - d. Completes all relevant checklists for the test
 - e. Records all test specific changes
 - f. Initiates launch
- IV. **Range Safety (multiple):**
 - a. In verbal or radio communication with the propulsion lead and safety director
 - b. Prevents bystanders from entering the restricted area
- V. **Ignition and Firing Control:**
 - a. Operates the ignition system and firing valves
 - b. Operates filling and venting system valves
 - c. Terminates main engine power as required
- VI. **Sensor Control:**
 - a. Operates all sensor and data acquisition equipment

- b. Responsible for monitoring supply tank weight during filling
- c. Responsible for checking flight tank oxidizer pressure
- d. Saves all data

VII. **Camera Control:**

- a. Operates cameras or webcams required for the test
- b. Saves camera data

VIII. **All Test Launch Personnel:**

- a. Responsible to act safely
- b. Responsible to carry out work to the best of their ability
- c. Responsible for calling an abort if they feel the test is unsafe

The preceding section has been read and understood by all personnel present:

Signature of Faculty Advisor: _____ **Date:** _____

Signature of Safety Officer: _____ **Date:** _____

Signature of Propulsion Lead: _____ **Date:** _____

Must be Completed Prior to Test Related Activities

Test Description:	Ambient Temperature:	Date:
Advisor/Supervisor:		Initials:
Safety Director:		Initials:
Propulsion Lead:		Initials:
Range Safety:		Initials:
Ignition and Firing Control:		Initials:
Sensor Control:		Initials:
Camera Control:		Initials:
First-Aiders:		Initials:
Other Personnel Present:		Initials:

The preceding section has been completed accurately and reviewed and understood by all personnel present:

Signature of Propulsion Lead: _____ **Date:** _____

Test Procedure Notes

Static Test Firing Checklist

Pre-Test Safety Checks

All personnel working on test fire are equipped with appropriate safety glasses (prescription glasses unacceptable) within test fire zone

All present personnel have hearing protection ready for use during engine firing

New clean gloves available for any work on the nitrous system

First-aid Kit present

Class B or multi-class fire extinguisher present

First-aiders present

Primary: _____

Secondary: _____

Physical barricade present

Phone available for emergency calls

Designated Caller: _____

Section 0.0 Pre-Test Safety Meeting

0.01 Safety Director to hold an initial safety meeting prior to beginning work

0.02 Highlight the locations of the first aid kit, fire extinguishers and muster points

0.03 Assign primary and secondary first aiders

0.04 Assign designated emergency caller

0.05 Verify Safety Director holds the launch keys

0.06 Give an inspirational speech (or sentence)

Section 1.0 Test Stand Check

1.01 Check all accessible bolts are torqued properly with a torque wrench or impact driver

1.02 Draw torque lines on bolts

1.03 Prepare the oxidizer cradle for oxidizer tank by removing the cross ribs

Section 2.0 Permanent Valve Check

2.01 Put on new and clean nitrile gloves before working on this system

2.02 Verify N2 bottle valve, MV1 closed

2.03 Verify N2O bottle valve, MV3 closed

2.04 Verify N2 fill line is disconnected on downstream engine side

- 2.05 ____ Verify N₂O fill line is disconnected on downstream engine side
- 2.06 ____ Open N₂ emergency vent valve MV2 to verify zero energy
- 2.07 ____ Open N₂O emergency vent valve MV4 to verify zero energy
- 2.08 ____ Uncap N₂ fill line on downstream side
- 2.09 ____ Uncap N₂O fill line on downstream side
- 2.10 ____ Verify opening and closing operations for N₂ pneumatic valve PBV1
- 2.11 ____ Verify opening and closing operations for N₂O pneumatic valve PBV2
- 2.12 ____ Close N₂ emergency vent valve MV2
- 2.13 ____ Close N₂O emergency vent valve MV4
- 2.14 ____ Verify N₂ bottle valve, MV1 closed
- 2.15 ____ Verify N₂ pneumatic valve PBV1 closed
- 2.16 ____ Verify N₂O bottle valve, MV3 closed
- 2.17 ____ Verify N₂O pneumatic valve PBV2 closed
- 2.18 ____ Verify N₂O vent valve SOL1 closed

Section 3.0 Motor Assembly Procedure

All motor components should be assembled as per the SOAR R-Ex 17 Hybrid Rocket Engine Assembly Manual Procedure

3.1 Post-Assembly Inspection

- 3.01 ____ Confirm cleaning and assembly tag is in place on the oxidizer tank
- 3.02 ____ Remove cleaning and assembly tag from the oxidizer tank
- 3.03 ____ Confirm cleaning and assembly tag is in place on the combustion chamber
- 3.04 ____ Remove cleaning and assembly tag from the combustion chamber

3.2 Test Stand Installation

- 3.05 ____ Place the oxidizer tank in the oxidizer cradle
- 3.06 ____ Install the restraining ribs on the oxidizer cradle
- 3.07 ____ Install the combustion chamber assembly to the linear motion plate, torque each bolt to 20 ft-lbs
- 3.08 ____ Connect oxidizer feed lines to the combustion chamber and torque each connection to 23 ft-lbs
- 3.09 ____ Connect N₂O supply line to the oxidizer fill valve and torque to 13 ft-lbs

Section 4.0 Engine Assembly Valve Check

- 4.01 ____ Verify opening and closing of oxidizer tank vent valve PBV3
- 4.02 ____ Verify opening and closing of oxidizer feed valve SOL2

- 4.03 ____ Verify opening and closing of oxidizer feed valve SOL3
- 4.04 ____ Verify opening and closing of oxidizer feed valve SOL4
- 4.05 ____ Verify oxidizer tank vent valve PBV3 closed
- 4.06 ____ Verify oxidizer feed vent valve SOL2 closed
- 4.07 ____ Verify oxidizer feed vent valve SOL3 closed
- 4.08 ____ Verify oxidizer feed vent valve SOL4 closed
- 4.09 ____ Connect N2 feed system to engine
- 4.10 ____ Connect N2O feed system to engine

Section 5.0 Sensor Check and Calibration

Pending review by electrical team

- ____ Set up Windaq data acquisition system
- ____ Ensure all data lines are hooked up
- ____ Oxidizer tank pressure transducer check
- ____ Combustion chamber pressure transducer check
- ____ Combustion chamber thermocouple exterior check/install
- ____ Nozzle thermocouple exterior check/install
- ____ Check communication with engine microcontroller

Section 6.0 Engine Assembly Purge

- 6.01 ____ Set N2 regulator to a suitable purge pressure (100 PSI)
- 6.02 ____ Activate exterior visual warning system
- 6.03 ____ Open N2 bottle valve MV1
- 6.04 ____ Remove all personnel from test firing area

Time Sensitive:

The following steps must be performed in ~15 seconds

- 6.05 ____ Open oxidizer vent valve
- 6.06 ____ Open throttle valves, SOL2, SOL3, SOL4
- 6.07 ____ Open pneumatic N2 valve PBV1, wait 15 seconds
- 6.08 ____ Close pneumatic N2 valve PBV2
- 6.09 ____ Close throttle valves, SOL2, SOL3, SOL4
- 6.10 ____ Close oxidizer vent valve

Section 7.0 Igniter Install

- 7.01 ____ Install electric match assembly and leads
- 7.02 ____ Connect leads to the engine ignition terminals
- 7.03 ____ Check for continuity along the ignition circuit using a multimeter

Section 8.0 Fill Flight Tank with Nitrous Oxide

- 8.01 ____ Hang warning tape for test
- 8.02 ____ Verify that test fan is on
- 8.03 ____ All personnel leave the pressure envelope and proceed to control room or designated safe area
- 8.04 ____ Range Safety completes a sweep of test site to ensure no personnel within pressure envelope
- 8.05 ____ Range Safety also checks for flammables inside flame containment area
- 8.06 ____ Take attendance of everyone
- 8.07 ____ Drone pilot is go to begin setting up
- 8.08 ____ Open N2 bottle valve MV1
- 8.09 ____ Set N2 regulator to boost pressure of 900 psi
- 8.10 ____ Open N2O bottle valve MV3
- 8.11 ____ Activate visual test warning
- 8.12 ____ Record pre-fill weight of oxidizer tank

Pre-fill weight: _____

- 8.13 ____ Open oxidizer tank vent valve PBV3
- 8.14 ____ Open N2O pneumatic valve PBV2
- 8.15 ____ Fill oxidizer tank until liquid N2O detected from vent line
- 8.16 ____ Record fill weight

Fill-weight: _____

- 8.17 ____ Close N2O pneumatic valve PBV2
- 8.18 ____ Close oxidizer tank vent valve PBV3
- 8.19 ____ Open N2O vent valve SOL1
- 8.20 ____ Wait until oxidizer tank pressure stabilizes
- 8.21 ____ Open N2 pneumatic valve PBV1
- 8.22 ____ Again wait until oxidizer tank pressure stabilizes

Section 9.0 Firing Procedure

- 9.01 ____ All personnel wearing hearing protection
- 9.02 ____ Confirm drone is in position
- 9.03 ____ Verbal confirmation of go from range safety at main gate
- 9.04 ____ Verbal confirmation of go from sensor control
- 9.05 ____ Verbal confirmation of go from ignition and firing control
- 9.06 ____ Verbal confirmation of go from camera control
- 9.07 ____ Verbal confirmation of go from propulsion lead
- 9.08 ____ Verbal confirmation of go from safety officer
- 9.09 ____ Test fire audio alarm activated
- 9.10 ____ Count-down initiated
- 9.11 ____ Ignition system activated at the end of the countdown. See section A.1 for off-nominal operation
- 9.12 ____ Confirm squib ignition using webcam imagery
- 9.13 ____ Initiate main burn. Proceed to injector valve failure procedure if required
- 9.14 ____ Close injector valves SOL2, SOL3, SOL4 to end the test fire
- 9.15 ____ Turn off test fire audio alarm

Section 10.0 Shutdown Procedure

- 10.01 ____ Main engine electrical supply powered off
- 10.02 ____ Initiate a 2-minute hold to ensure that all combustion has ended
- 10.03 ____ Close pneumatic N2 valve PBV1
- 10.04 ____ Open oxidizer tank vent valve PBV3
- 10.05 ____ Open throttle valves SOL2, SOL3, SOL4
- 10.06 ____ Confirm oxidizer tank is at atmosphere via flight tank pressure transducer
- 10.07 ____ Close throttle valves SOL2, SOL3, SOL4
- 10.08 ____ Close oxidizer tank vent valve PBV3
- 10.09 ____ Wait 5 minutes for the air in the sea can to vent
- 10.10 ____ Turn off N2O bottle valve MV3
- 10.11 ____ Turn off N2 bottle valve MV1
- 10.12 ____ Open manual valve MV2
- 10.13 ____ Remove all personnel from the test firing area
- 10.14 ____ Open N2 pneumatic valve PV1

- 10.15 ____ Open N2O fill line vent valve SOL1
- 10.16 ____ Open N2O pneumatic valve PV2
- 10.17 ____ Wait 30 seconds to ensure all lines have fully vented
- 10.18 ____ Close N2O pneumatic valve PV2
- 10.19 ____ Close N2O fill line vent valve SOL1
- 10.20 ____ Close N2 pneumatic valve PV1
- 10.21 ____ Wait 5-minutes for any residual N2O in the sea can air to dissipate
- 10.22 ____ De-activate exterior visual warning system
- 10.23 ____ Sea can is now safe to approach
- 10.24 ____ Range safety at front gate no longer required

Section 11.0 Post-Firing Procedure

- 11.01 ____ Remove test warning tape
- 11.02 ____ Disconnect N2O fill line from the oxidizer tank lower manifold
- 11.03 ____ Install protective caps on both sides of the connection
- 11.04 ____ Disconnect N2 fill line from the oxidizer tank upper manifold
- 11.05 ____ Install protective caps on both sides of the connection
- 11.06 ____ Engine may now be disassembled as per SOAR 2018 Hybrid Rocket Cleaning and Assembly/Dis-Assembly Procedure

Section A.1 Off-Nominal Procedures

Abort Procedure

- ____ Abort declared
- ____ Main engine electrical supply powered off

N2O Leak Procedure

- ____ Main engine electrical supply powered off
- ____ Close both pneumatic valves valve PBV1, PBV2
- ____ Range Safety to close nitrous tank bottle valve MV3, if applicable
- ____ Vent flight oxidizer tank via the oxidizer tank valve PBV3
- ____ Wait until pressure in system is atmospheric
- ____ Current Time: _____
- ____ Allow 5 minutes for the nitrous to dissipate via the fan
- ____ Proceed to step 10.22 of Section 10.0 Shutdown Procedure

Disassemble leaking component and investigate leak

Catastrophic Combustion Chamber Failure

Main engine electrical supply powered off

Camera Control check for visible indications of fire inside sea can

If fire detected inside sea can:

Call 911 for Fire Department

GPS coordinates: Lat 50.868039 deg N, Long 114.291142 deg W

Highway Address: 200, 198070 Hwy 22

Shut off sea can fan

Vent flight oxidizer tank via the oxidizer tank valve PBV3

Wait until pressure in system is atmospheric

If no fire detected inside sea can:

Vent flight oxidizer tank via the oxidizer tank valve PBV3

Wait until pressure in system is atmospheric

Current Time: _____

Allow 2 minutes for the nitrous to dissipate via the fan

Range Safety to approach sea can from blast wall side in full PPE with radio and fire extinguisher class B or multiclass B to check for fire

If Range Safety finds a fire inside the sea can then proceed to steps above

If Range Safety finds a fire inside containment fence then fight it with fire extinguisher or call 911 if deemed large enough

Close the emergency N2 valve MV2

Close the emergency N2O valve MV4

Proceed to step 10.22

Catastrophic Oxidizer Tank Failure

Main engine electrical supply powered off

Camera Control check for visible indications of fire inside sea can

If fire detected inside sea can:

Call 911 for Fire Department

GPS coordinates: Lat 50.868039 deg N, Long 114.291142 deg W

Highway Address: 200, 198070 Hwy 22

- Close all pneumatic valves if not already
- Shut off sea can fan
- Evacuate to muster location
- Ensure all personnel are accounted for and injury free. Call 911 if anyone is seriously injured
- Check for visible fire. Call 911 if a fire is present
- Seek guidance from advisor or supervisor

Ignition Failure Procedure

- Ensure the ignition system is properly armed
- Re-attempt ignition
- If successful proceed to Step 9.12
- Disable ignition system electrical supply
- Disable main engine electrical supply
- Wait 5 minutes to ensure that no combustion is occurring
- Notify all personnel that the flight tank will be vented
- Vent flight oxidizer tank via the oxidizer tank vent valve PBV3
- Wait until pressure in system is atmospheric
- Current Time: _____
- Allow 5 minutes for the nitrous to dissipate via the fan
- Close the emergency N2 valve MV2
- Close the emergency N2O valve MV4
- Proceed to step 10.22

N2O Injector Valve Failure (SOL2, SOL3, SOL4)

- Main engine electrical supply powered off
- Monitor squib burn via webcam imagery
- Current time: _____
- Time 5 minutes from the last visual indication of combustion occurring in the chamber
- Notify all personnel that the flight tank will be vented
- Close pneumatic N2 valve PBV2

Vent flight oxidizer tank via the oxidizer tank valve PBV3

Wait until pressure in system is atmospheric

Current Time: _____

Allow 5 minutes for the nitrous to dissipate via the fan

Close the emergency N2 valve MV2

Close the emergency N2O valve MV4

Proceed to step 10.22

Loss of Remote Valve Control

Attempt to re-establish remote control of the valves

Remove power from the microcontroller board

Alert all personnel that the oxidizer tank will be vented

Range Safety to approach sea can in Full PPE and close the N2O tank valve MV3

Close the N2 tank valve MV1

Open the emergency oxidizer tank dump valve MV2

Open the emergency N2O fill system dump valve MV4

Wait until pressure in system is atmospheric

Current Time: _____

Allow 5 minutes for all nitrous to dissipate via fan

Close the emergency N2 valve MV2

Close the emergency N2O valve MV4

Proceed to step 10.22

Completion of Testing Activities

Signature of Propulsion Lead: _____ **Date:** _____

Signature of Safety Officer: _____ **Date:** _____

Signature of Faculty Advisor: _____ **Date:** _____

APPENDIX VI: Aero-Structures Simulations & Analysis

Design Loads:

Calculated by finding the total applied loads, then using the method of sections to calculate the loads at key points/interfaces in the rocket

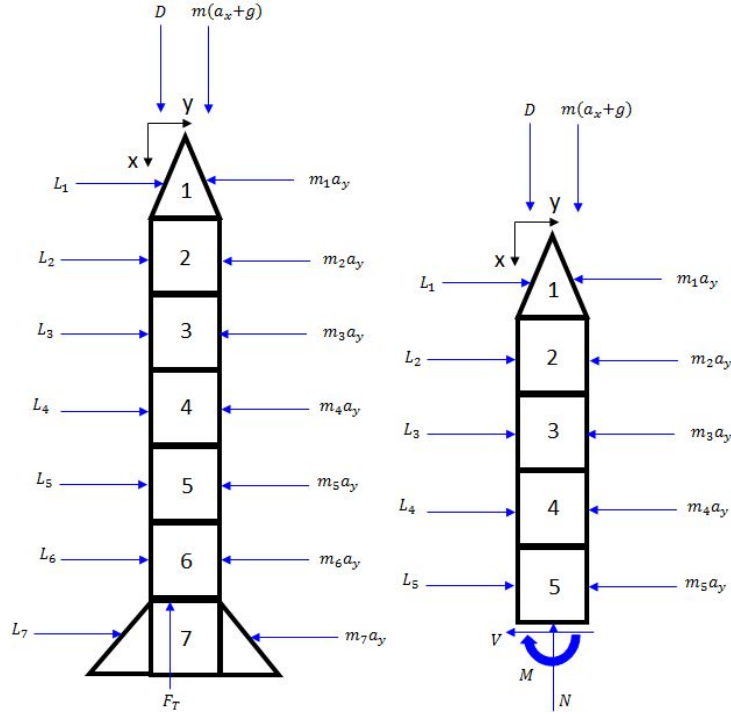
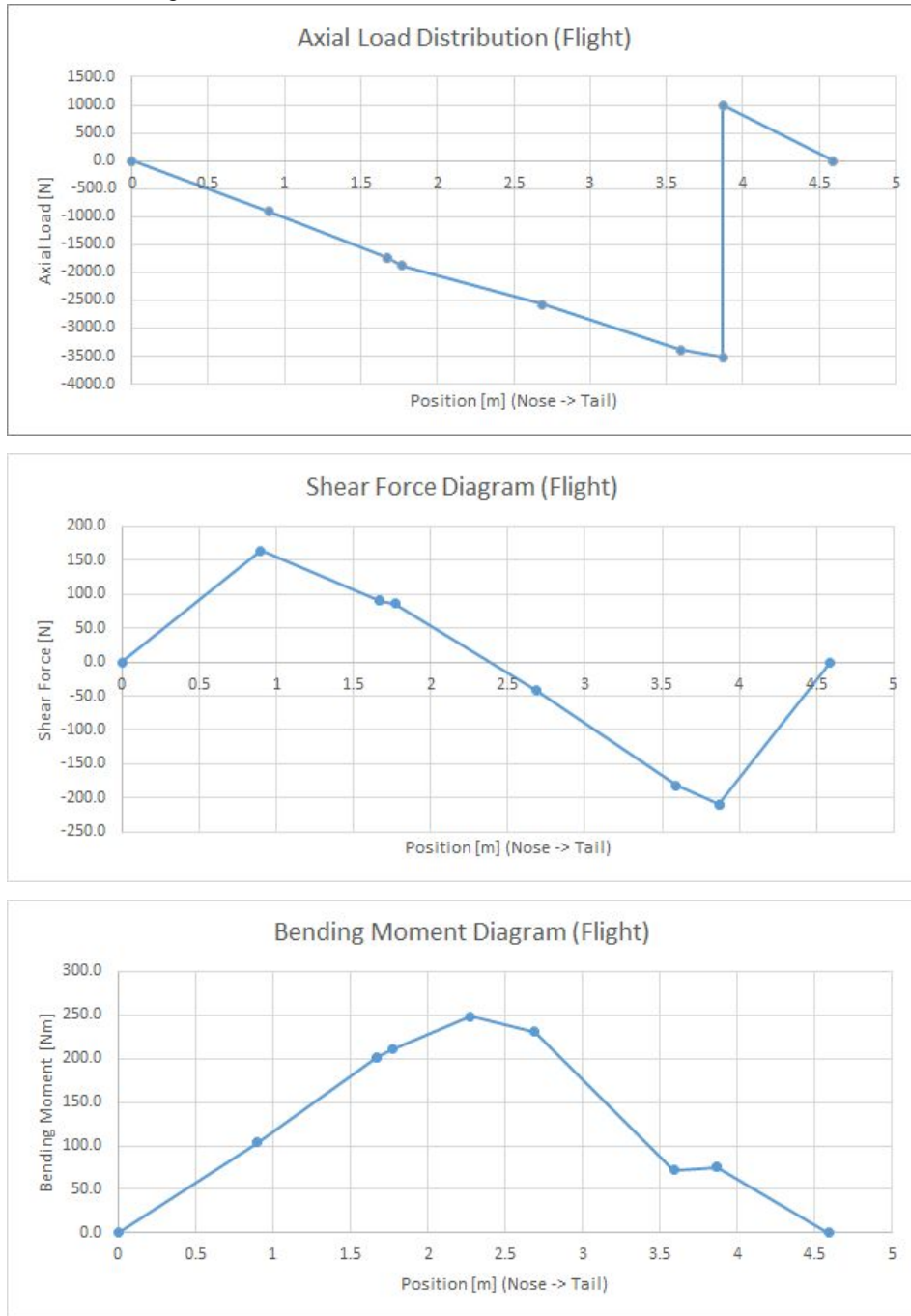
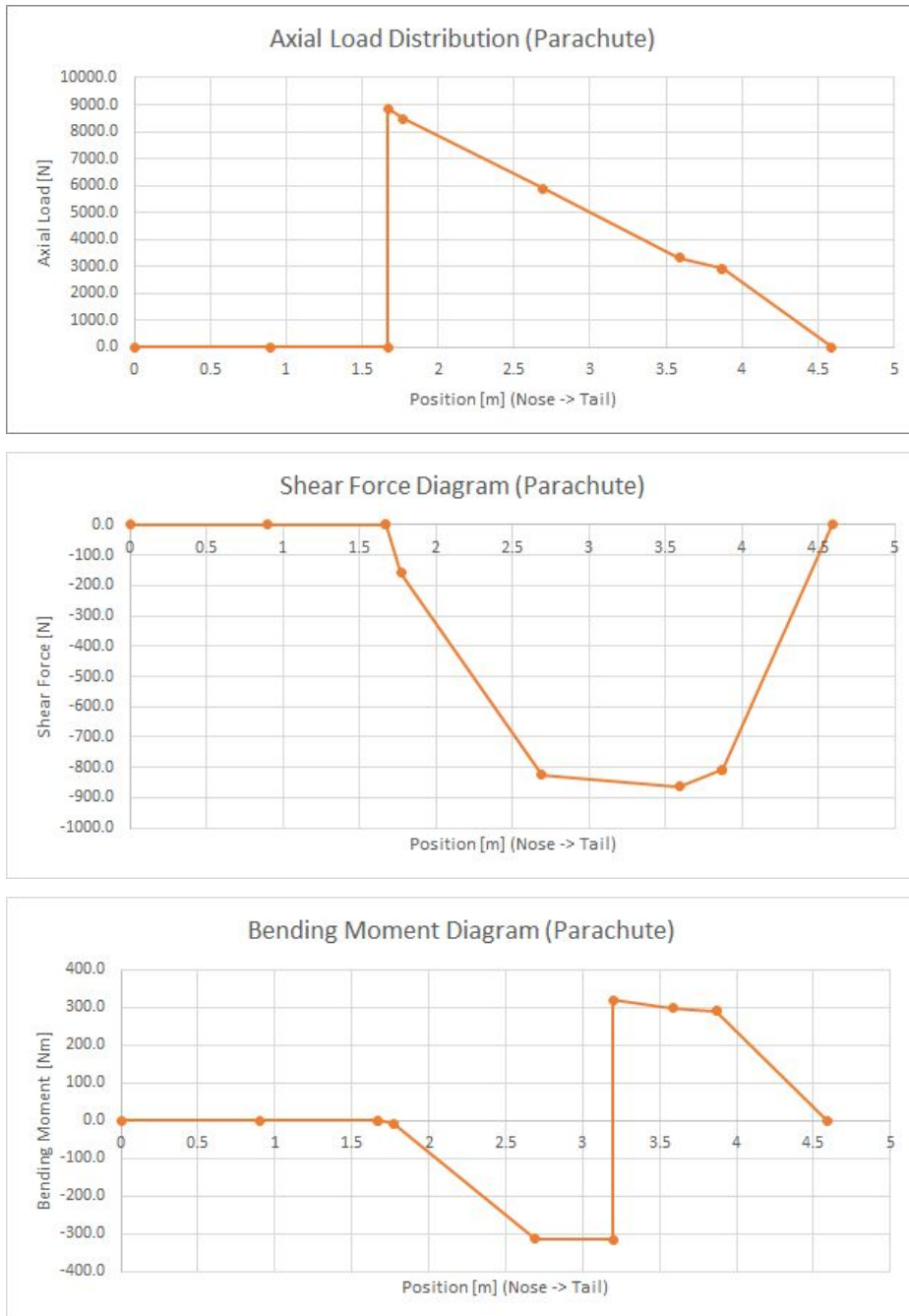


Figure: Method of Sections

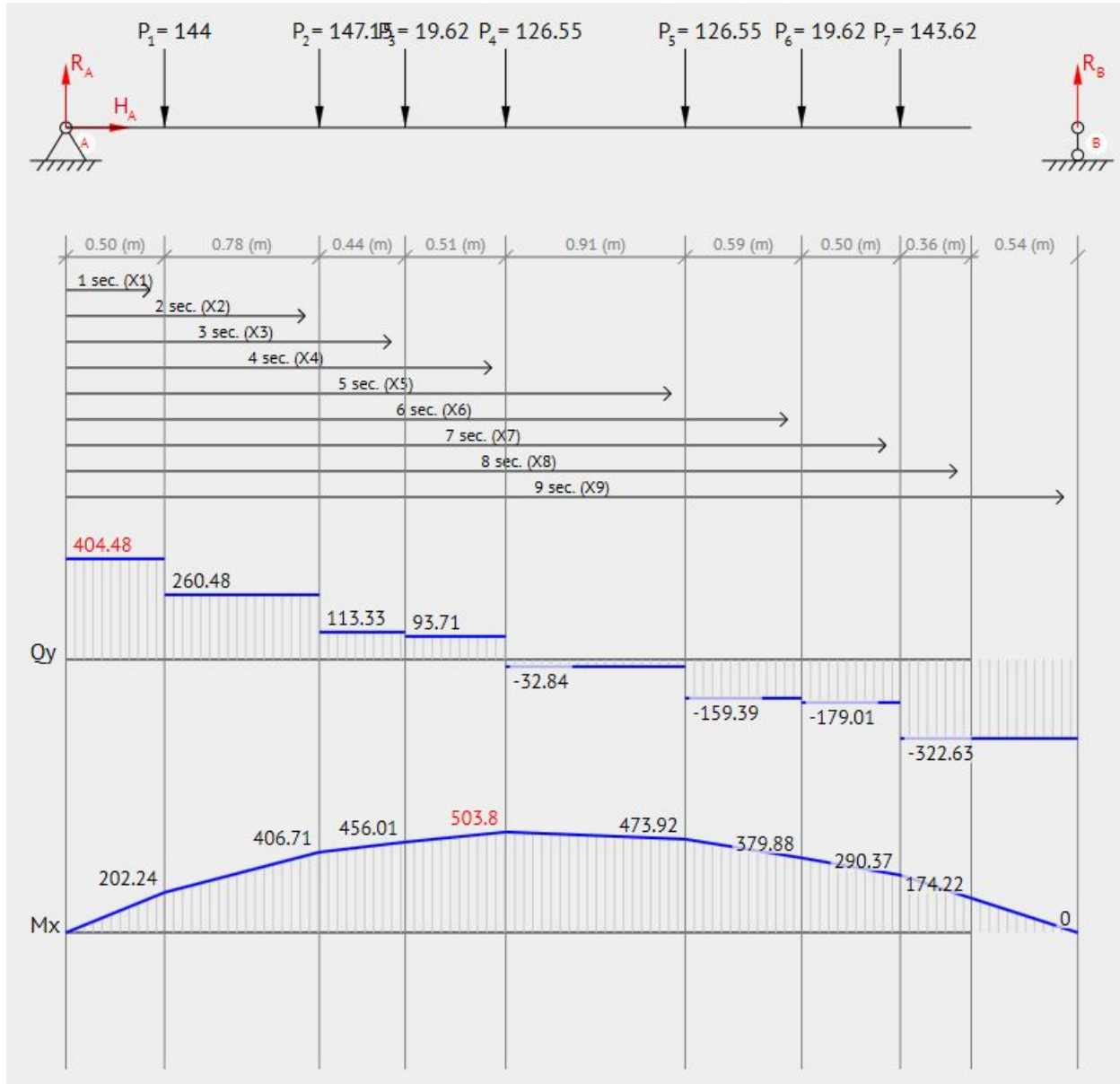
Flight Loading Case: Maximum speed & thrust, sharp edged wind gust encountered. Total sideways wind loading determined through a CFD simulation of the rocket flying. Load distribution and CP location for each section determined in OpenRocket.



Parachute Opening Case: Main parachute opens instantly, rocket body is 15° from the vertical when the parachute deploys and applies a vertical force of 9,500 N. Fuel / Oxidizer are depleted and the parachute, nose cone and payload are no longer contributing to the weight of the main rocket body.



Ground Handling Case: Rocket is lifted by two individuals, one at each end (or lifted at one end by one individual) and a 1G acceleration is applied by said individual(s). Oxidizer tank is empty, otherwise the rocket is fully loaded.



Body Tube Simulations

Screenshots of Flight Load Simulation with winding angle orientation of 33°,33°,33°,85°

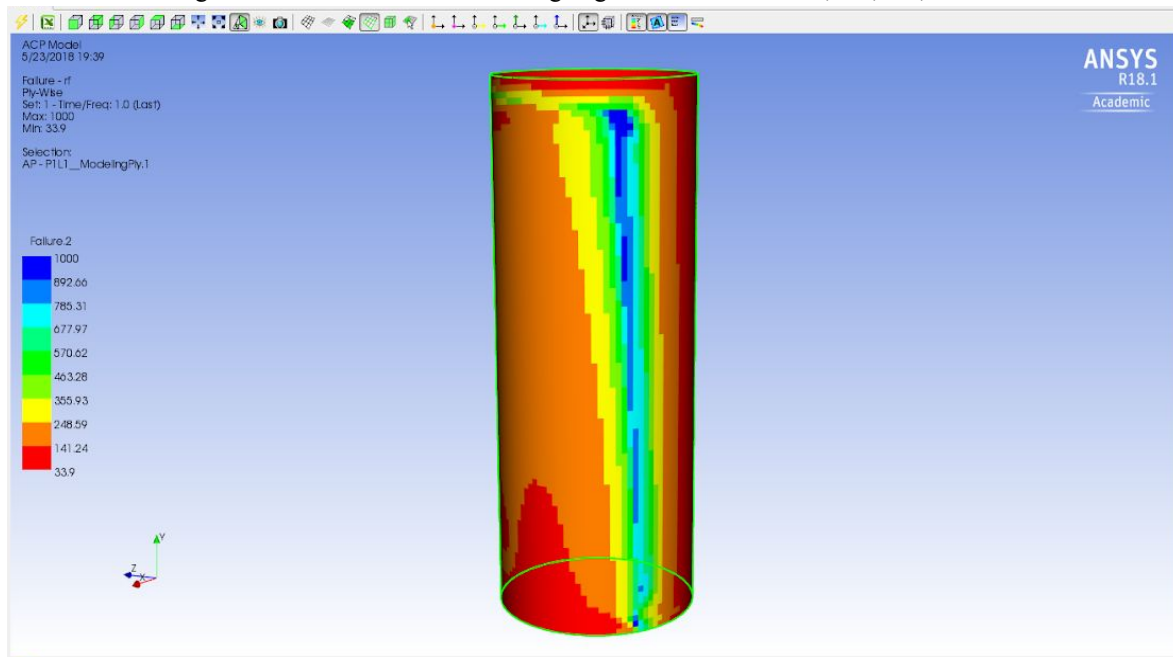


Figure: Layer 1 Results

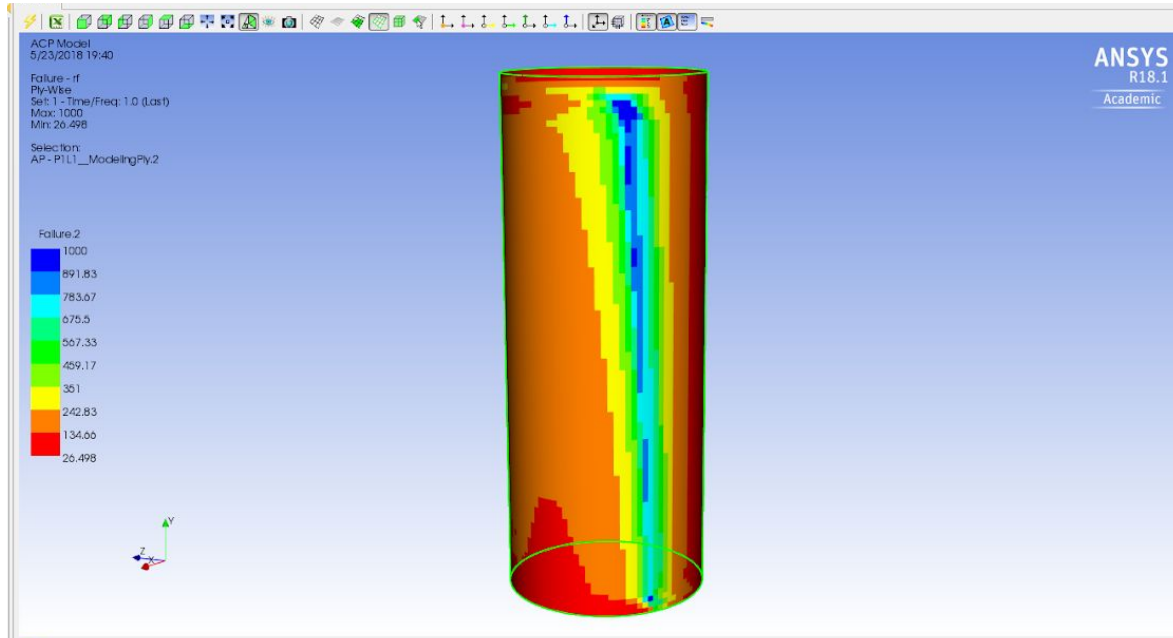


Figure: Layer 2 Results

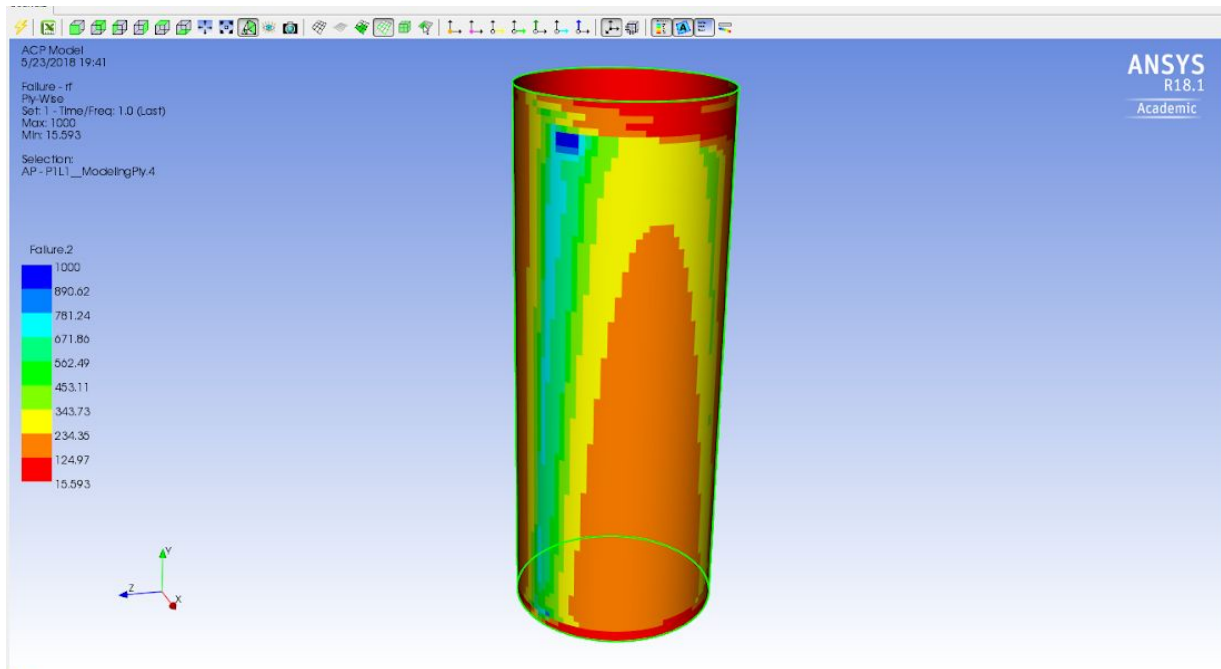


Figure: Layer 3 Results

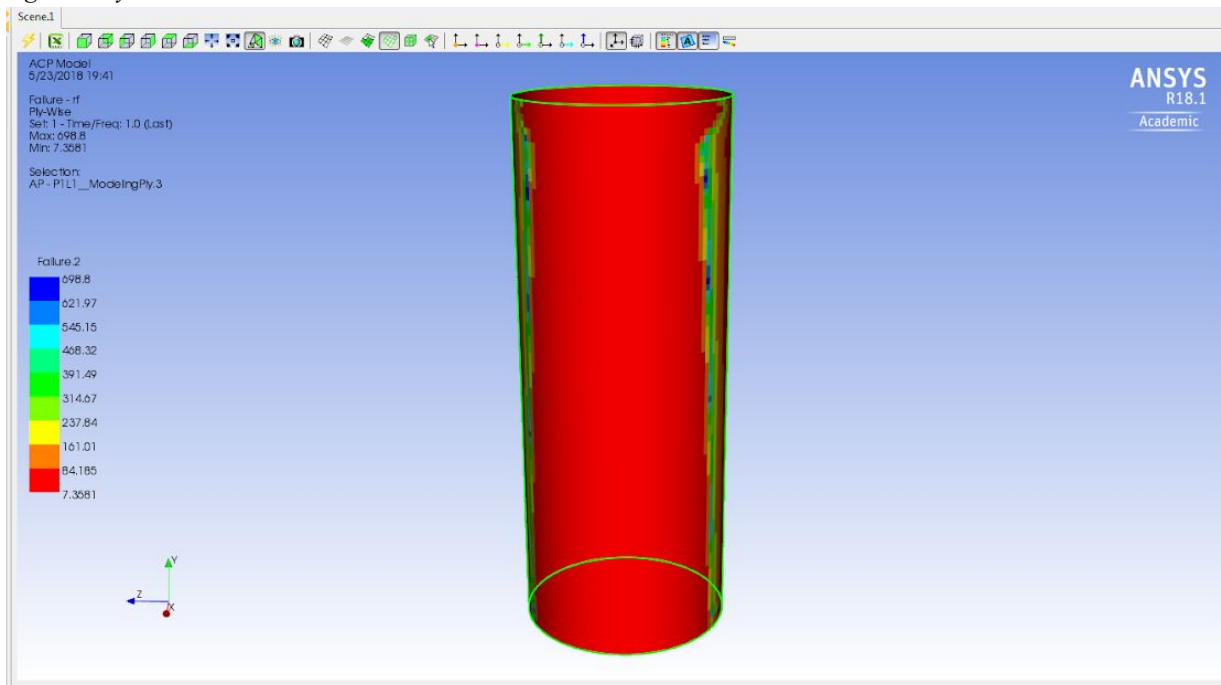


Figure: Layer 4 Results

Nose Cone Simulations

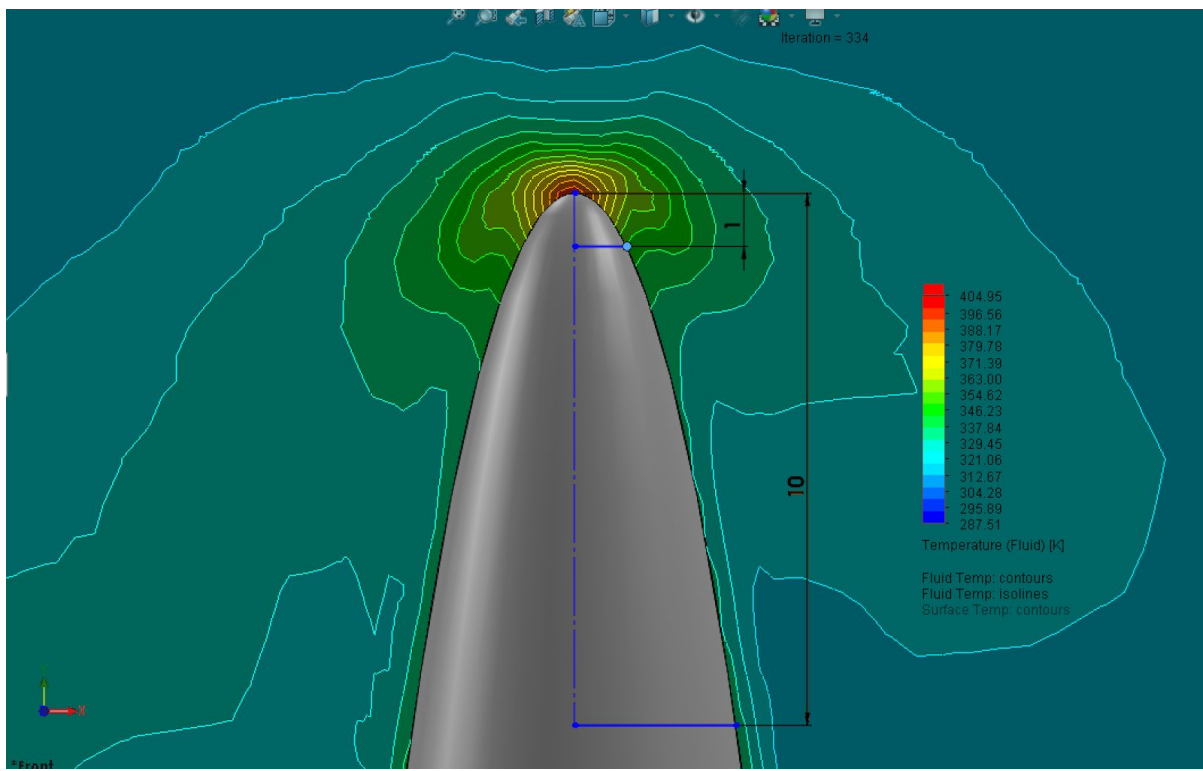


Figure: Nose Cone Pressure Profile at maximum expected airspeed, estimated Spaceport America Conditions

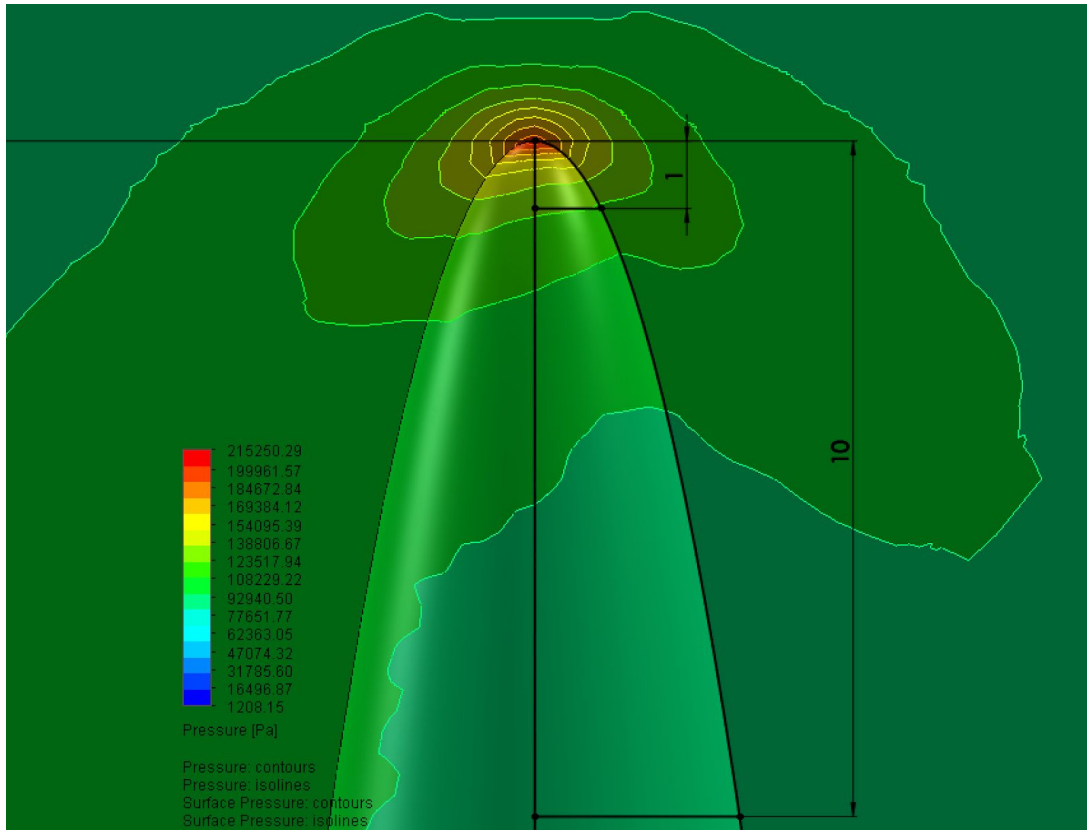


Figure: Nose Cone Pressure Profile at maximum expected airspeed, estimated Spaceport America Conditions

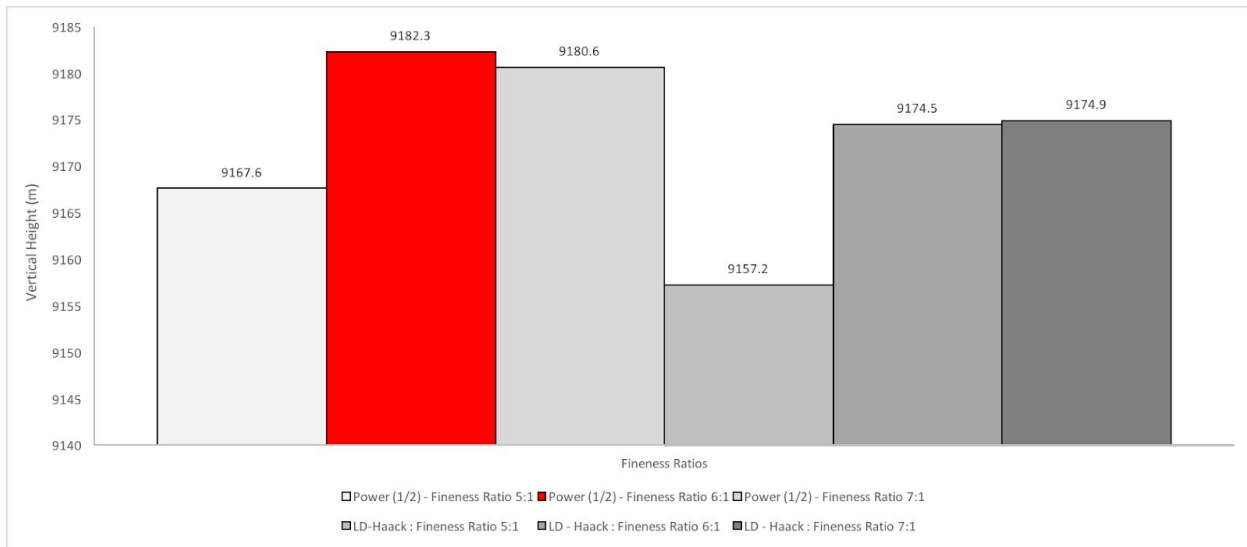


Figure: Nose Cone Simulation Altitude Results - holding all other parameters constant

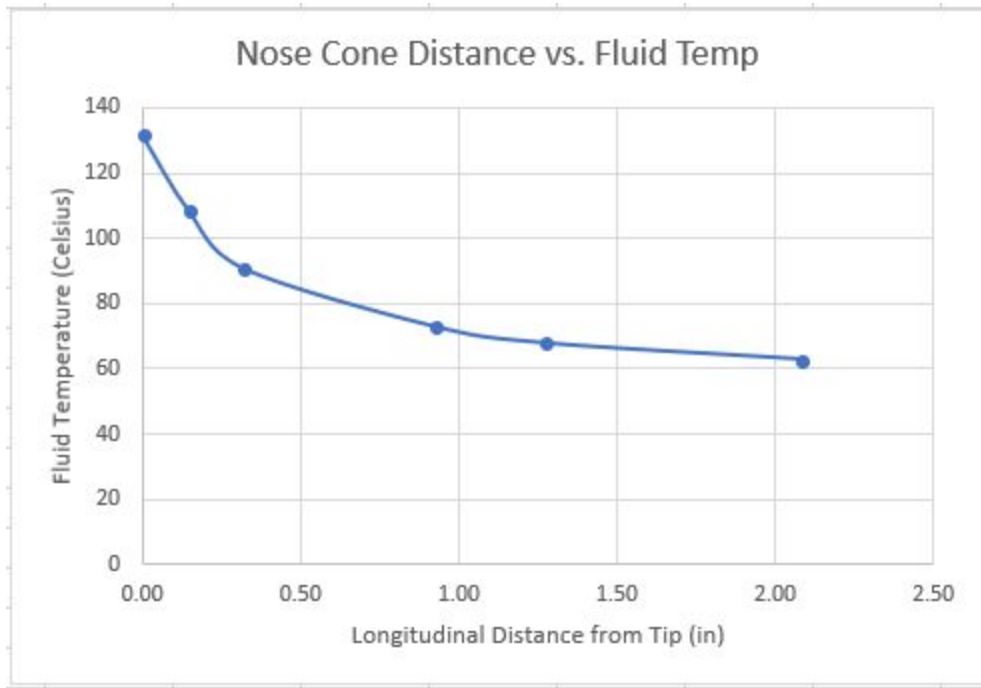


Figure: Nose Cone Distance vs. Fluid Temp

Radax Joint Length & Aluminum Thickness Calculations

Inputs	Value	Units	Imperial	Units	Metric	Units	
Shear strength of epoxy	1500.00	psi	1500.00	psi	10342.12	kPa	
Yield Strength of Al	275.00	Mpa	39.89	ksi	275.00	Mpa	
Peak Expected Axial Tensile Load (Parachute)	9500.00	N	2135.68	lbf	9500.00	N	
Peak Expected Axial Compressive Load (Thrust)	1000.00	lbf	1000.00	lbf	4448.22	N	
Peak Expected Bending Load (Carrying)	500.00	N*m	368.78	lb*ft	500.00	N*m	
Outer Diameter of radax	6.98	in	6.98	in	17.73	cm	
Inner Diameter of radax	6.74	in	6.74	in	17.13	cm	
Radax Length	1.50	in	1.50	in	3.81	cm	
Axial Load							
Area per length of bond	21.93	in	21.93	in	55.70	cm	
Area required for axial load	1.42	sq in	1.42	sq in	9.19	sq cm	
Length required for axial load	0.06	in	0.06	in	0.16	cm	
Uncertainty factor	1.50						
Length required for axial load	0.10	in	0.10	in	0.25	cm	Total SF
Axial SF	15.40						23.1
Bending Load							
M	500.00	N*m	368.78	lb*ft	500.00	N*m	
Y	3.49	in	3.49	in	8.86	cm	
I	14.98	in^4					
Peak Stress	1031.22	psi	1031.22	psi	7110.01	kPa	
Radial length	0.236	in	0.24	in	0.60	cm	
Adhesive length required	0.16	in	0.16	in	0.41	cm	
Uncertainty factor	5.00						
Adhesive length required	0.81	in	0.81	in	2.06	cm	Total SF
Bending SF	1.85						9.2
Match Aluminum and epoxy strength							
Radial length	0.118	in	0.12	in	0.30	cm	
Adhesive length required	3.138	in	3.14	in	7.97	cm	
Min Thickness	0.06	in	0.06	in	0.14	cm	

Motor Mount Beam Sizing

Situation Definition		Imperial	Units	Metric	Units
Max Tensile Loading	3320 N	746.37 lbf		3320.00 N	
Max Compressive Loading	3515 N	790.20 lbf		3515.00 N	
Max Bending Moment	380 Nm	#N/A	#N/A	#N/A	#N/A
Max Shear	860 N	193.34 lbf		860.00 N	
Free Length	6 in	6.00 in		15.24 cm	
Material Yield Strength (Axial)	186 Mpa	26.98 ksi		186.00 Mpa	(HAZ)
Material Yield Strength (Buckling)	275 Mpa	39.89 ksi		275.00 Mpa	(non HAZ)
Modulus of Elasticity	68.9 Gpa	9993.12 ksi		68.90 Gpa	
K (Column Length Factor)	0.5				
Number of Beams	4				
Beam Definition					
Shape	Square				
Side	0.75 in	0.75 in		1.91 cm	
Wall Thickness	0.125 in	0.13 in		0.32 cm	
Second Moment of Area	8.80698E-09 m^4				
Area	0.000201613 sq m	0.31 sq in		0.00 sq m	
Assembly Definition					
Radial distance to centroid	2.875 in	2.88 in		7.30 cm	
Radial distance to outer edge	3.25 in	3.25 in		8.26 cm	
Second Moment of Area	2.18549E-06 m^4				
Results					
Axial Strength	37500 N	8430.32 lbf		37499.93 N	
Buckling Load	1031421 N	231872.70 lbf		1031421.16 N	
Bending Compression / Tension	2602 N	584.92 lbf		2601.85 N	
Bending Stress	14.35 Mpa	2.08 ksi		14.35 Mpa	
Shear Force	1128.47 N				
Axial SF	42.67				
Bending SF	12.96				
Buckling SF	396.42				
Shear SF	5.25				

Engine Mount Bolt Sizing

Bolt Diameter Calculation			
Bolt Tensile Strength	60 ksi	60.00 ksi	413.68 MPa
Number Bolts	2		
Desired SF	2		
Max Force / bolt	584.919 lbs	584.92 lbs	265.31 kg
Area	0.010 sq in		
Minor Diameter	0.111	#8-32	http://www.engineershandbook.com
Major Diameter	0.164		
Bolt Thread Length Calculation			
Aluminum Yield	275.0 Mpa	39.89 ksi	275.00 Mpa
Thread Major Dia	0.2 in	0.16 in	0.42 cm
Force Applied	2601.8 N	584.92 lbf	2601.85 N
Desired SF	3.0		
Length Needed	0.196 in	0.20 in	0.50 cm
Chosen Length	0.375 in	0.38 in	0.95 cm
SF	5.73		

Rocket Diameter Sizing

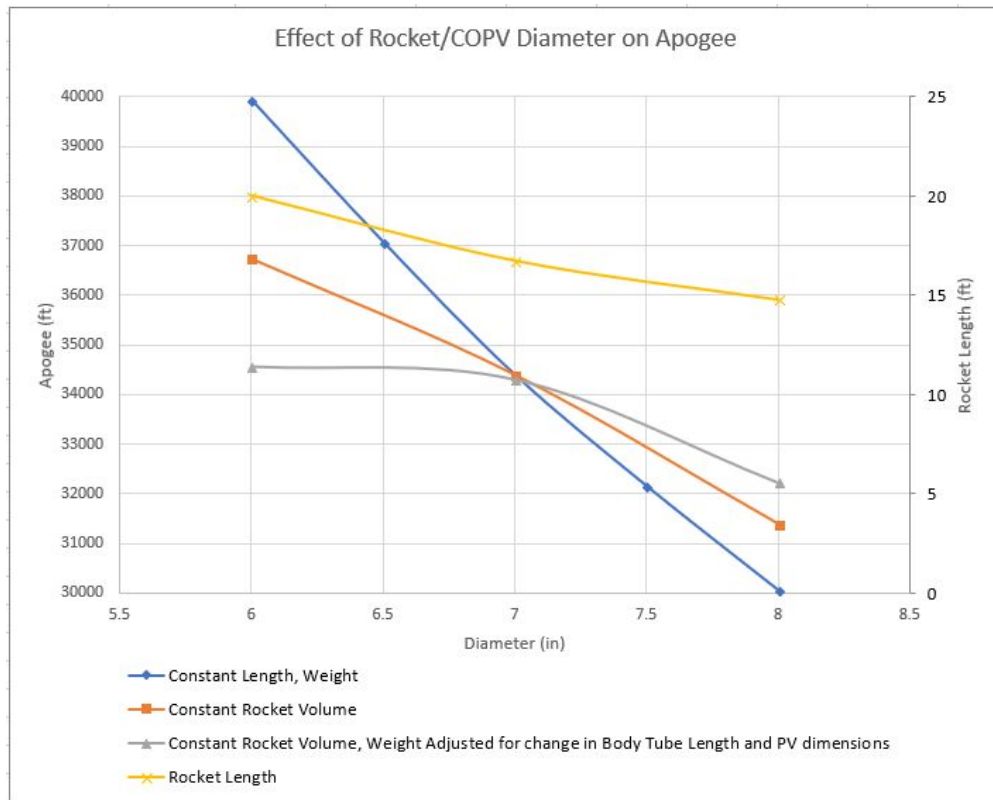
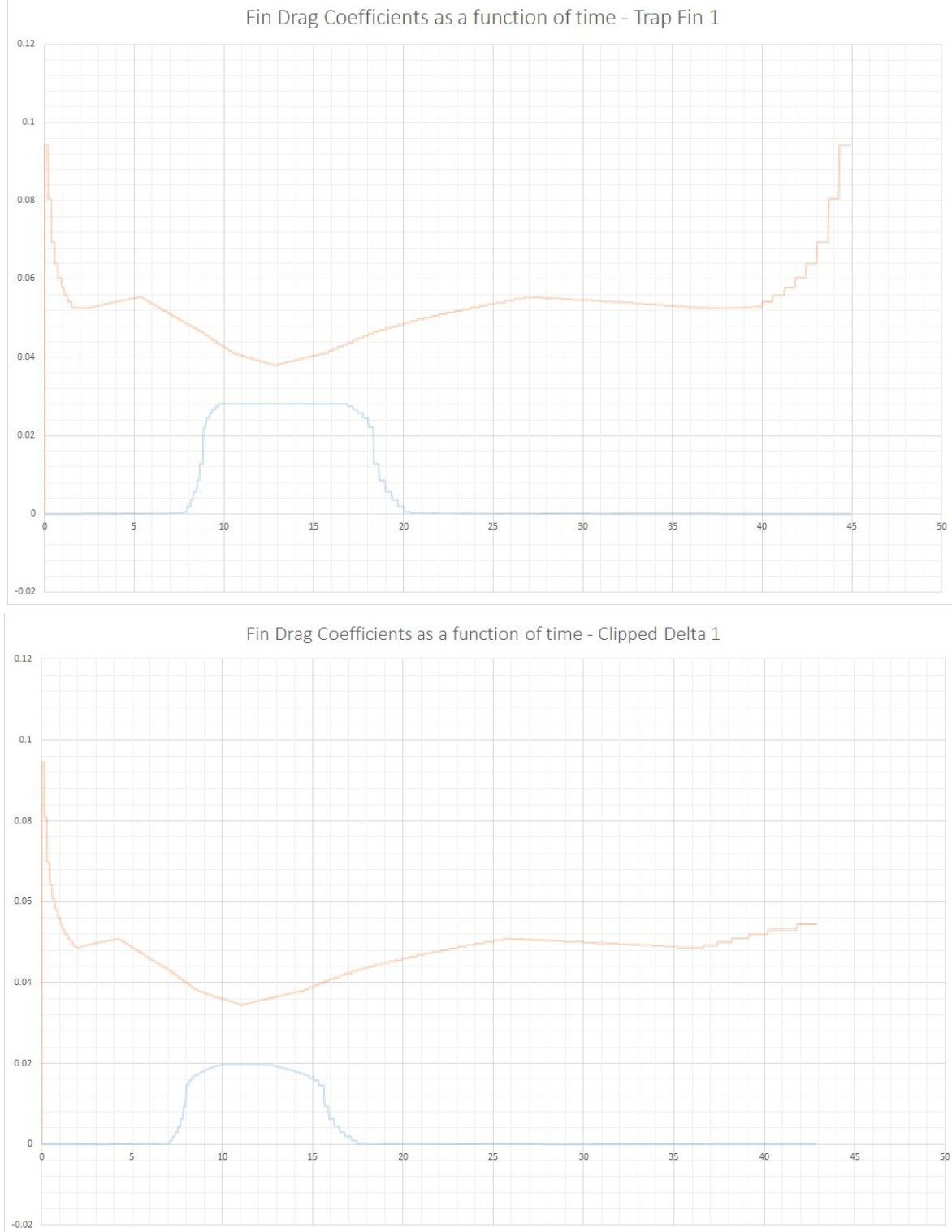


Figure: Effect of Rocket / COPV Diameter on Apogee

- 7" OD selected due to negligible loss in altitude compared to a 6" rocket while greatly easing transportation (by making the rocket shorter) and internal system packaging (by increasing the internal diameter).
- Simulations conducted in OpenRocket

Fin Shape Choice

The charts below show drag vs time for a trapezoidal and clipped delta fins. In orange is the estimated skin friction drag and in blue is the estimated pressure drag.



COPV Design and Simulations

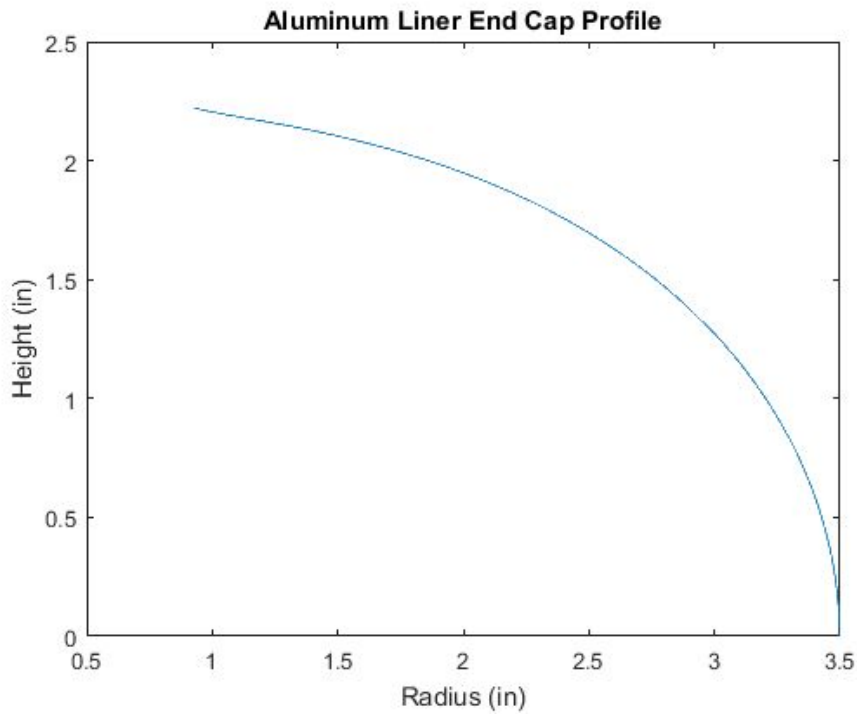


Figure : COPV Aluminum Liner Optimal End Cap Profile

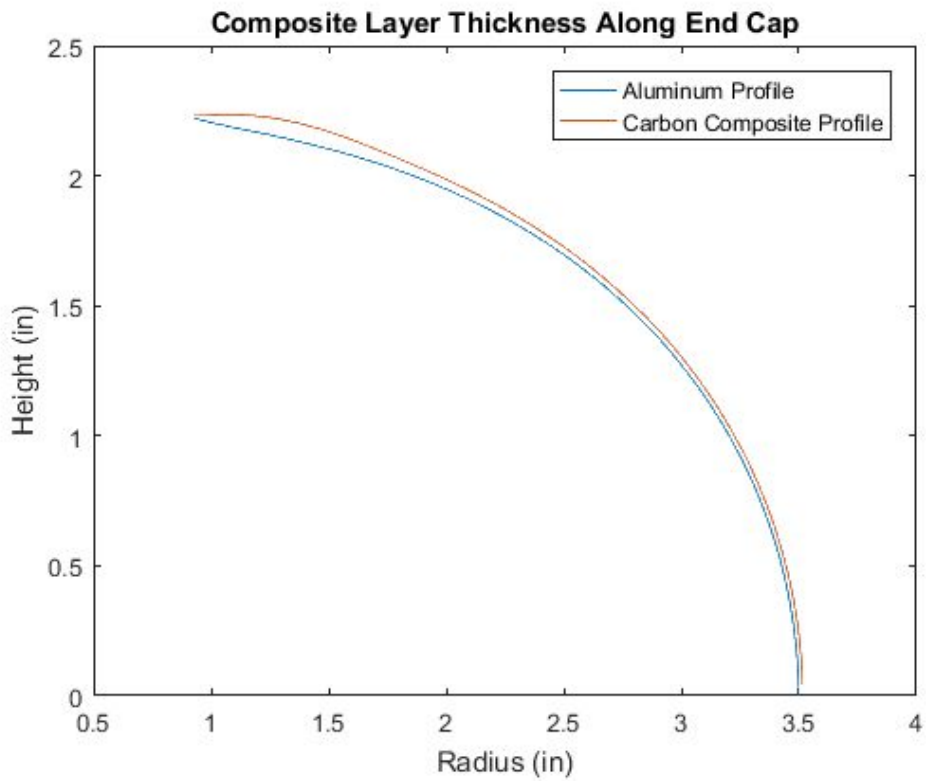


Figure: Composite Layer Thickness Along End Cap

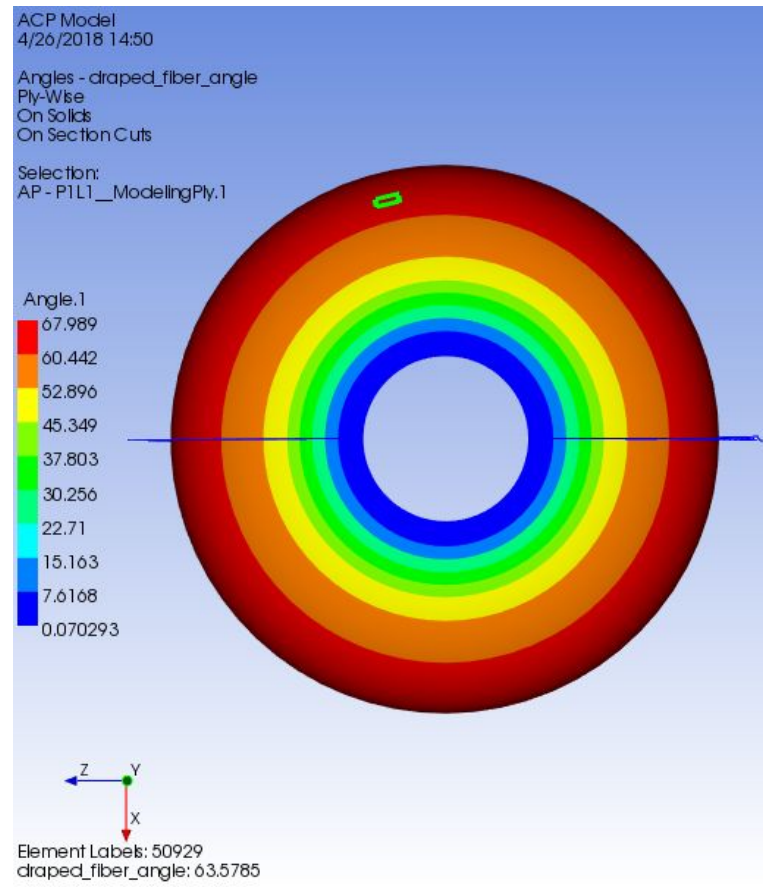


Figure : Fiber Angle on COPV End Cap

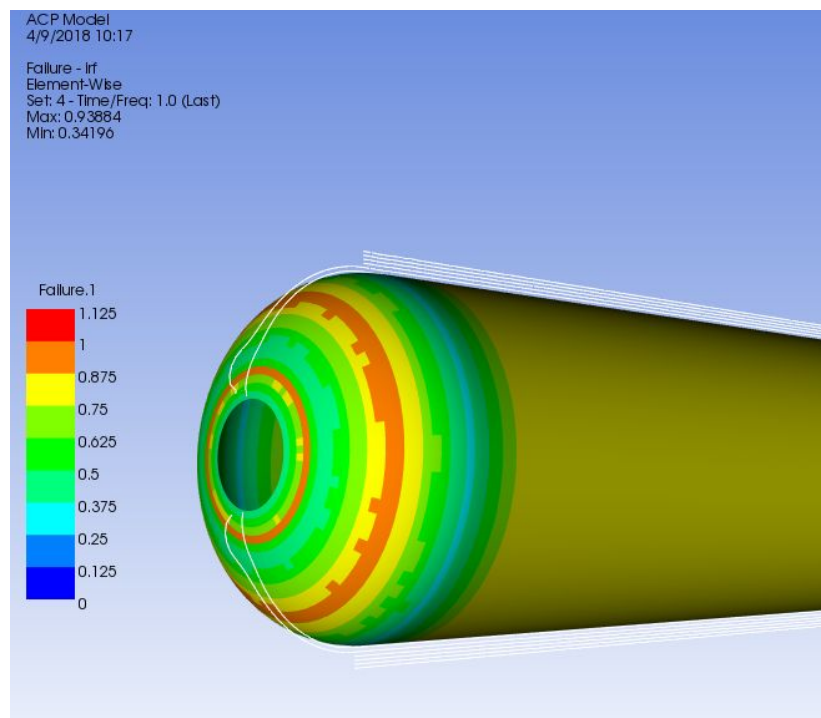


Figure : Safety Factor Diagram of 3x Flight Loads and Internal Pressure Applied

Table : Safety Factor of Each COPV Test Case

	Safety Factor
Internal Pressure	3.198
Carrying Load	60
Flight Loads	3.195
Parachute Loads	63.5

APPENDIX VII: Engineering Drawings

Aero-structures Subsystems Drawings

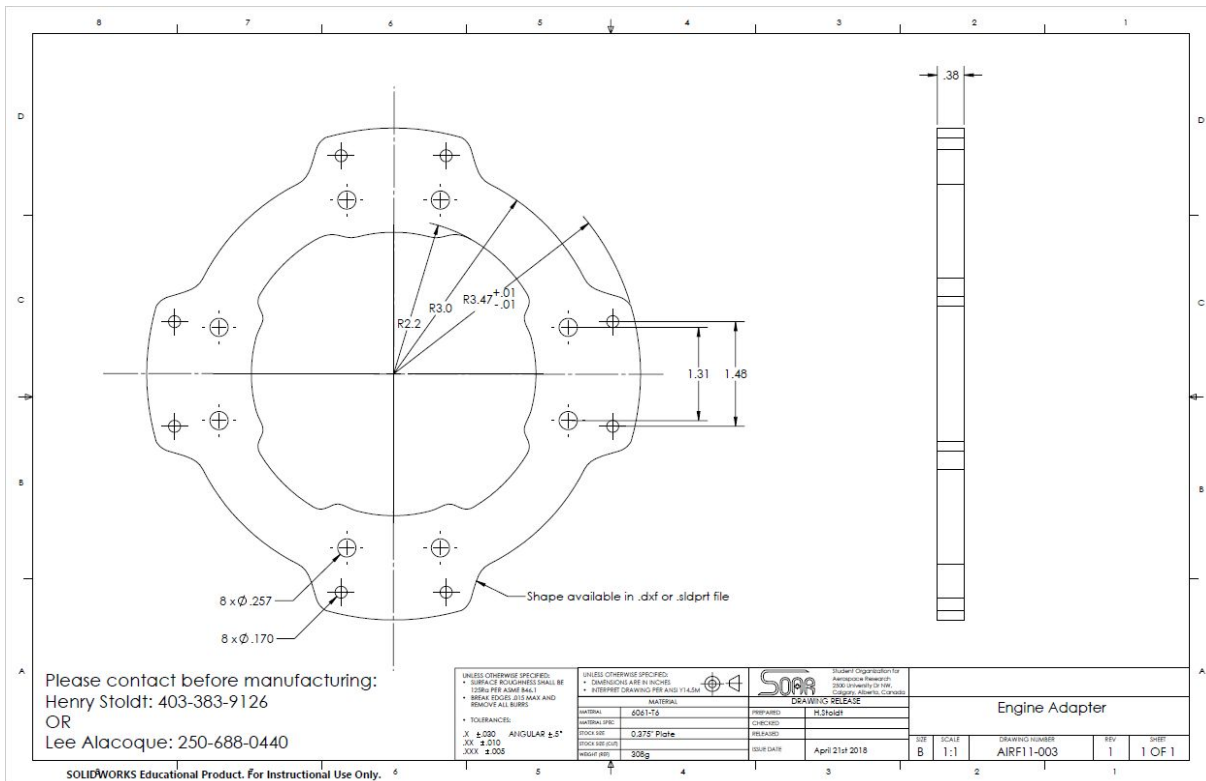


Figure. Engine Adapter Drawing

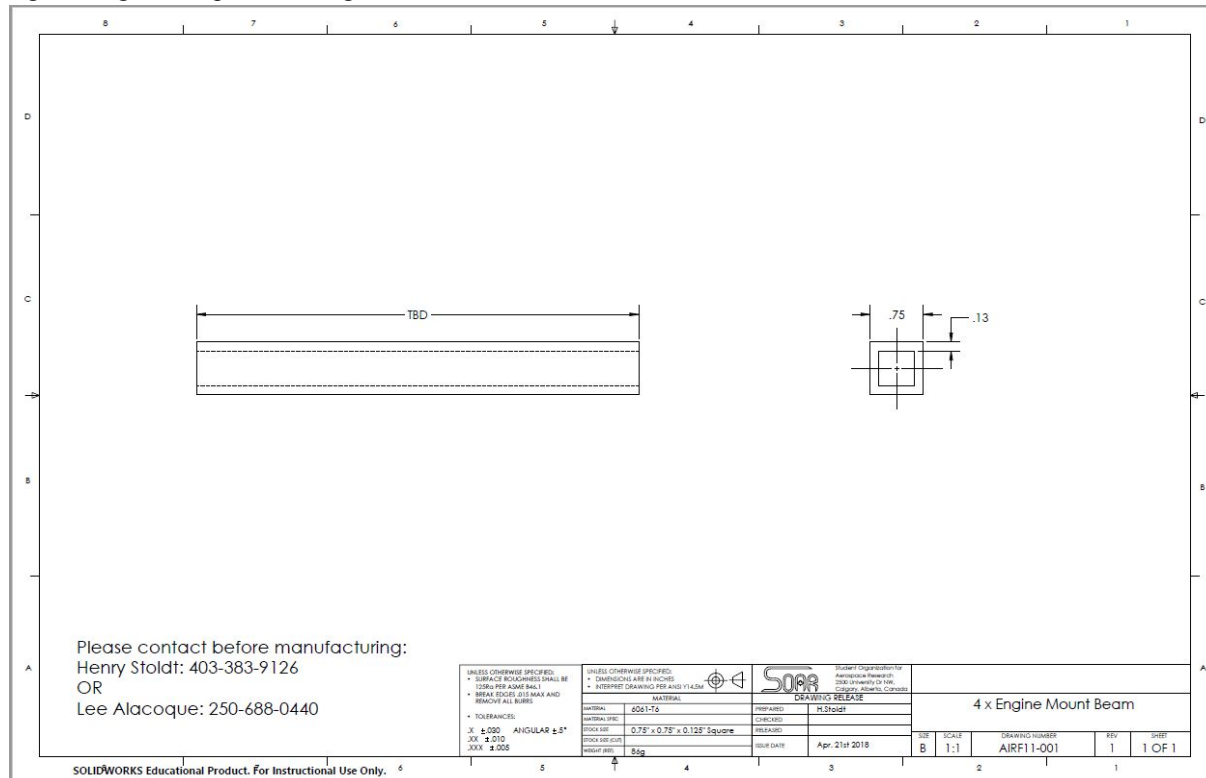


Figure. Engine Mount Beam Drawing

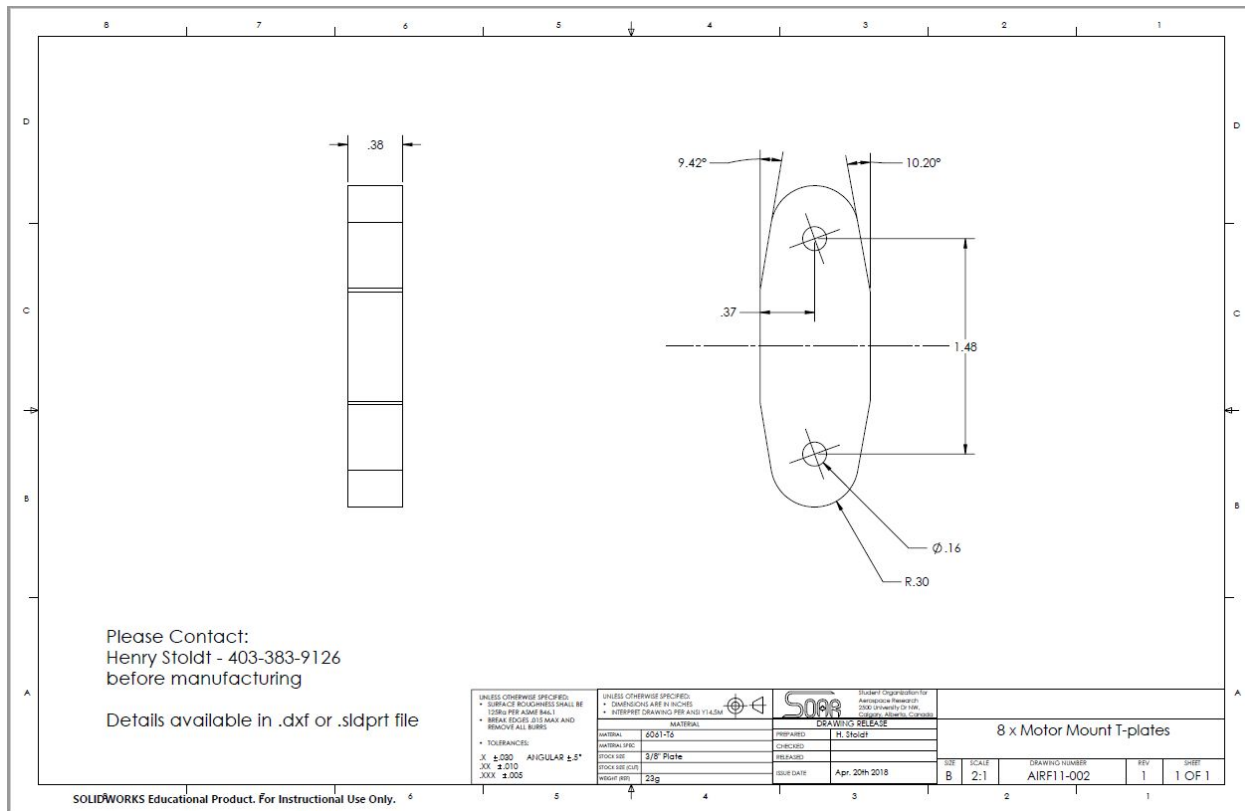


Figure. Motor Mount T-plates Drawing

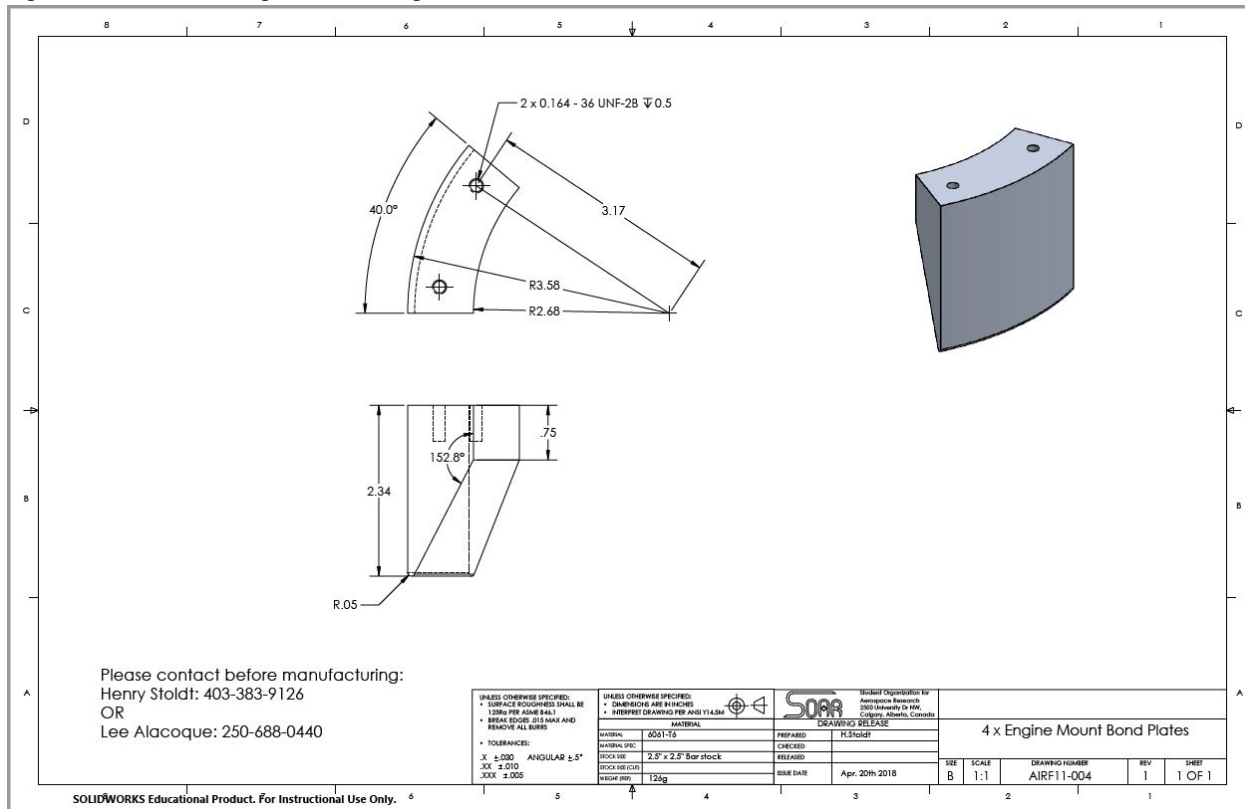


Figure. Engine Mount Bond Plate Drawing

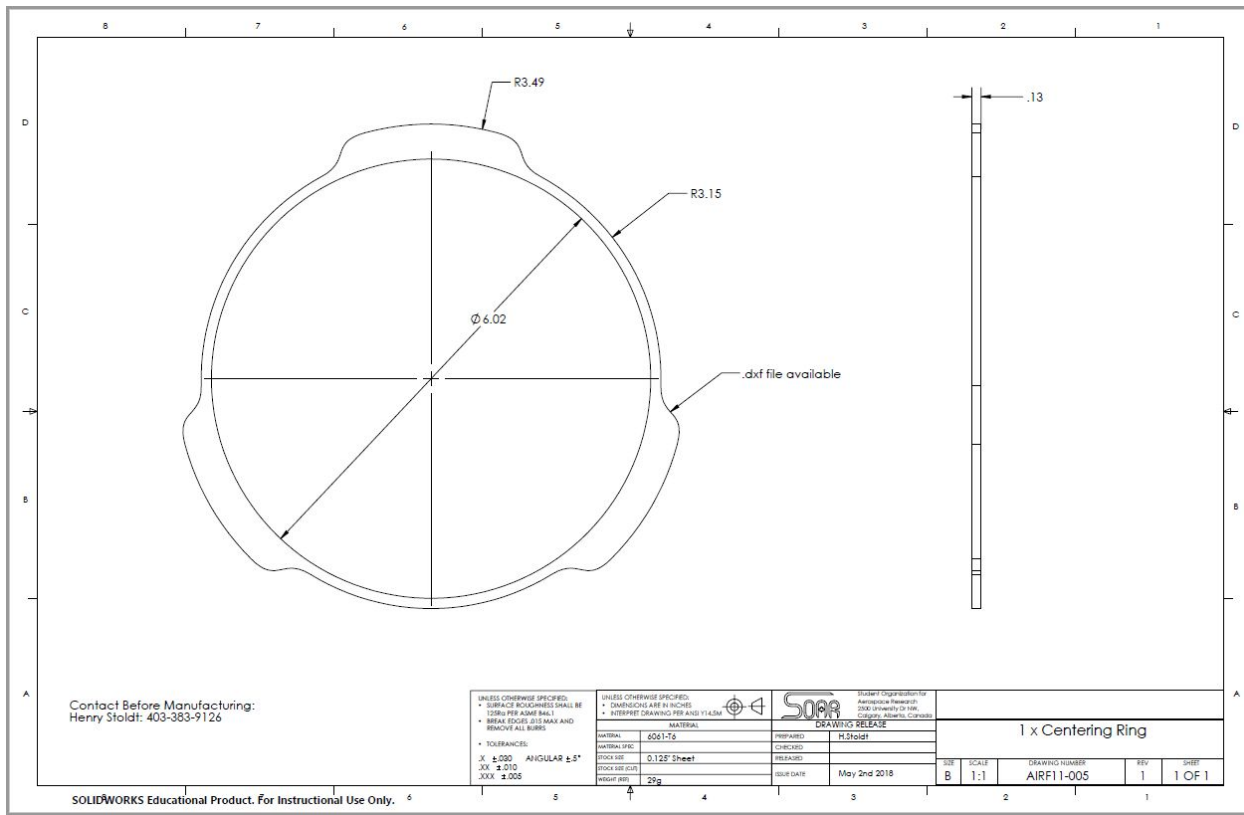


Figure. Centering Ring Drawing

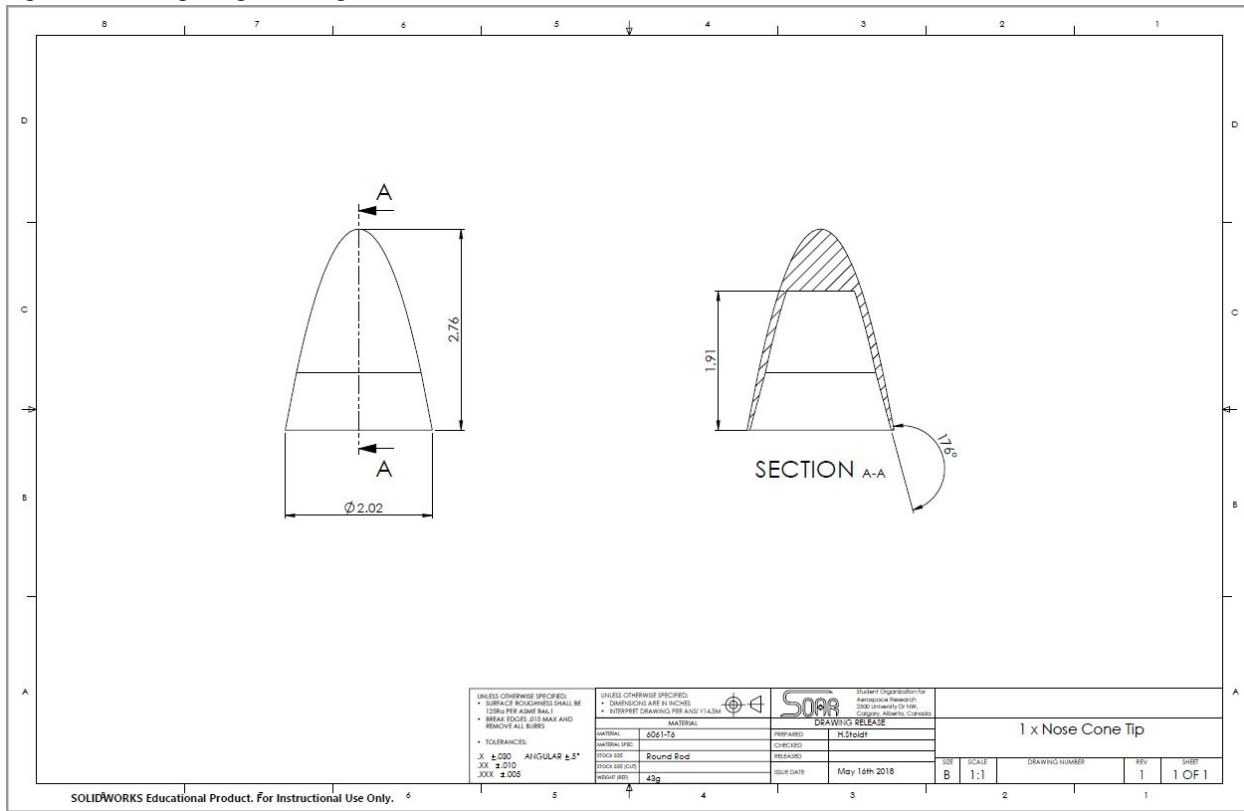


Figure. Nose Cone Tip Drawing

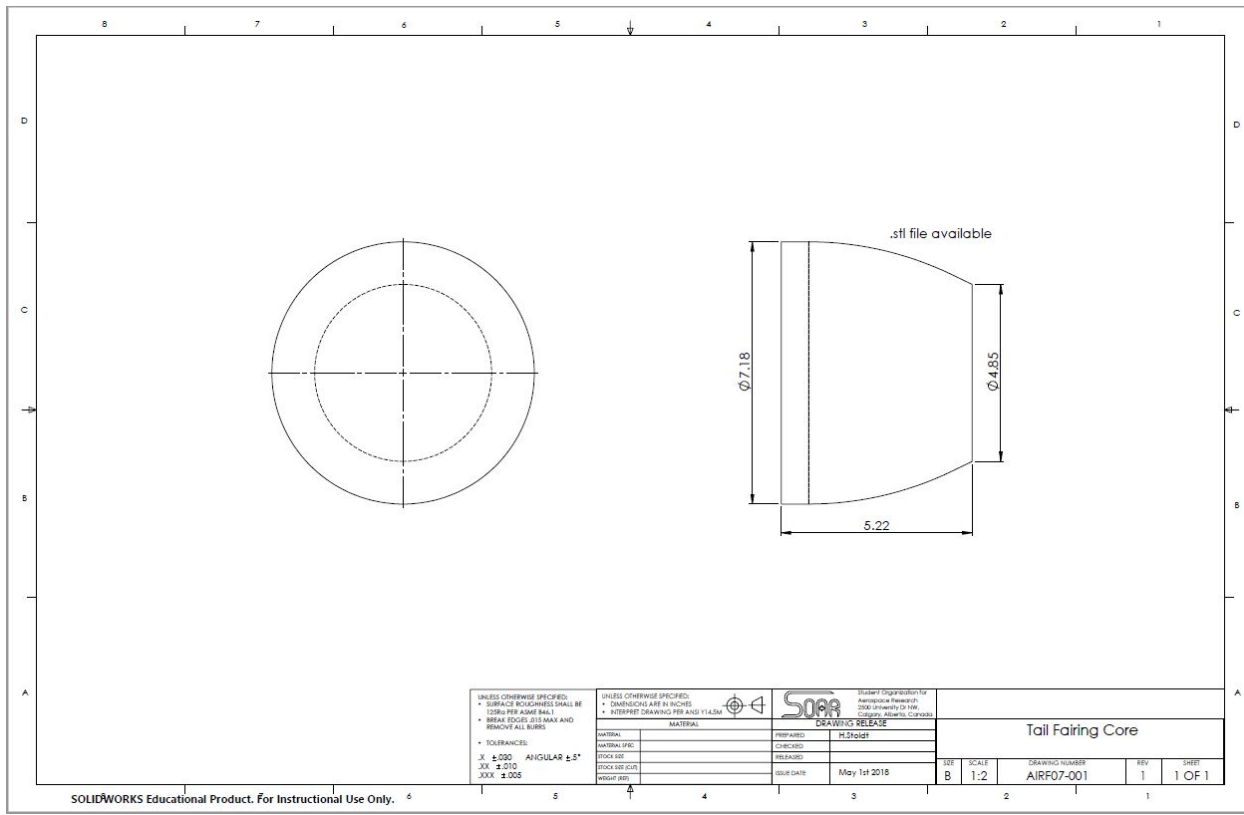


Figure. Tail Fairing Core Drawing

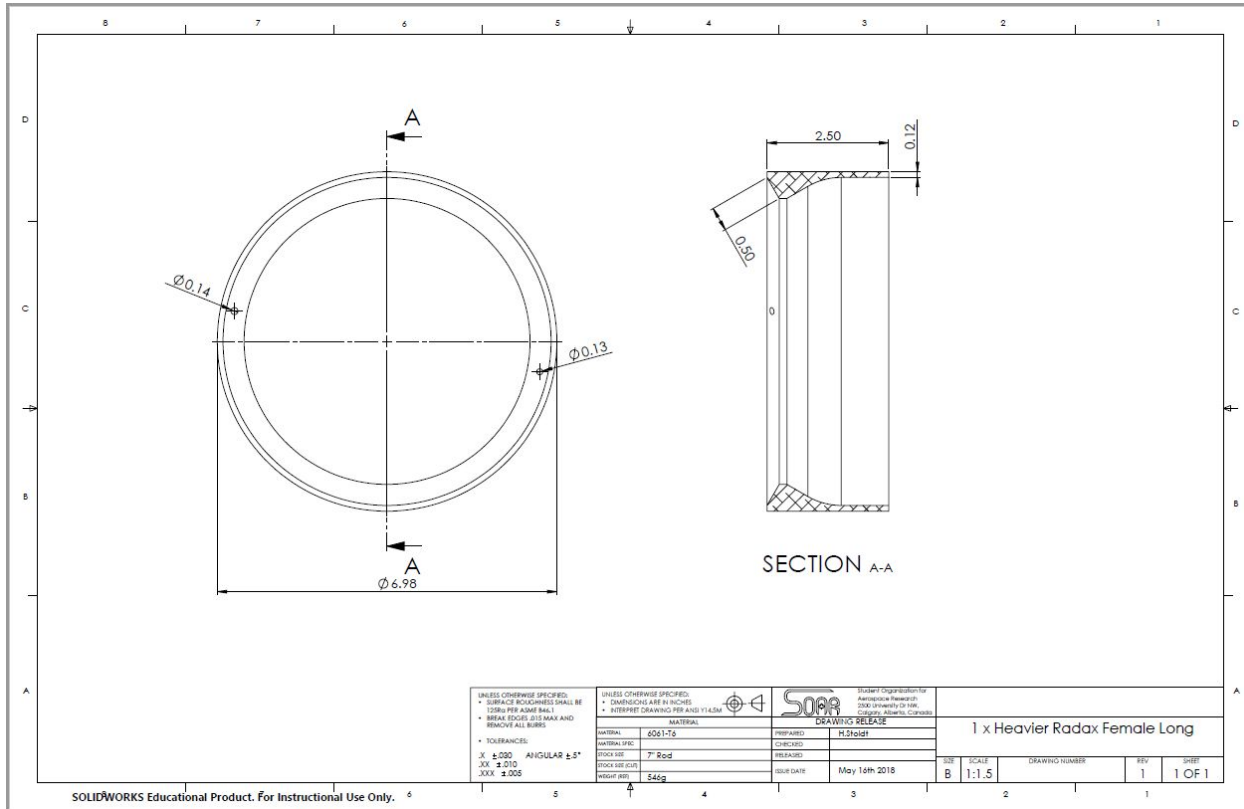


Figure. Long (Upper) Female Radax Joint Drawing

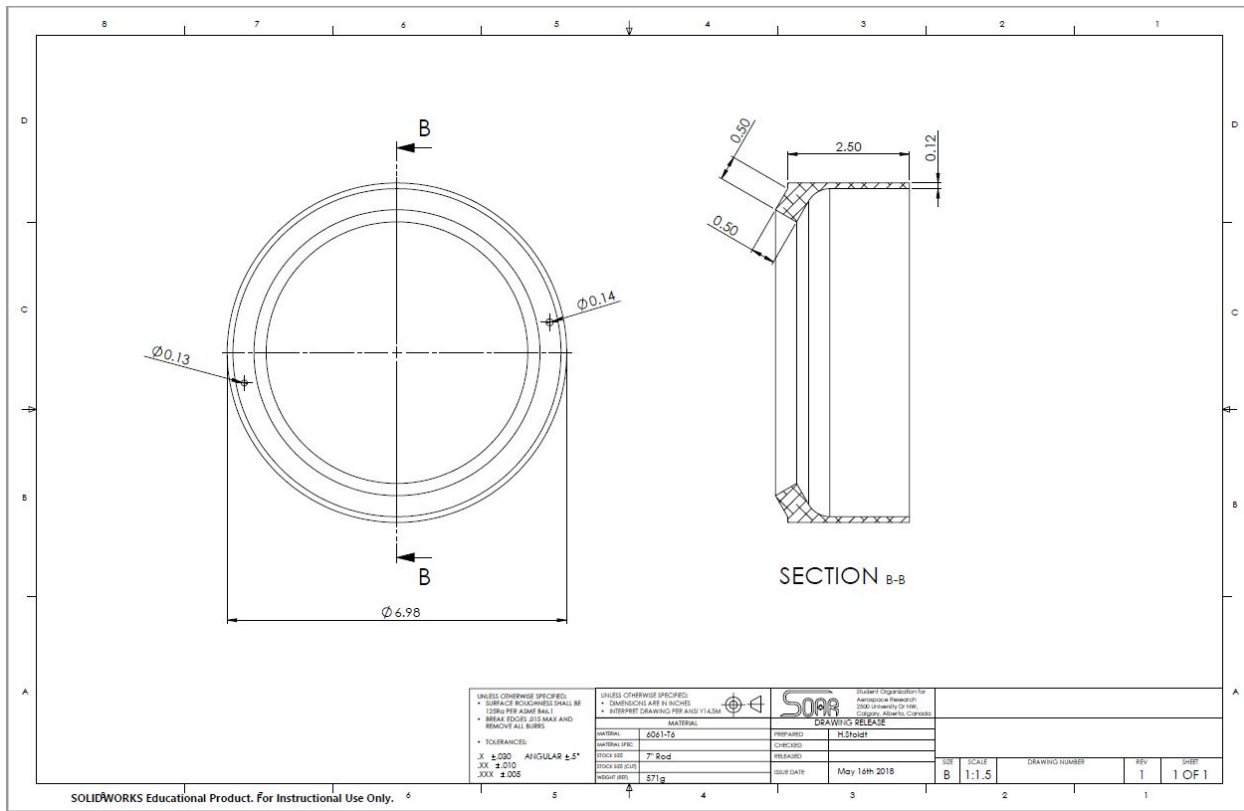


Figure. Long (Upper) Male Radax Joint Drawing

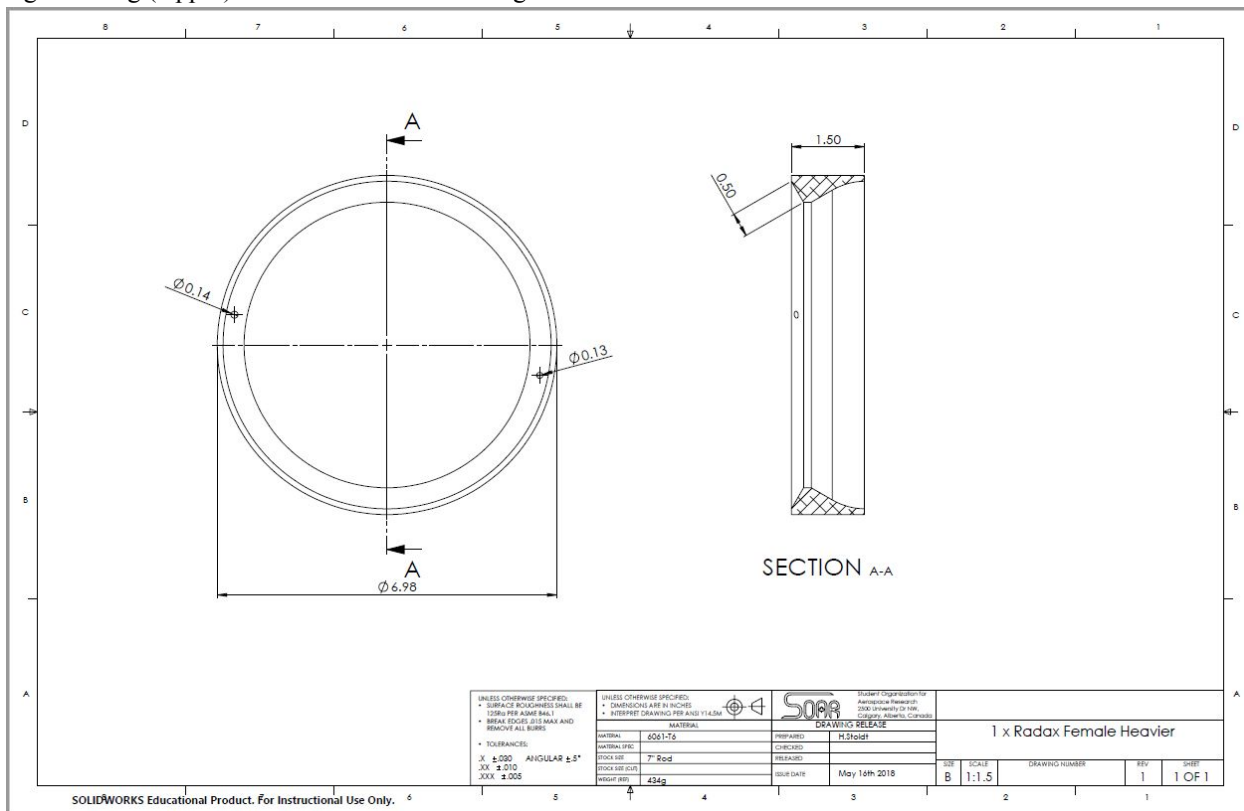


Figure. Short (Lower) Female Radax Joint Drawing

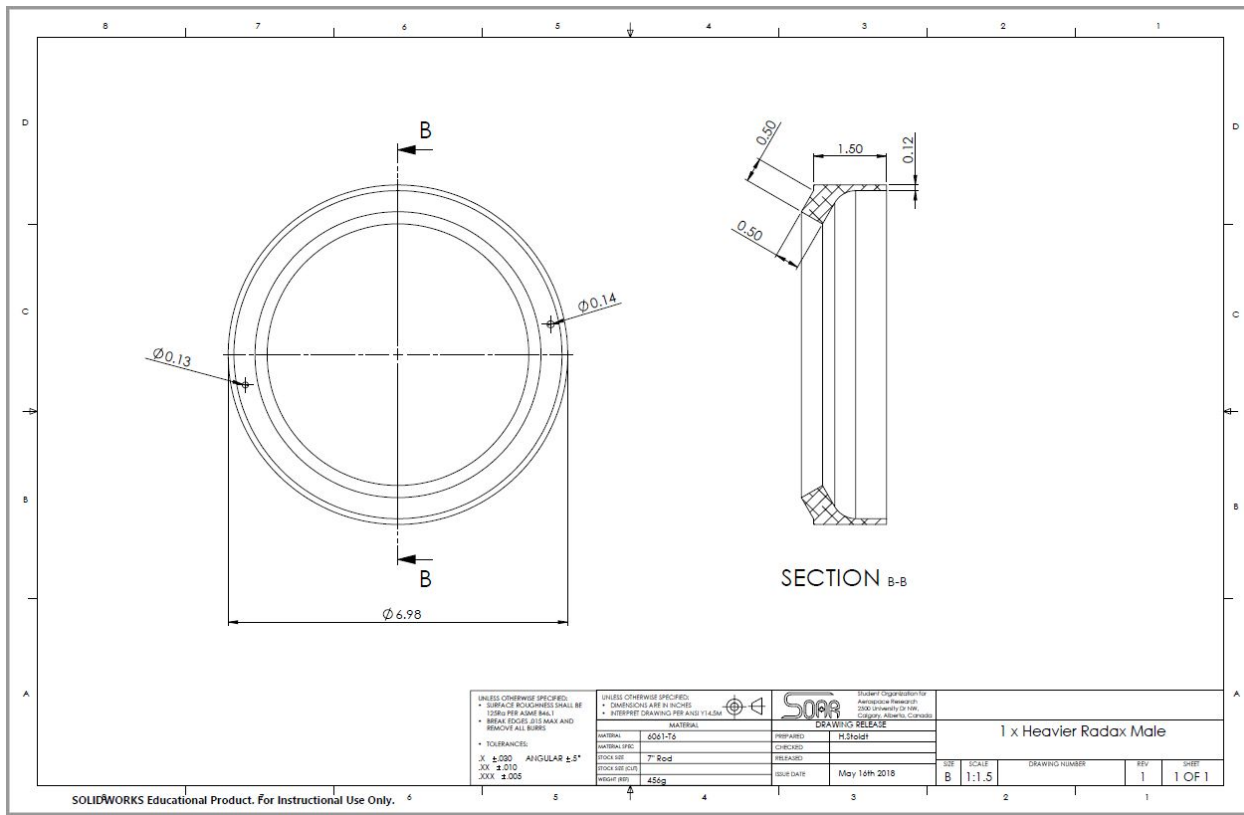


Figure. Short (Lower) Male Radax Joint Drawing

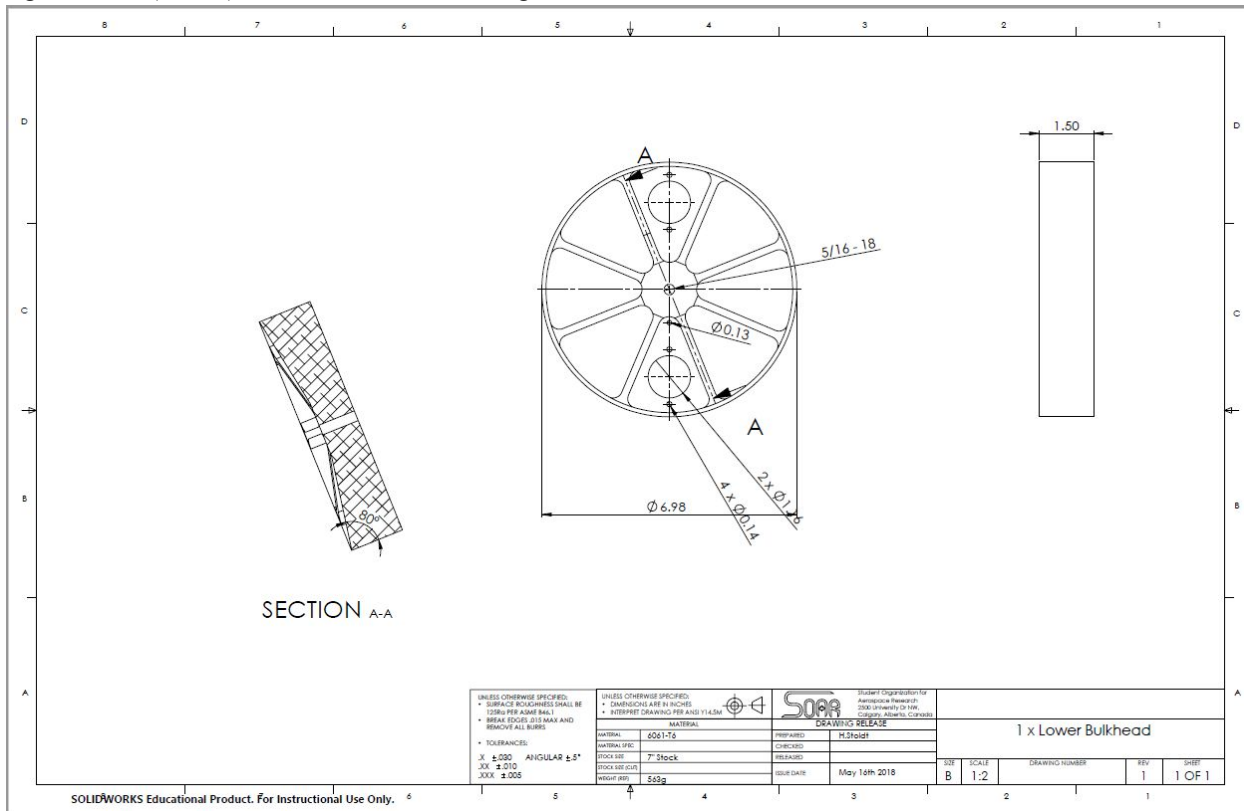


Figure. Lower Bulkhead Drawing

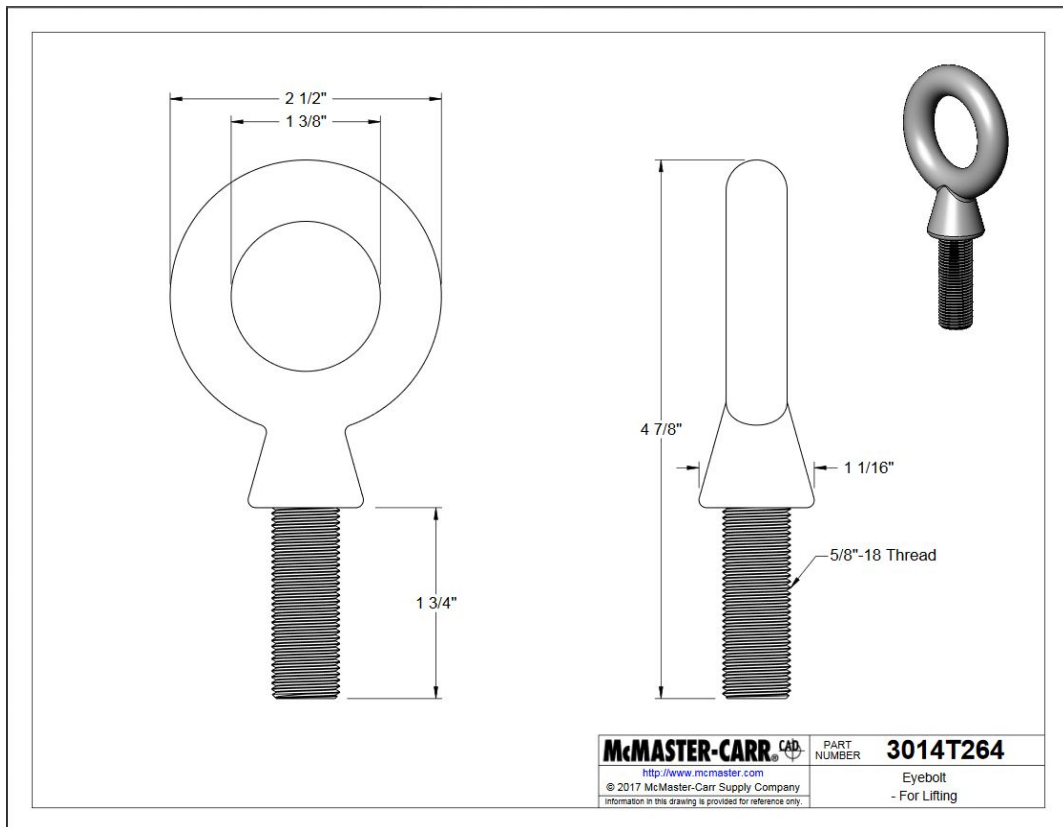


Figure. Lower Bulkhead Eye Bolt Drawing

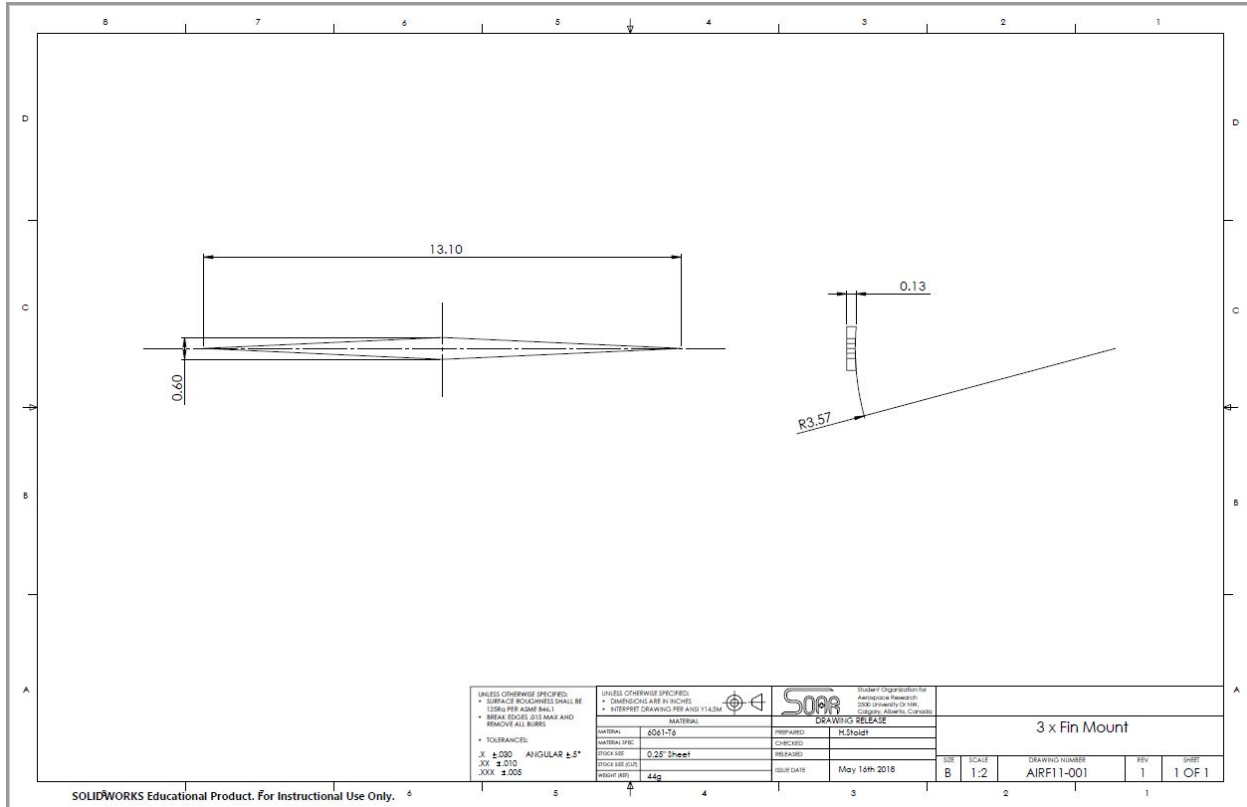


Figure. Fin Mount Drawing

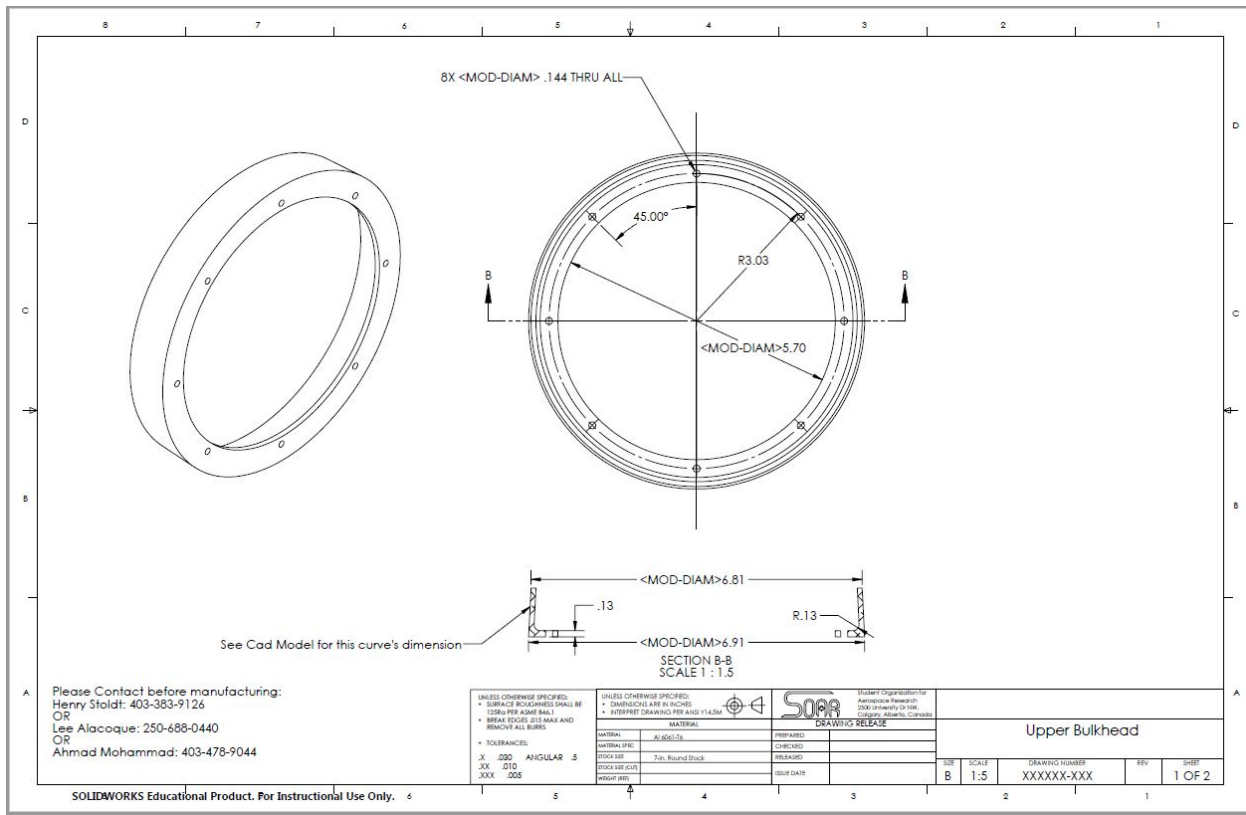


Figure. Upper Bulkhead Drawing

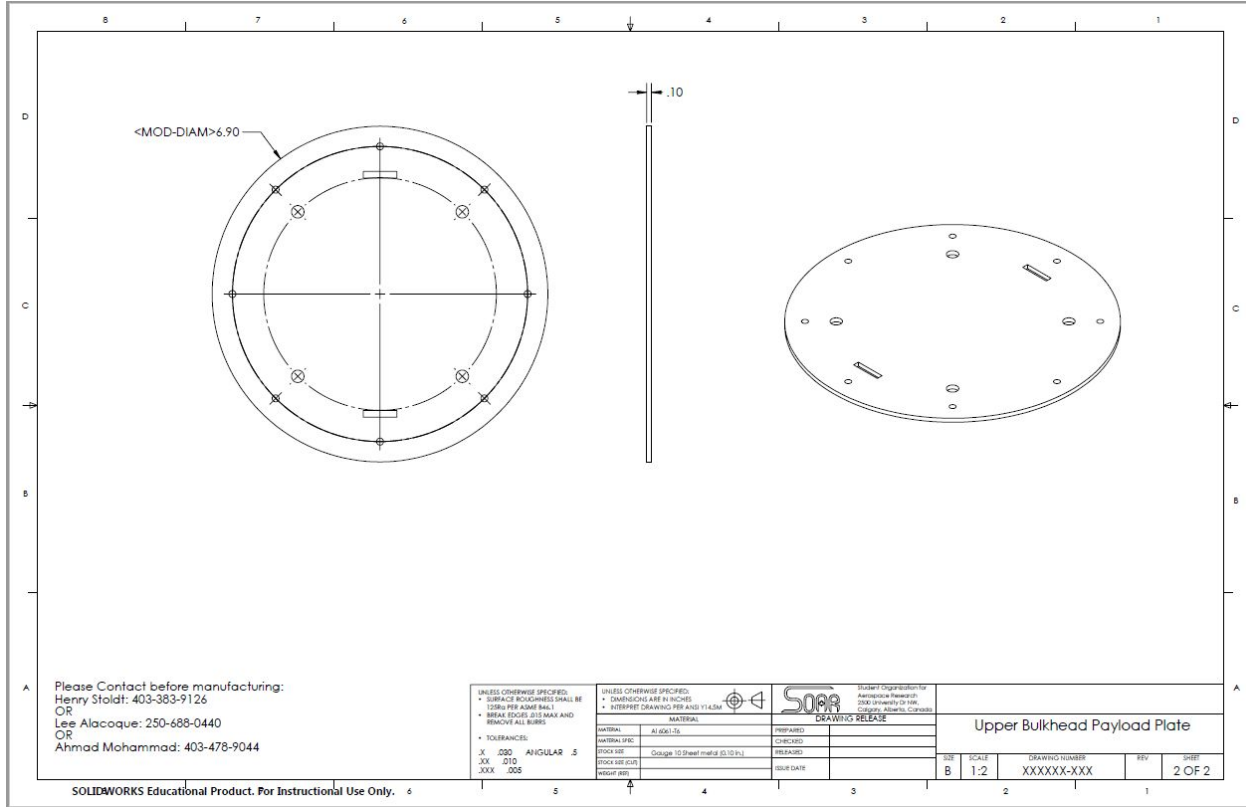


Figure. Upper Bulkhead Payload Plate Drawing

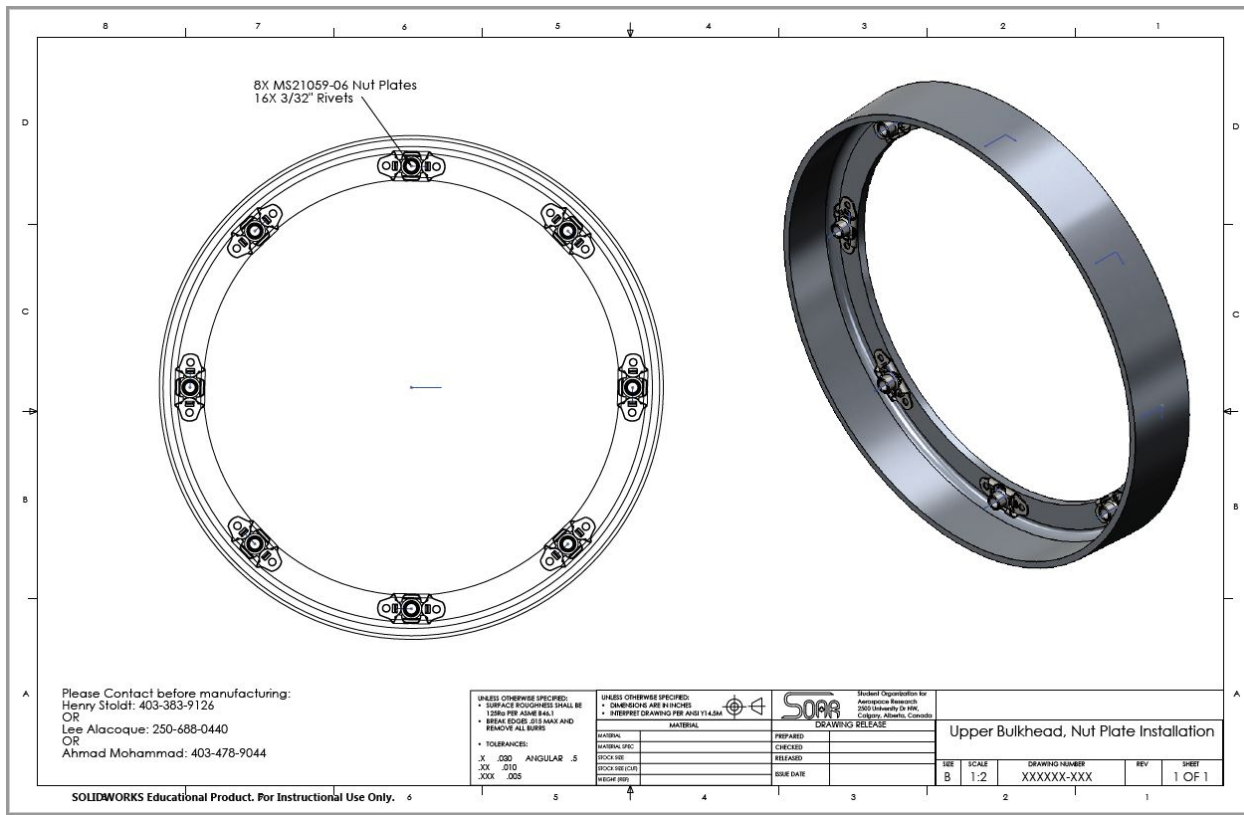


Figure. Upper Bulkhead with nut plates installed

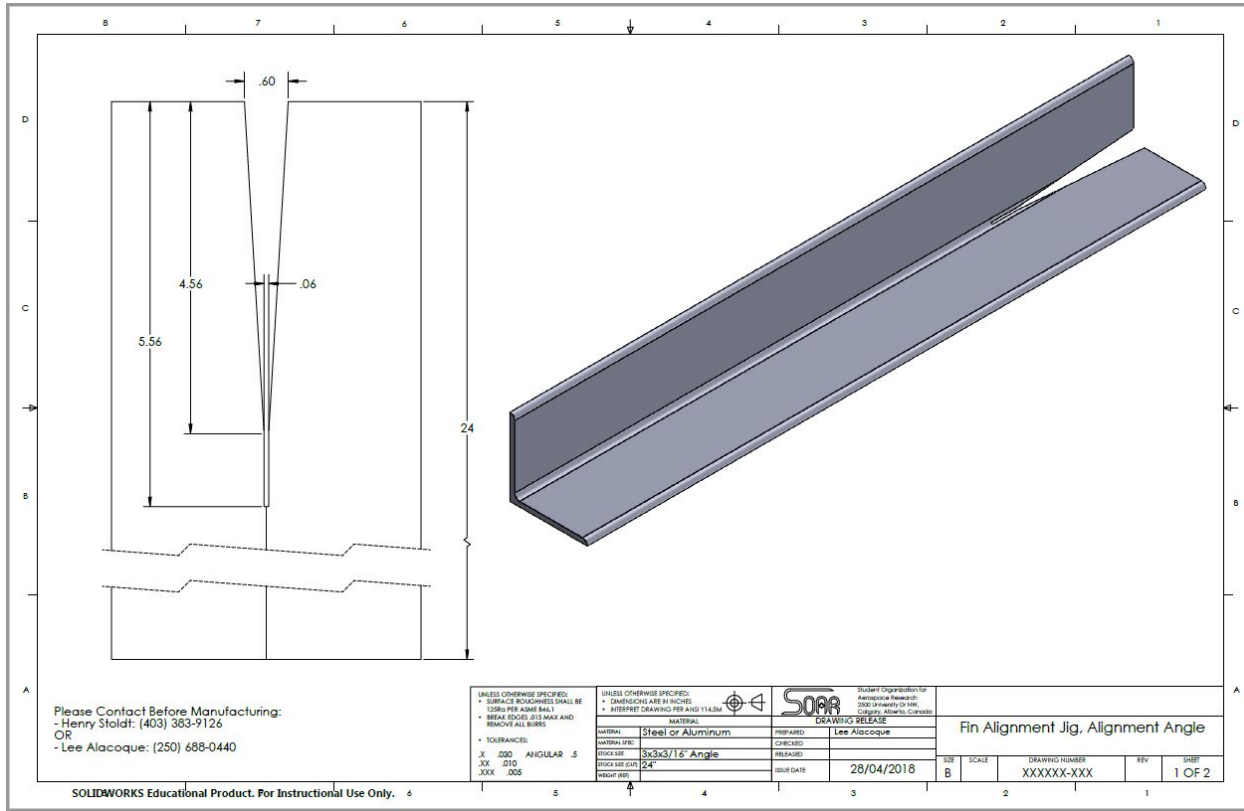


Figure. Fin Alignment Jig, Alignment Angle Drawing

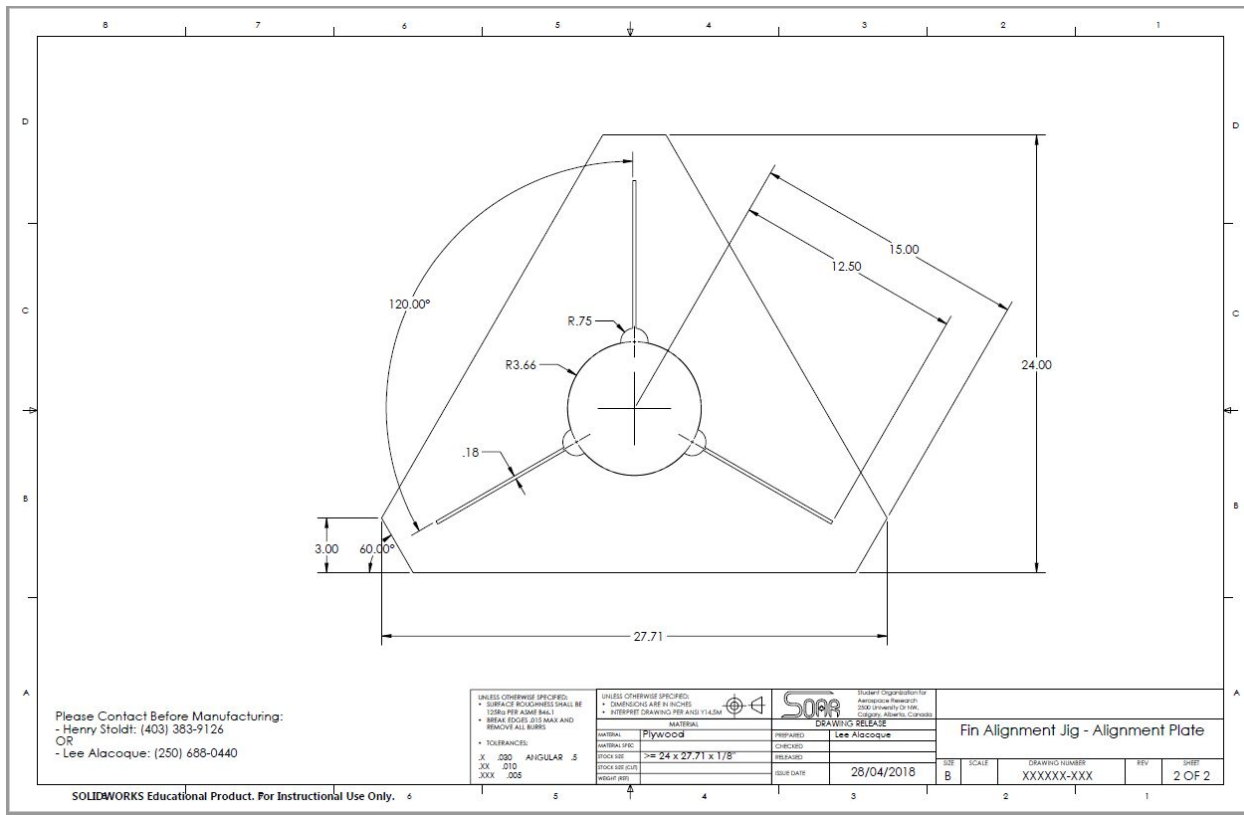


Figure. Fin Alignment Jig, Alignment Plate Drawing

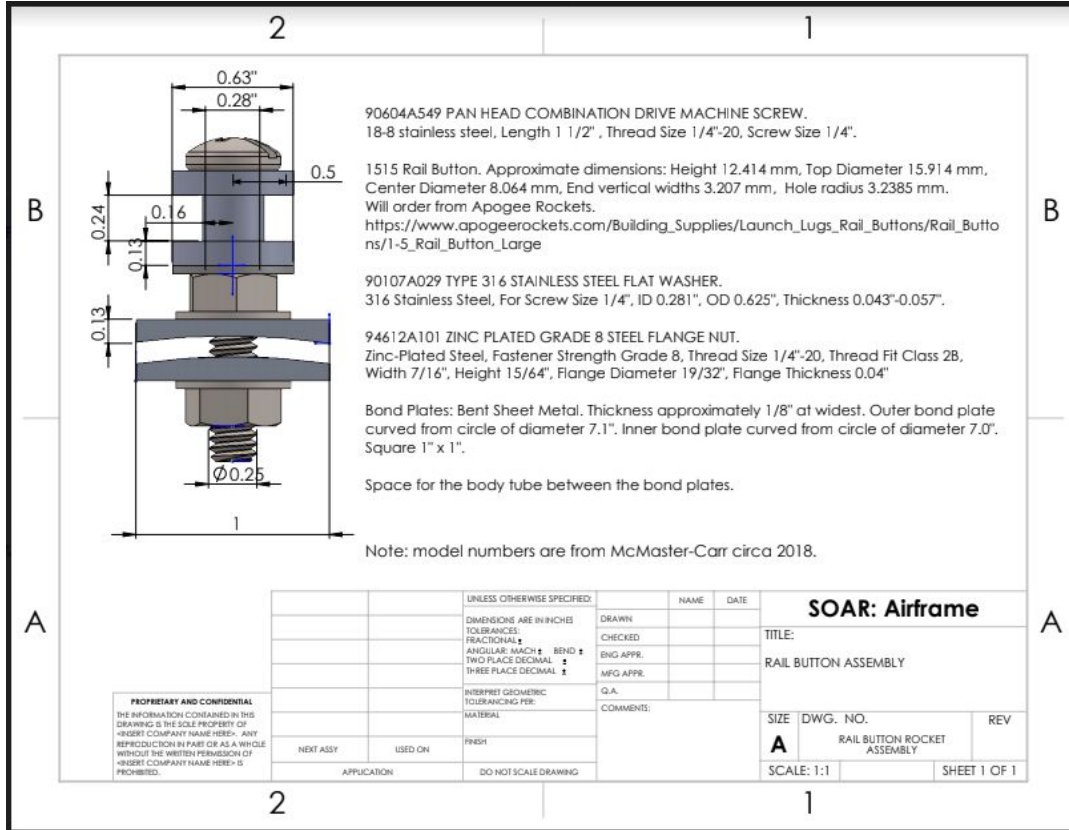


Figure. Launch Lug Assembly Drawing

Recovery Subsystem Drawings

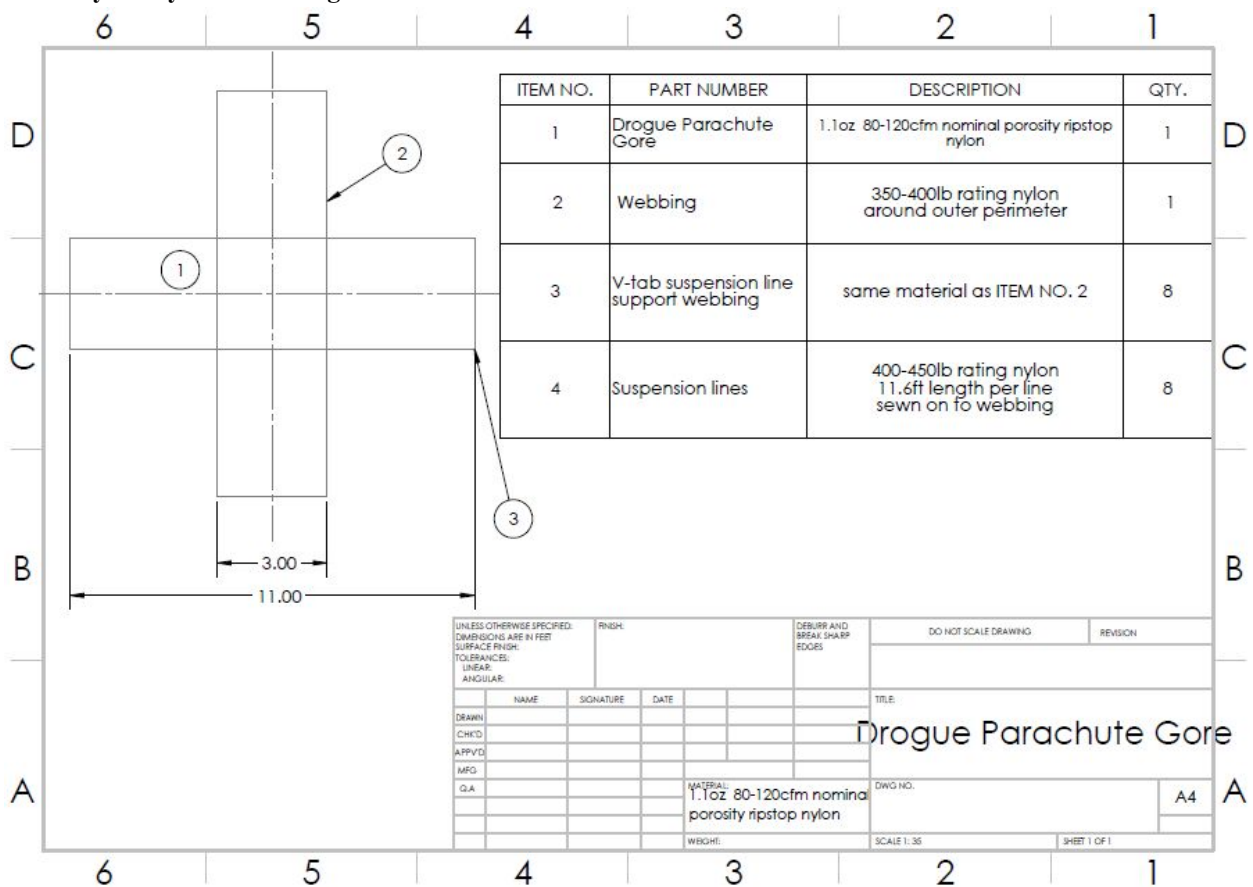


Figure : Drogue Parachute Gore

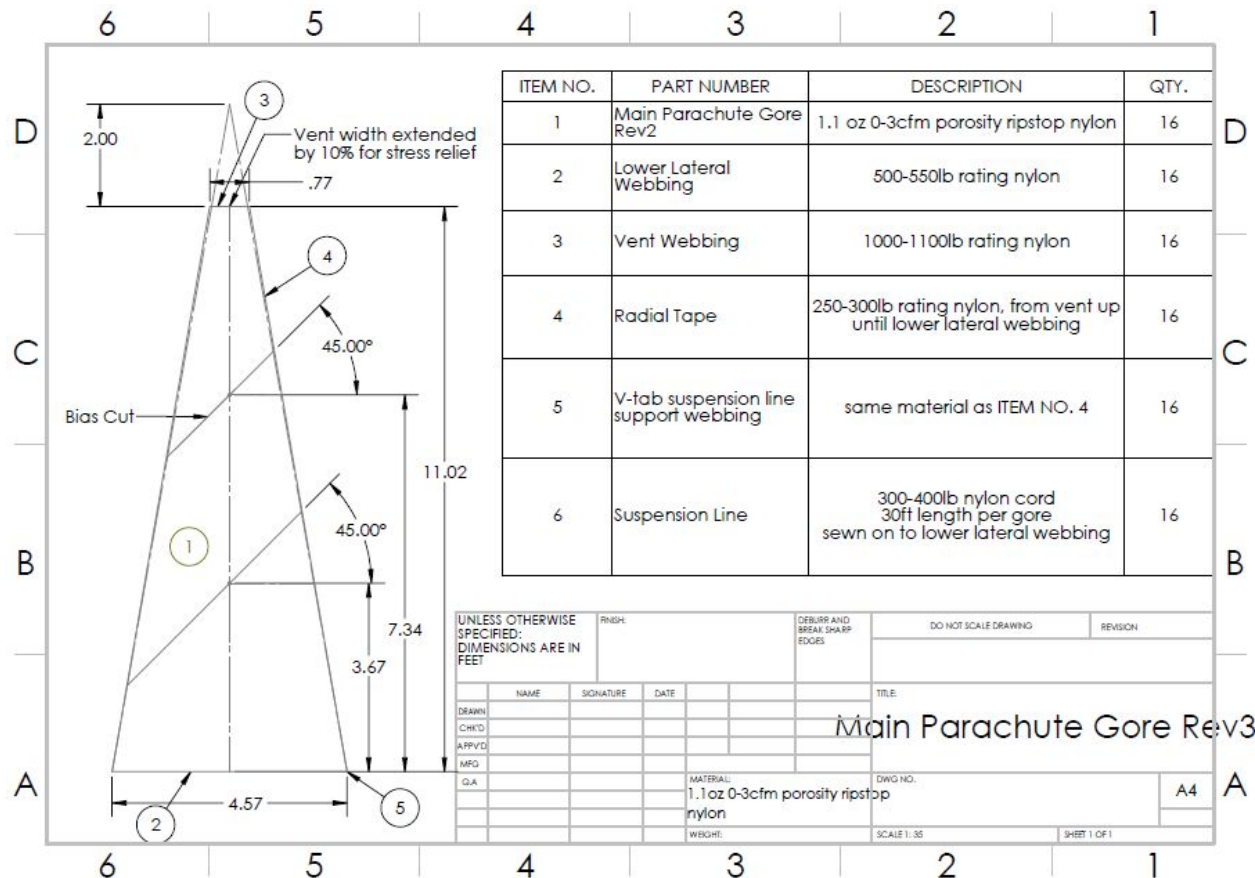


Figure : Main Parachute Gore

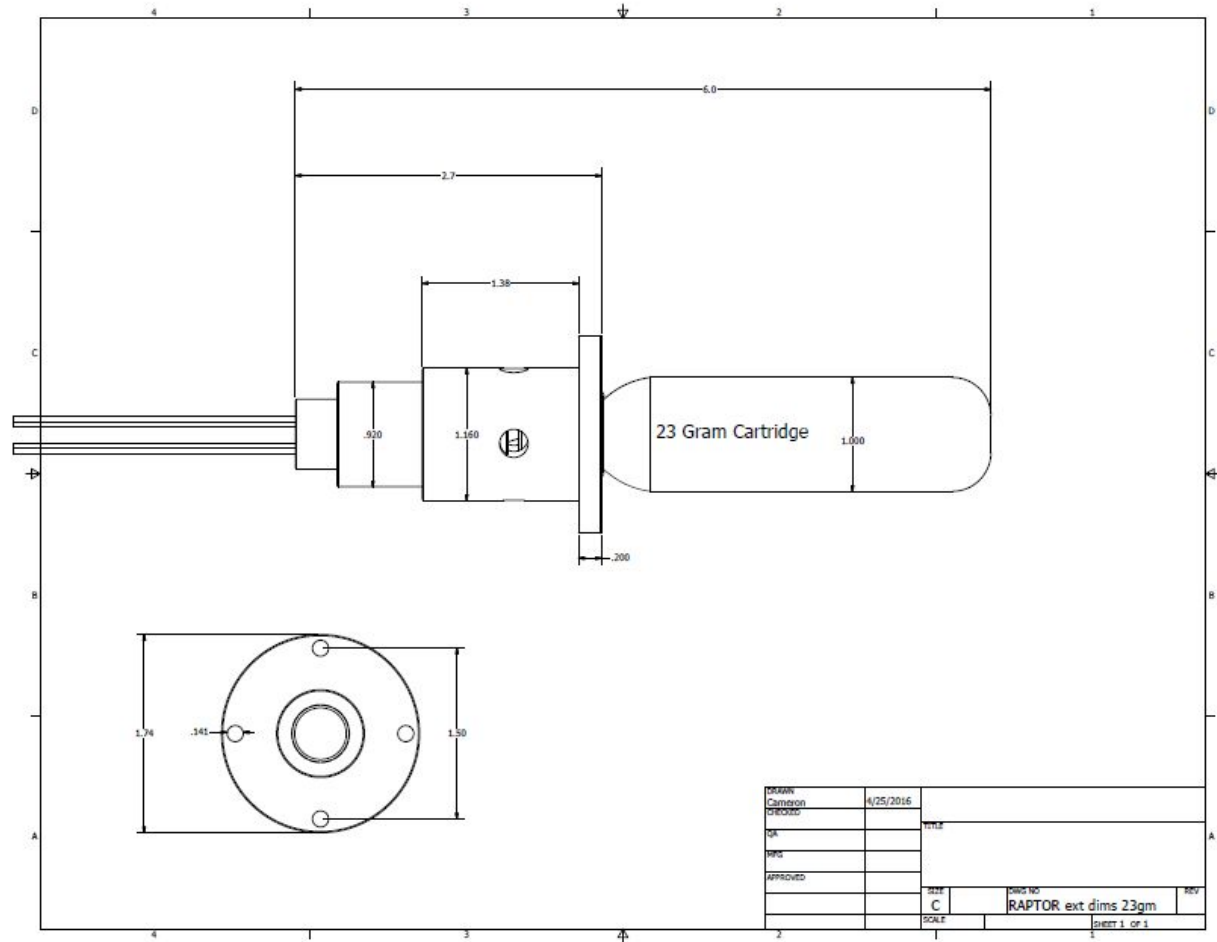


Figure : Drogue Parachute CO₂ Release System - 23 gram cartridge shown

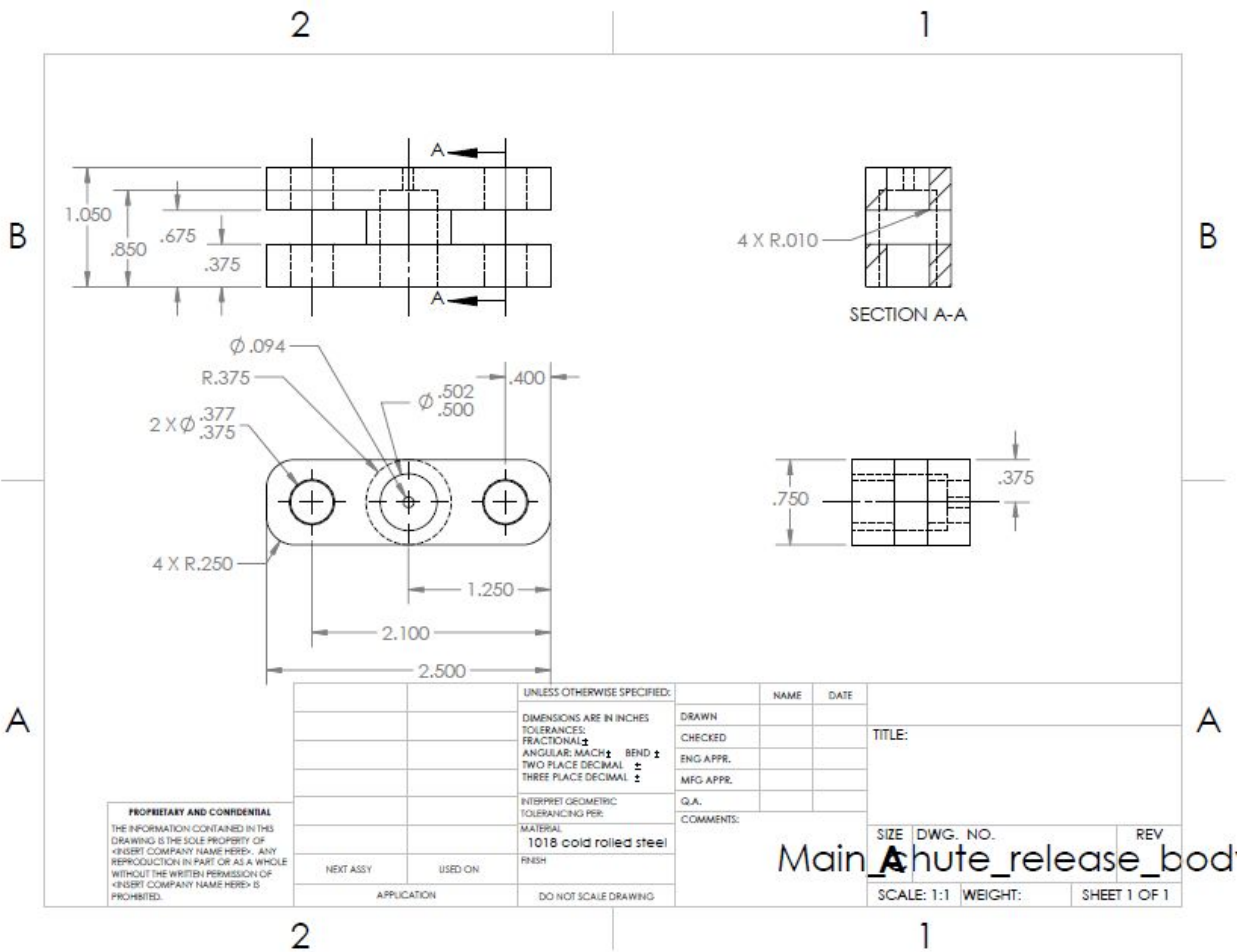


Figure : Main Parachute Release System - Main Body

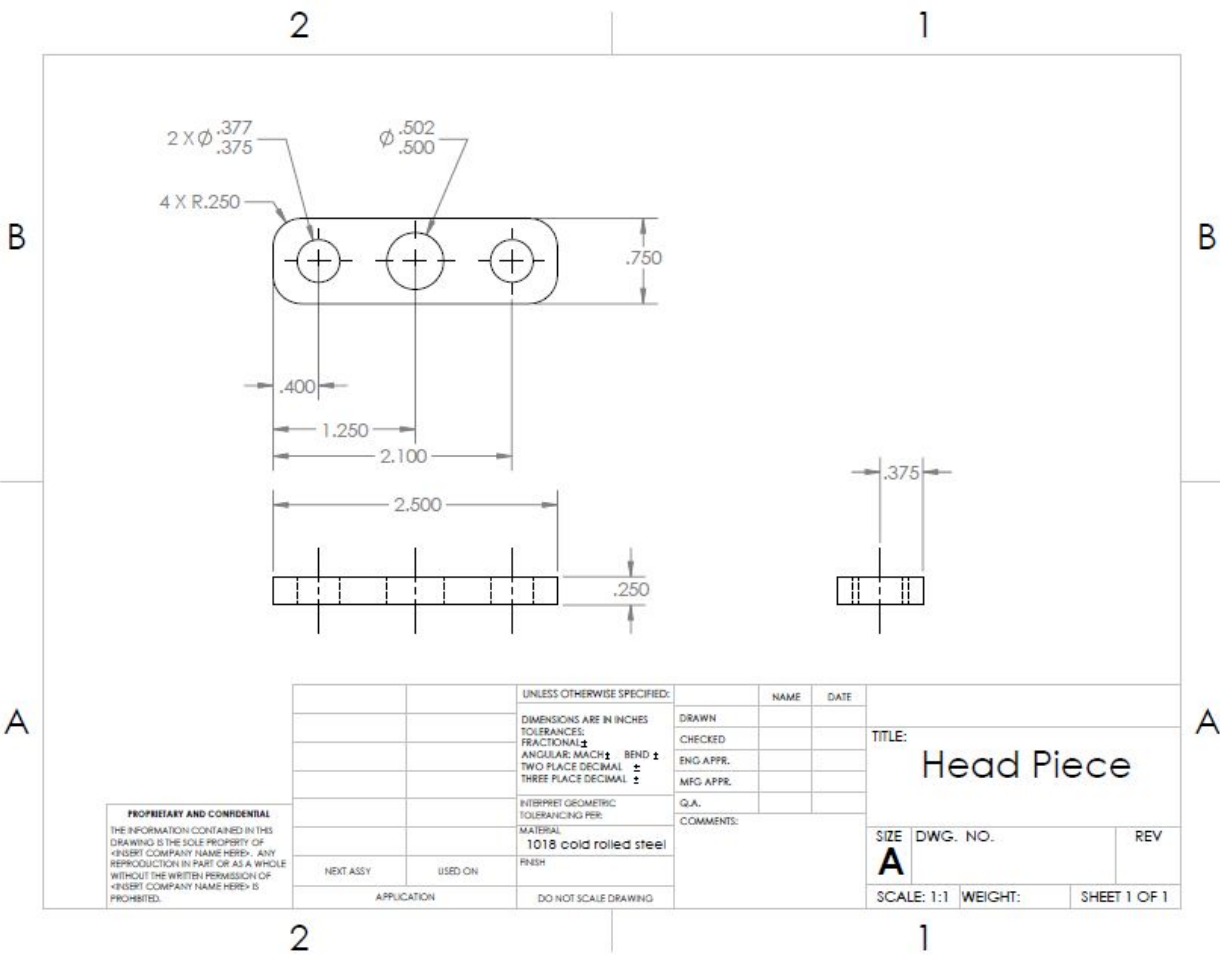


Figure : Main Parachute Release System - Pin Part

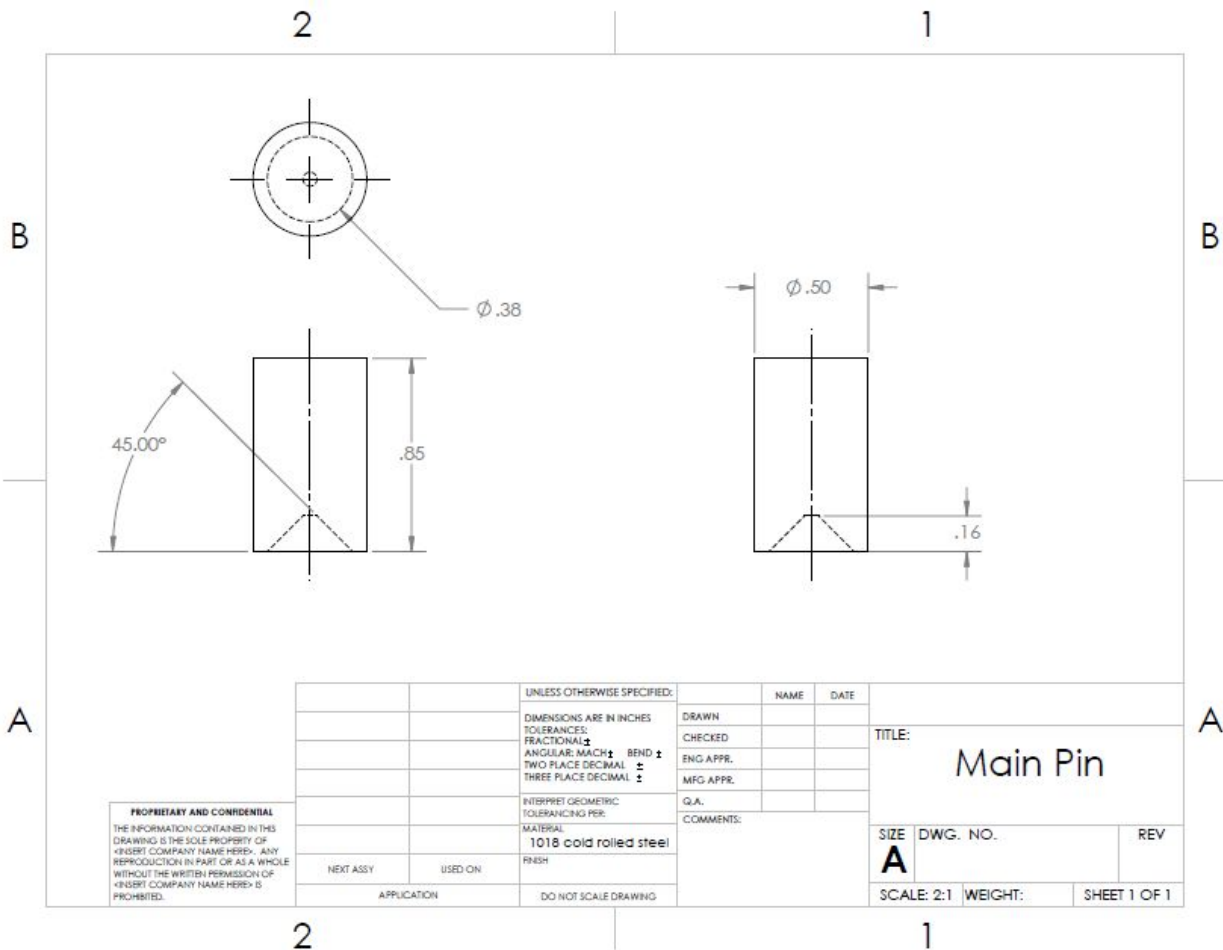


Figure : Main Parachute Release System - Center Pin

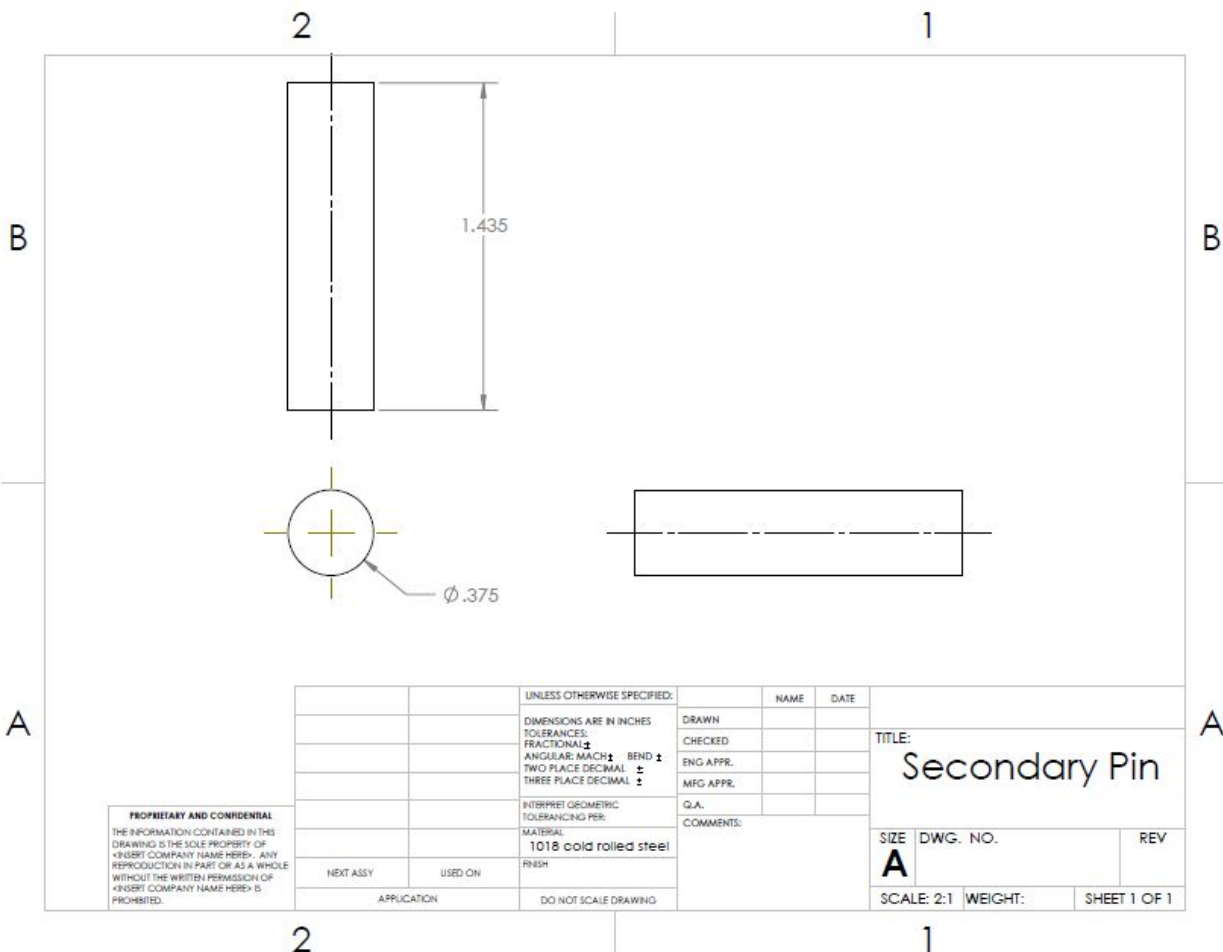


Figure. Main Parachute Release System - Side Pins

Propulsion Subsystems Drawings

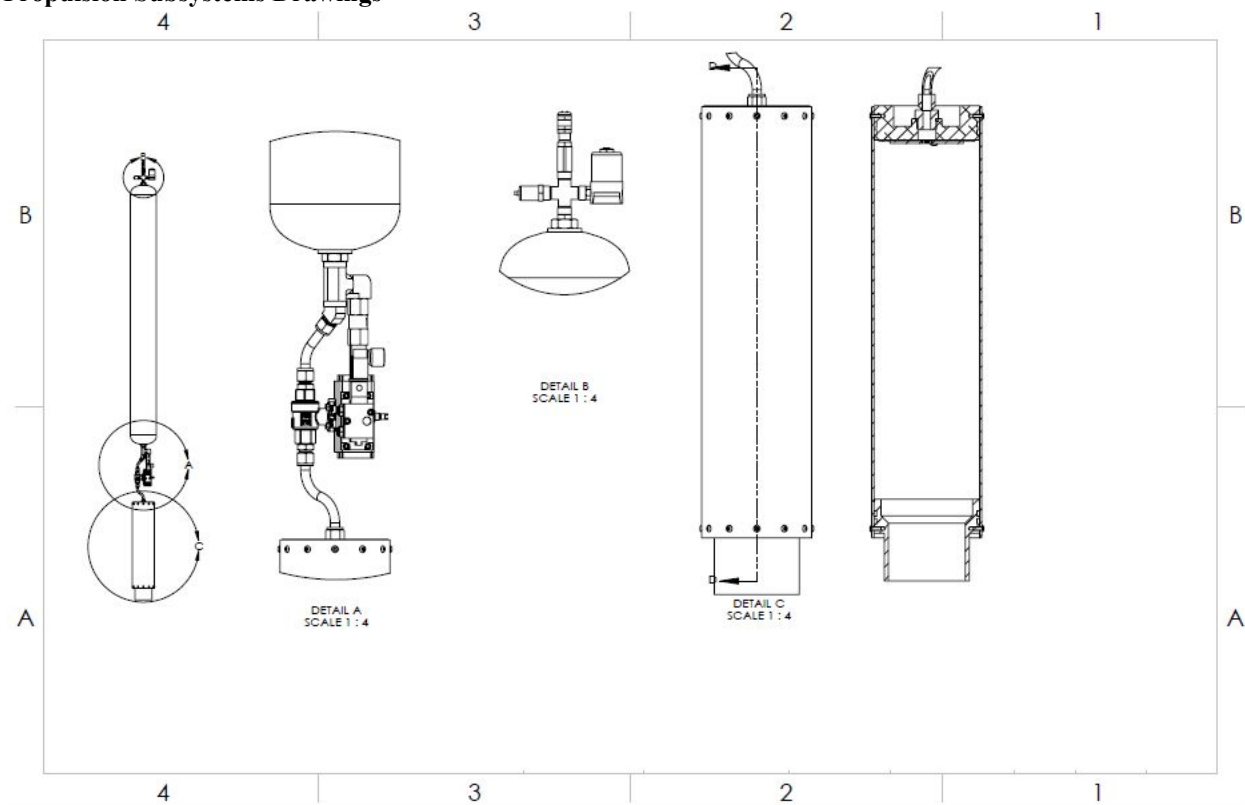


Figure. Propulsion system Assembly Drawing

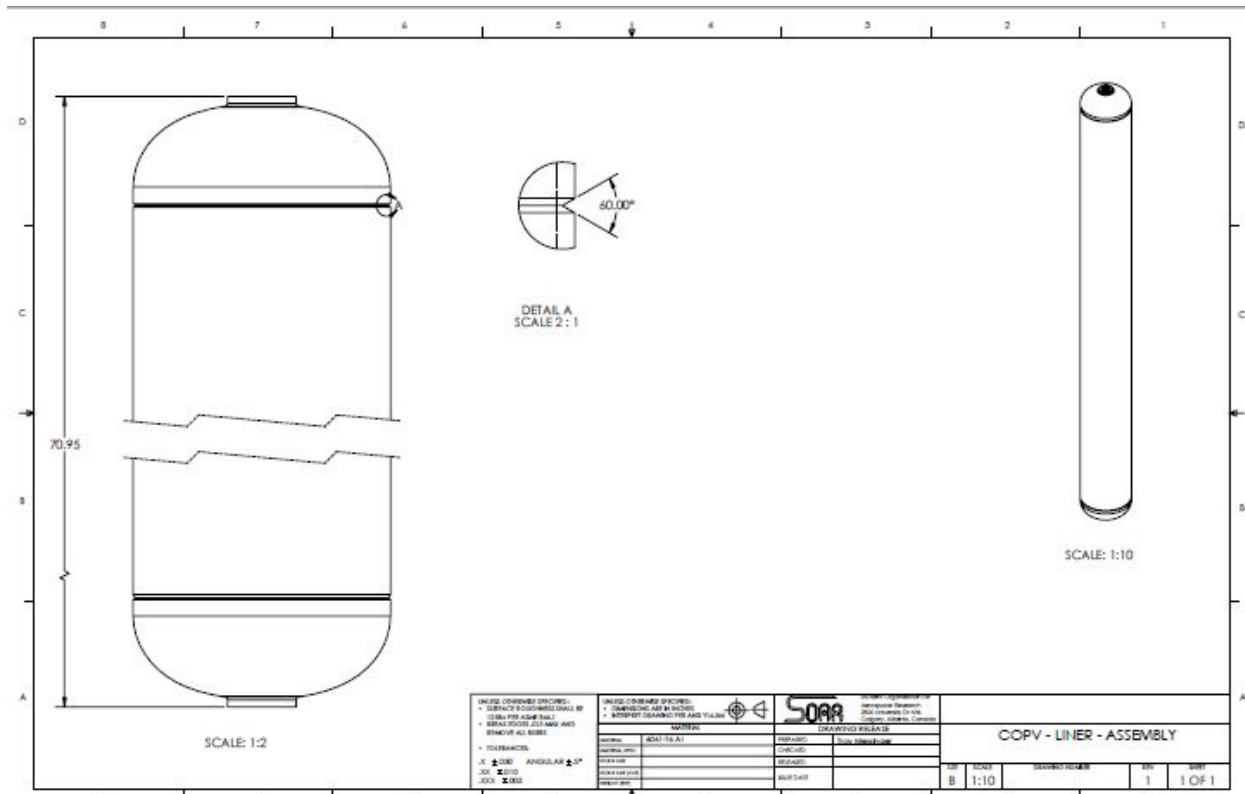


Figure. COPV Liner Assembly

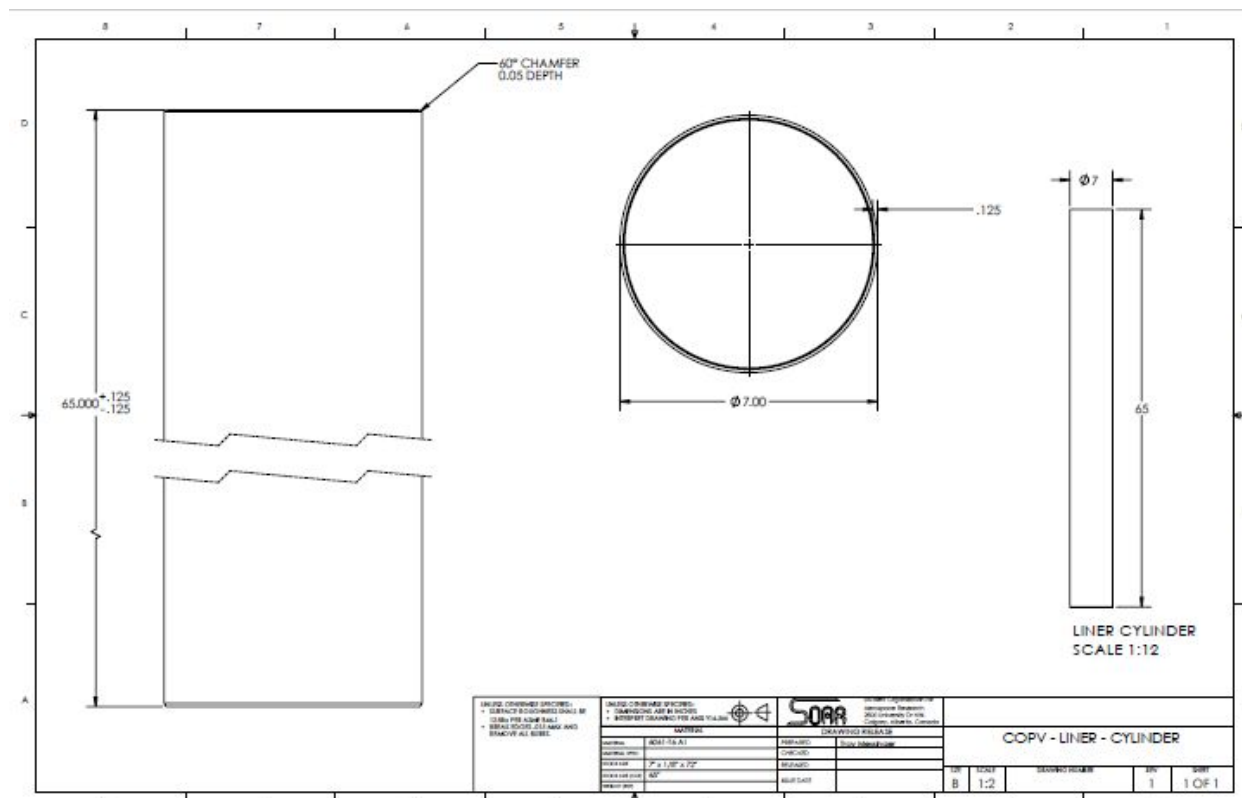


Figure. COPV liner cylinder

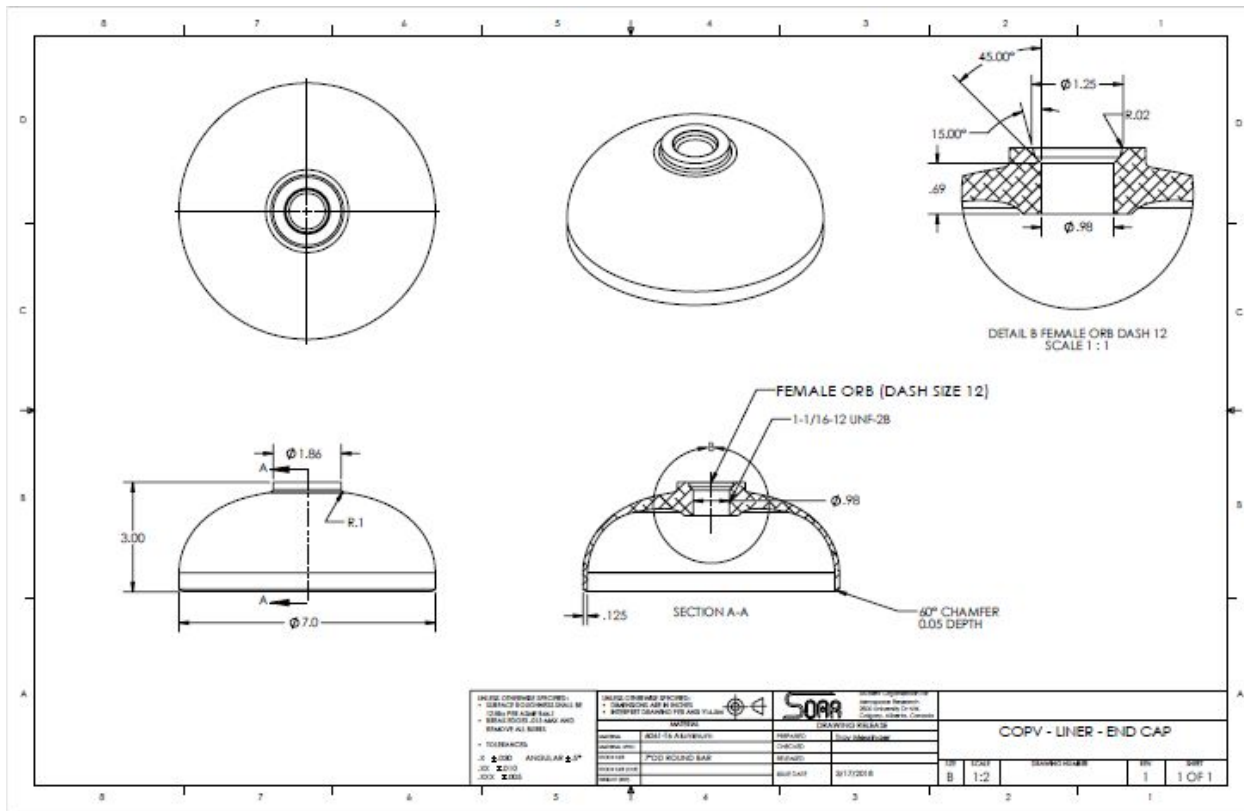


Figure. COPV Liner End Cap

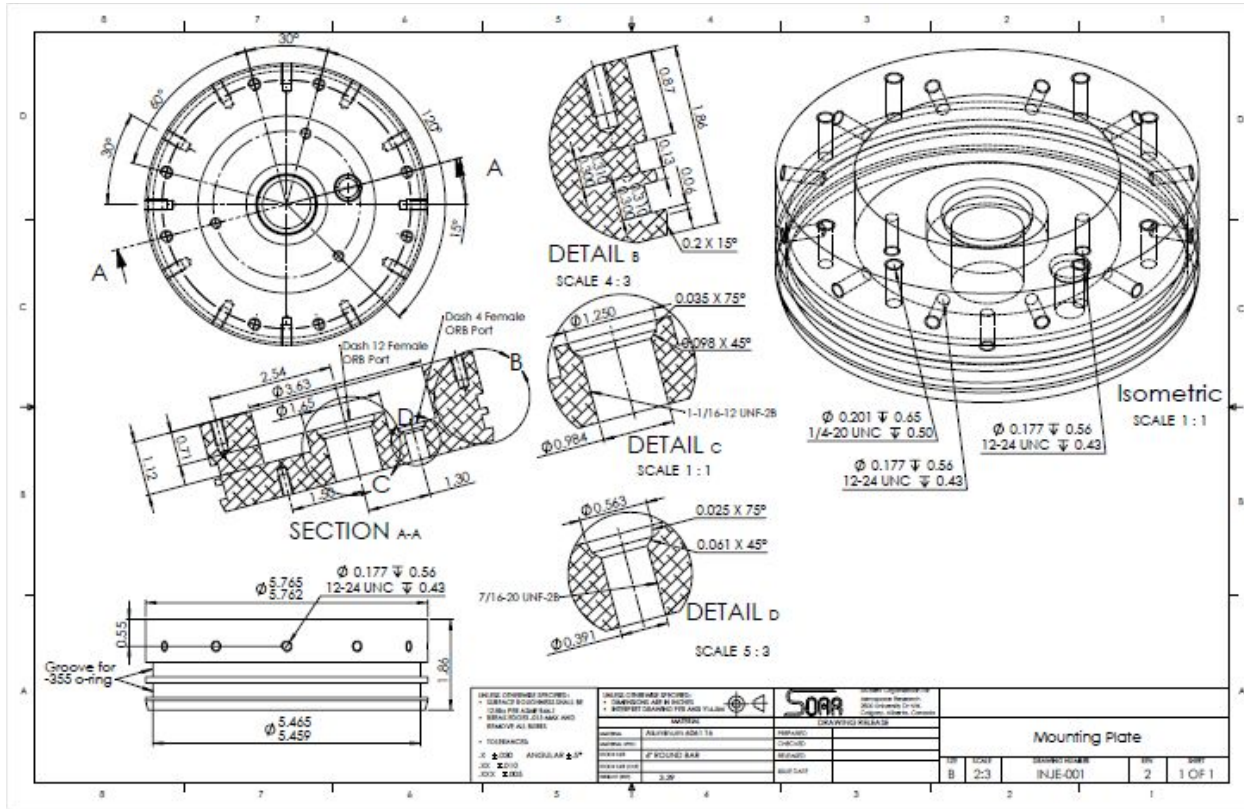


Figure. Axial Injector

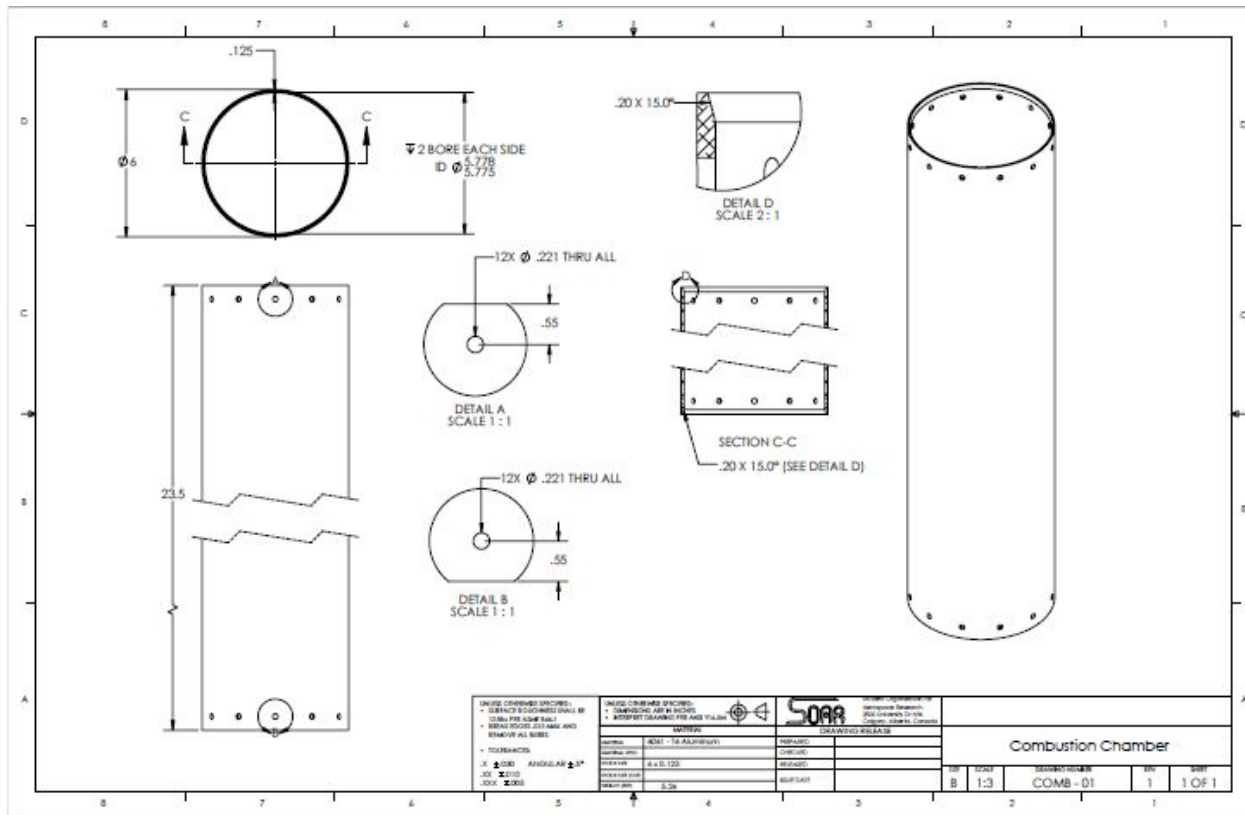


Figure. Combustion Chamber

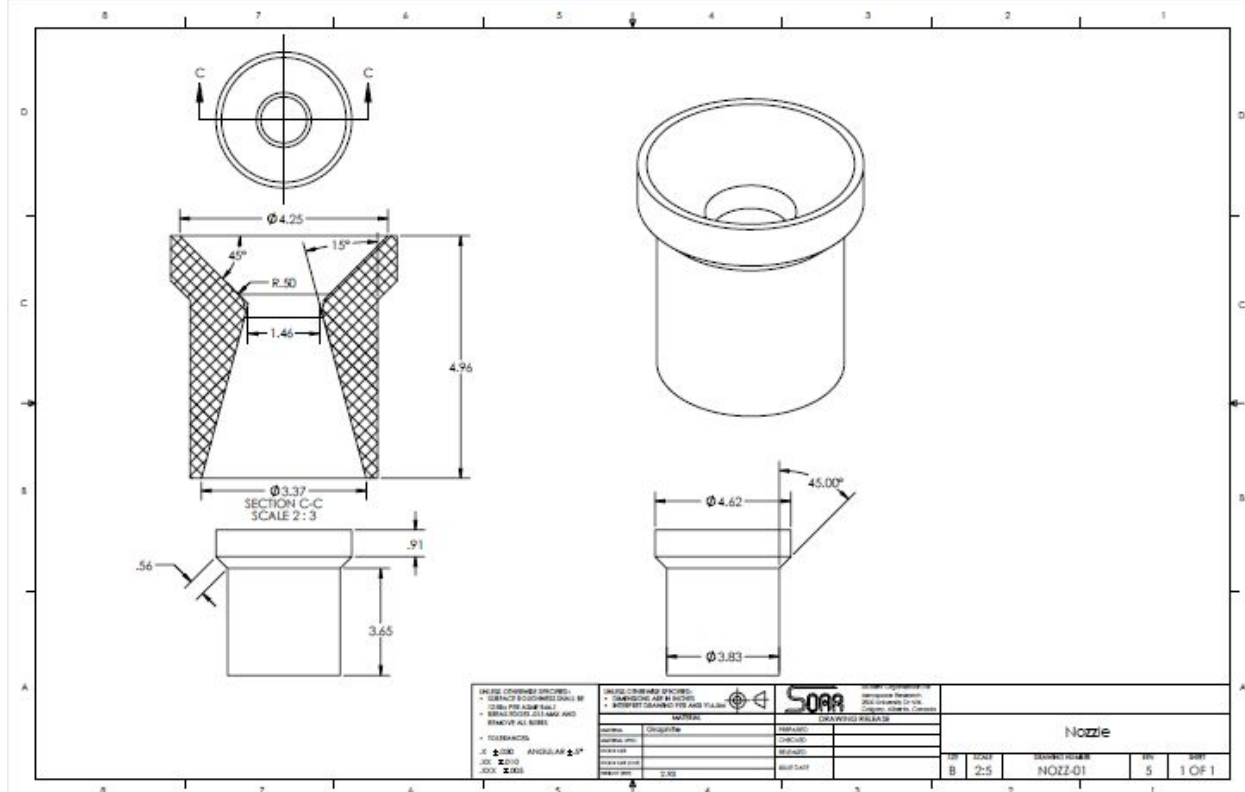


Figure. Nozzle Graphite

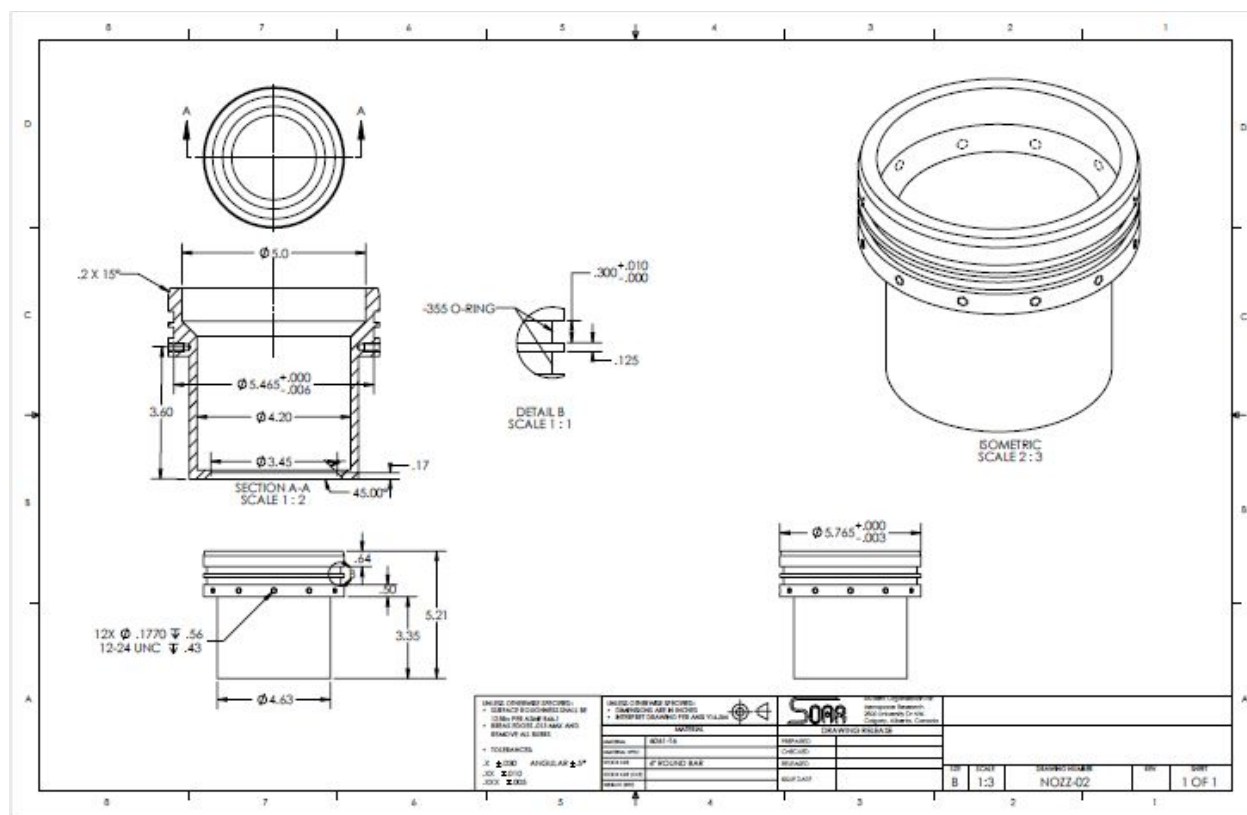


Figure. Nozzle Aluminum Housing

Avionics / Electronics Subsystems Drawings:

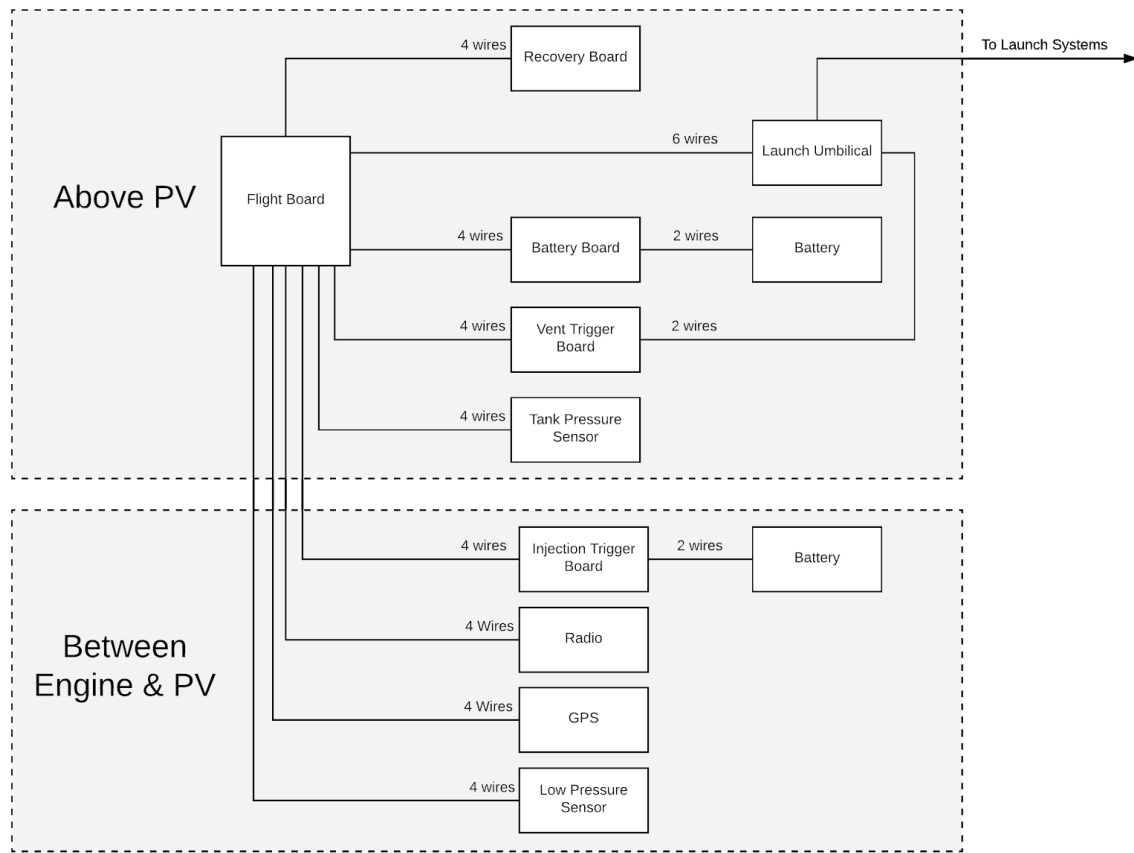


Figure. Overview of Internal Electronic Systems (Excluding Payload)

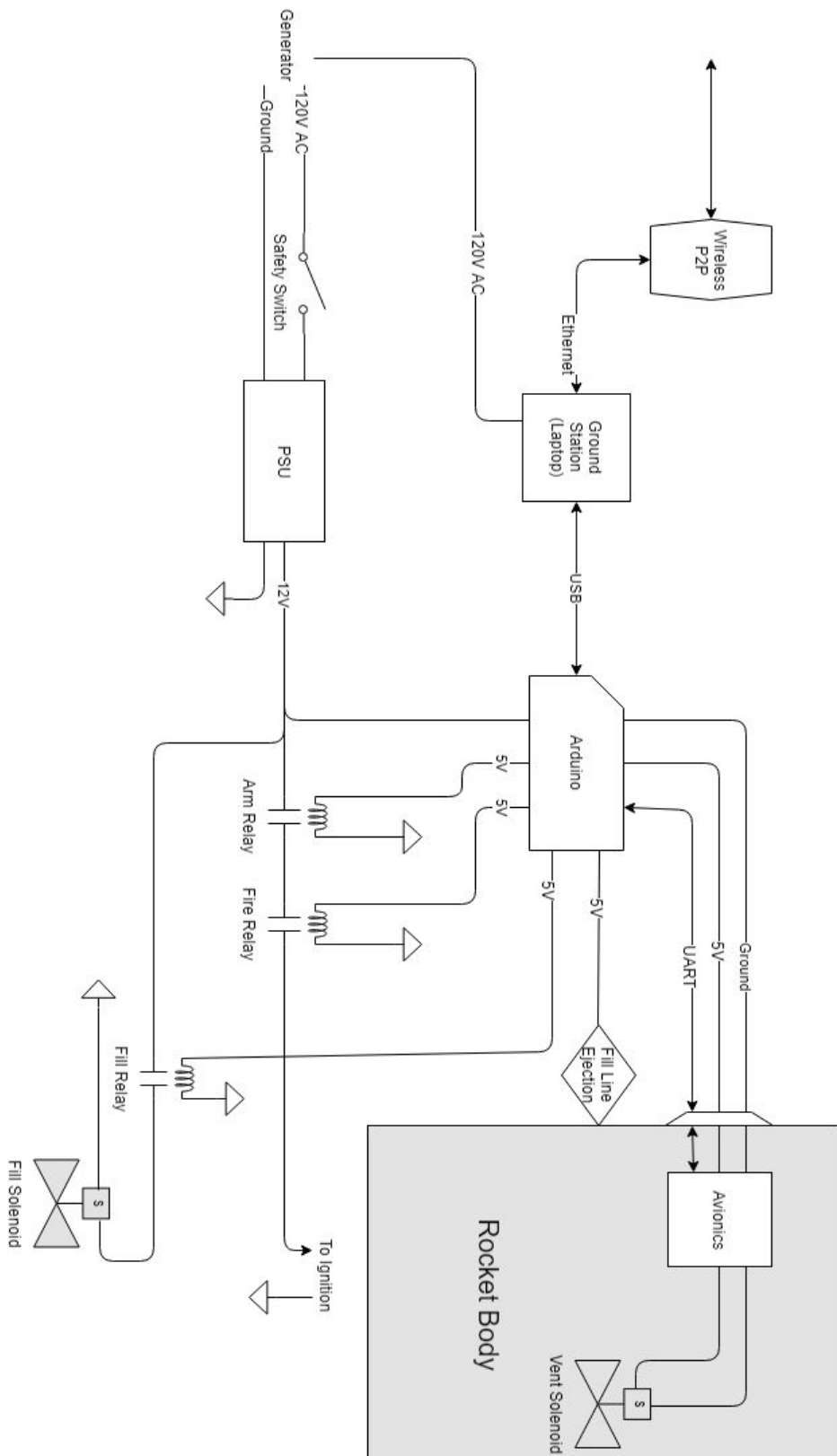


Figure. Overview of External Electronic Systems

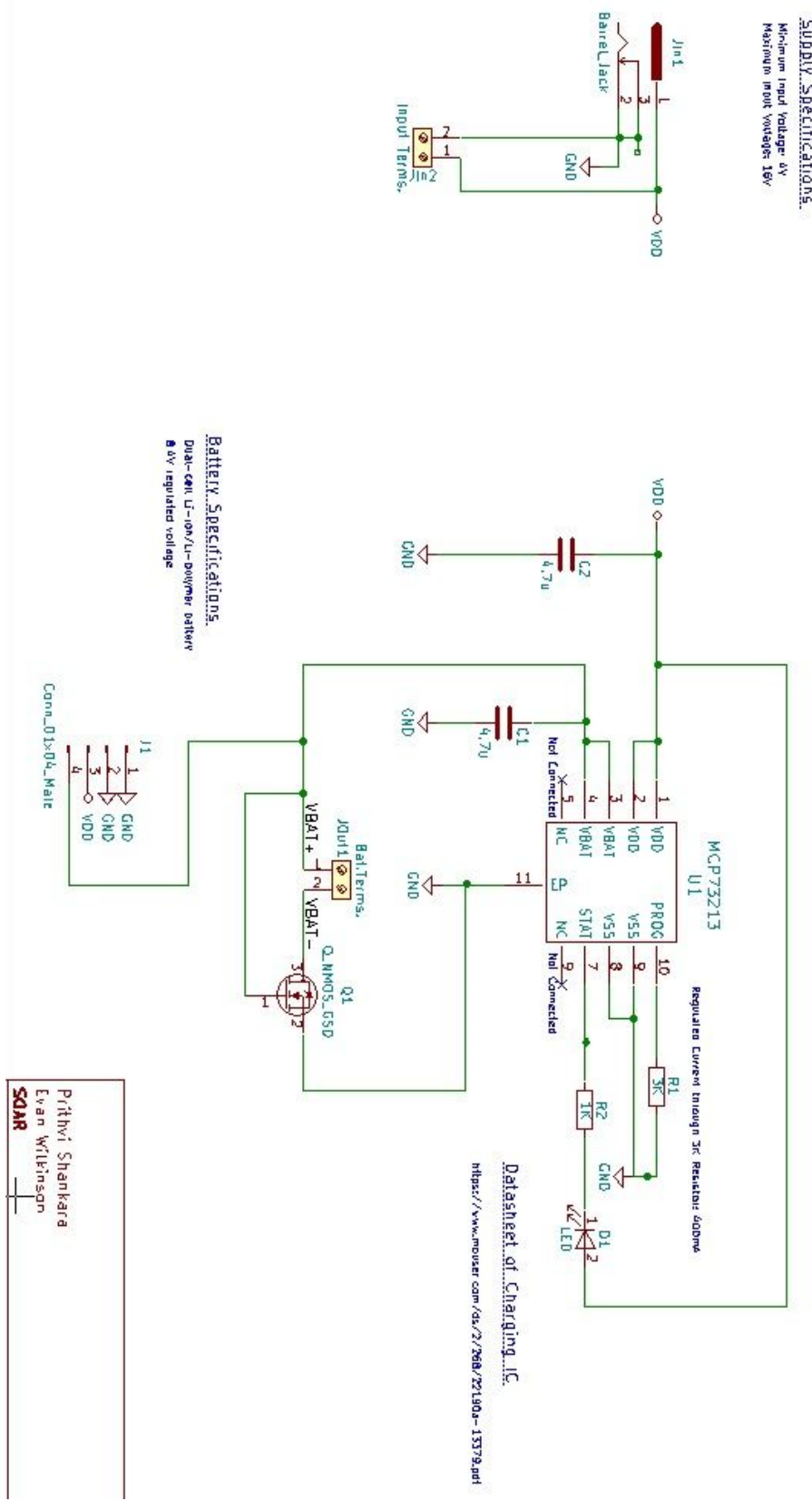


Figure. Main Avionics Board Schematic

APPENDIX VIII: Arming / Ignition Sequence

- 1) Arming Prechecks
 - a) Check N20 Tank is filled
 - b) Check Tank temperature
 - c) Check Avionics signals read Ok
 - d) Check permission to fire is granted from supervisors
- 2) Arm
 - a) Fill valve ejection
- 3) Fire Precheck
 - a) Check Tank is filled
 - b) Check Tank temperature
 - c) Check Avionics signals read Ok
 - d) Begin countdown
- 4) Fire
 - a) N20 valve is opened by Avionics
 - b) Igniter is shorted
 - c) Rocket Lifts off
 - d) Electrical Umbilical detach

Acknowledgments

The SOAR organization would like to express their sincere appreciation to their engineering advisor Dr. Craig Johansen for providing the appropriate resources,, technical knowledge, and opportunity to complete this ambitious project.

The SOAR organization would like to thank their science advisor Dr. Christopher Cully for his support of the scientific experimental components and electrical systems.

The SOAR organization would also like to thank Dr. Phil Langill, and the Rothney Astrophysical Observatory for providing the space, and resources for our testing facility.

The SOAR organization would like to thank Luxfer Gas Cylinders for the large amount of help and resources they provide to our team.

Lastly, the SOAR organization would like to thank the Schulich School of Engineering and the Faculty of Science for their generous contributions to the rocket project. Without your contribution the project would not be possible.

References

1. R. Aburashed, O. Almoqadam, S. Baumann, K. Griswold, J. Pawa, and S. Sridharan, “Design An Innovative Launch Vehicle,” Calgary, 2016.
2. C. Lanczos, The variational principles of mechanics. Dover Publications, 1986.
3. E. Oberg, F. D. Jones, H. L. Horton, and H. H. Ryffel, Machinery’s handbook. .
4. B. S. Waxman, J. E. Zimmerman, B. J. Cantwell, G. G. Zilliac, and E. C. Wells, “Mass Flow Rate and Isolation Characteristics of Injectors for Use with Self-Pressurizing Oxidizers in Hybrid Rockets.”
5. G. Dyer, J., Doran, E., Dunn, Z., Lohner, K., and Zilliac, “Modeling Feed System Flow Physics for Self-Pressurizing Propellants,” 43rd AIAA/ASME/SAE/ASEE Jt. Propuls. Conf. Exhib.
6. C. Snyder, “NASA Chemical Equilibrium with Applications (CEA).” [Online]. Available: <https://www.grc.nasa.gov/WWW/CEAWeb/>. [Accessed: 09-Apr-2017].
7. W. Devenport, “Ideal Flow Machine.” [Online]. Available: <http://www.dept.aoe.vt.edu/~devenpor/aoe5104/ifm/ifm.html>. [Accessed: 09-Apr-2017].
8. Z. Arena, A. Athouges, A. Rodulfo, A. Athouges, and D. Deturris, “Hybrid Rocket Motor,” 2010.
9. D. Bartz, “A simple Equation for Rapid Estimation of Rocket Nozzle Convective Heat Transfer Coefficients.,” Jet Propuls. Lab., 1957.
10. B. Widrow, Y. Kim, and D. Park, “The Hebbian-LMS Learning Algorithm,” IEEE Comput. Intell. Mag., vol. 10, no. 4, pp. 37–53, Nov. 2015.
11. “Adaptive Filter System.” [Online]. Available: <http://archive.cnx.org/contents/88b55b0b-1ca2-42bc-9302-c0928f16d2e2@1/adaptive-filter-system>. [Accessed: 09-Apr-2017].
12. Newlands R. Modelling the nitrous run tank emptying. 2011.
13. NASA Chemical Equilibrium with Applications (CEA). <https://www.grc.nasa.gov/WWW/CEAWeb/>.
14. ASME Boiler and Pressure Vessel Code Section II-B Nonferrous Material Specifications and Section VIII Rules for Construction of Pressure Vessels. 2015.
15. Waxman BS, Cantwell B, Zilliac G, Zimmerman JE. Mass Flow Rate and Isolation Characteristics of Injectors for Use with Self-Pressurizing Oxidizers in Hybrid Rockets. In: *49th AIAA/ASME/SAE/ASEE Joint Propulsion Conference*. Reston, Virginia: American Institute of Aeronautics and Astronautics; 2013. doi:10.2514/6.2013-3636.
16. Karabeyoglu A. High regression rate hybrid rocket propellants and method of selecting. 2000.
17. Arena Z, Athouges A, Rodulfo A, Athouges A, Deturris D. Hybrid Rocket Motor. 2010.
18. Sutton GP, Biblarz O. *Rocket Propulsion Elements, 8th Edition*. 8th ed. New Jersey: John Wiley & Sons, Inc.; 2010. <http://ca.wiley.com/WileyCDA/WileyTitle/productCd-0470080248.html>.
19. Devenport WJ. Converging Diverging Nozzle. <http://www.engapplets.vt.edu/fluids/CDnozzle/cdinfo.html>. Published 2001. Accessed November 10, 2016.
20. ASM Material Data Sheet. <http://asm.matweb.com/search/SpecificMaterial.asp?bassnum=MA6061t6>.
21. Standard: Space Systems – Metallic Pressure Vessels, Pressurized Structures, and Pressure Components (AIAA S-080-1998). In: *Standard: Space Systems – Metallic Pressure Vessels, Pressurized Structures, and Pressure Components (AIAA S-080-1998)*. Washington, DC: American Institute of Aeronautics and Astronautics, Inc.; 1998. doi:10.2514/4.473654.001.
22. MIL-STD-889 Dissimilar metals. 1993.
23. Sayyar-Rodsari B. ESTIMATION-BASED ADAPTIVE FILTERING AND CONTROL. 1999.
24. Least Mean Square Algorithm (using C++) - CodeProject. <http://www.codeproject.com/Articles/1000084/Least-Mean-Square-Algorithm-using-Cplusplus>.
25. Gordon Sanford Gordon S, Cleveland A, McBride BJ. Finite Area Combustor Theoretical Rocket Performance. 1988.
26. Standard: Space Systems — Composite Overwrapped Pressure Vessels (COPVs) (AIAA S-081A-2006). In: *Standard: Space Systems — Composite Overwrapped Pressure Vessels (COPVs) (AIAA S-081A-2006)*. Washington, DC: American Institute of Aeronautics and Astronautics, Inc.; 2006. doi:10.2514/4.478437.001.
27. Tsohas J, Appel B, Rettenmaier A, Walker M, Heister S. Development and Launch of the Purdue Hybrid Rocket Technology Demonstrator. In: *45th AIAA/ASME/SAE/ASEE Joint Propulsion Conference & Exhibit*. Reston, Virginia: American Institute of Aeronautics and Astronautics; 2009. doi:10.2514/6.2009-4842.
28. Richard Nakka’s Experimental Rocketry Site. <http://www.nakka-rocketry.net/nozmach.html>.
29. Carbon Fiber Properties. <http://www.christinedemerchant.com/carboncharacteristics.html>.
30. Fastenal industries stander. Fastenal Technical Reference Guide. 2015
31. Roylance, D., “Pressure Vessels.” Dept. of Materials Science and Engineering, Massachusetts Institute of Technology, Cambridge, MA, 2001
32. Lutdke, W. P., “Effects of Canopy Geometry on the Drag coefficient of a cross parachute in the fully open and reefed conditions for a W/L ratio of 0.264,” NOLTR 71-111, 1971
33. Niccum, R. J., Haak, E. L., Guttenkauf, R., “Drag and Stability of cross type parachutes,” FDL-TDR-64-155
34. Jorgensen, D. S., “Cruciform Parachute Aerodynamics,” Ph.D. Dissertation, University of Leicester, 1982

35. Knacke, T. W., *Parachute Recovery Systems Design Manual*, Para Publishing, Santa Barbara, 1992
36. Bixby, H. W., Ewing, E. G., Knacke, T. W., *Recovery Systems Design Guide*, Gardena, CA, AFDL-TR-78-151
37. Newlands, R., “Parachute recovery system design for large rockets,” December 2014
38. Tinder Rocketry, “Peregrine Raptor Manual,” URL: https://fruitychutes.com/docs/Peregrine_Raptor_Manual.pdf
39. Tender Descender, “Recovery Tether Manual,” URL: https://fruitychutes.com/Recovery_Tether_Manual.pdf
40. “Department of Defence Handbook, Global Climatic Data for Developing Military Products,” MIL-HDBK-310
41. EuroLaunch, “REXUS User Manual v7.15”, URL: http://rexusbexus.net/wp-content/uploads/2017/12/RX_UserManual_v7-15_07Nov17.pdf
42. Niskanen, S., “OpenRocket Technical Documentation v13.05”, URL: https://github.com/openrocket/openrocket/releases/download/OpenRocket_technical_documentation-v13.05/OpenRocket_technical_documentation-v13.05.pdf
43. Apogee Components, “How To Calculate Fin Flutter Speed”, URL: <https://www.apogeerockets.com/education/downloads/Newsletter291.pdf>
44. Martin, D., “Summary of Flutter Experiences as a Guide to the Preliminary Design of Lifting Surfaces on Missiles”, NACA Technical Note 4197, URL: <https://ntrs.nasa.gov/archive/nasa/casi.ntrs.nasa.gov/19930085030.pdf>
45. Crowell, G., “The Descriptive Geometry of Nose Cones” URL: https://web.archive.org/web/20110411143013/http://www.if.sc.usp.br/~projetoisulfos/artigos/NoseCone_EQN2.PDF